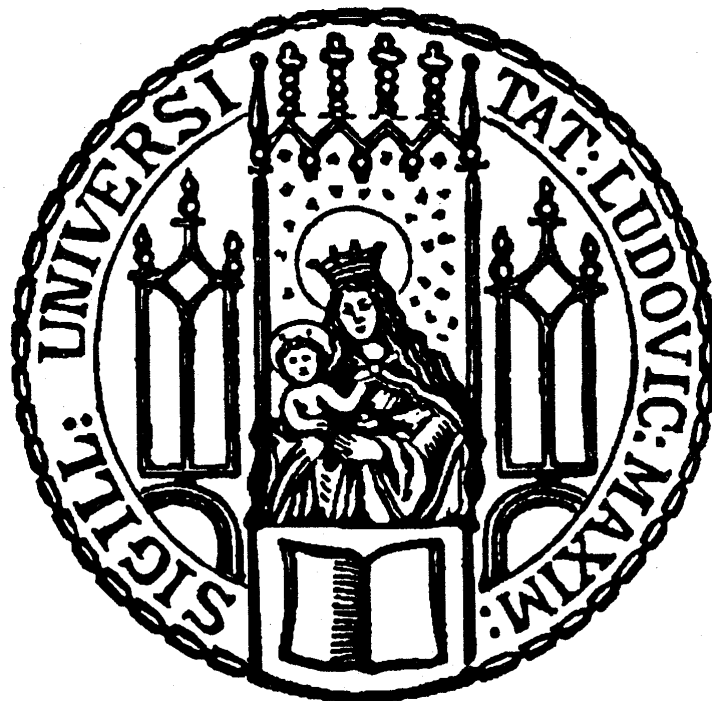

Divergent Functions of IL-4R α and STAT6 in a Model of Colitis-Associated Carcinogenesis



Tiago Azambuja De Oliveira

2016

Divergent Functions of IL-4R α and STAT6 in a Model of Colitis-Associated Carcinogenesis

Dissertation

der Fakultät für Biologie
der Ludwig-Maximilians-Universität München

vorgelegt von

Tiago Azambuja De Oliveira

aus Pelotas, Brasilien

München, den 27 Oktober 2016

Erstgutachter: Prof. Dr. Heinrich Leonhardt

Zweitgutachter: PD. Dr. Eric Lambie

Betreuer: Prof. Dr. Florian R. Greten

Tag der Abgabe: 27 Oktober 2016

Tag der mündlichen Prüfung: 29 Mai 2017

TABLE OF CONTENTS

| | |
|--|------------|
| ABSTRACT | vi |
| ZUSAMMENFASSUNG | vii |
| 1. INTRODUCTION | 1 |
| 1.1 The Large Intestine | 1 |
| 1.1.1 Anatomy, structures and cell composition | 1 |
| 1.1.2 Intestinal microbiota | 10 |
| 1.1.3 Immune cells | 13 |
| 1.2 The IL-4 Signaling Pathway | 18 |
| 1.2.1 IL-4, IL-13, IL-4R α and Stat6 | 18 |
| 1.2.2 IL-4 signaling involvement in tumorigenesis | 21 |
| 1.3 Colonic Carcinogenesis | 24 |
| 1.3.1 Colonic carcinogenesis | 24 |
| 1.3.2 Molecular events of colonic carcinogenesis | 25 |
| 1.3.3 Mouse models of colonic carcinogenesis | 29 |
| 2 AIM | 31 |
| 3 MATERIAL AND METHODS | 32 |
| 3.1 Materials | 32 |
| 3.1.1 Chemicals, reagents and kits | 32 |
| 3.1.2 Oligonucleotides | 33 |
| 3.1.3 Antibodies | 34 |
| 3.2 Cell Culture-Based Methods | 34 |
| 3.2.1 Extraction and stimulation of mouse bone marrow derived macrophages (BMDM) | 34 |
| 3.2.2 Extraction and stimulation of mouse peritoneal macrophages | 35 |
| 3.2.3 Intestinal epithelial cell isolation | 36 |
| 3.2.4 Intestinal fibroblast isolation | 36 |
| 3.2.5 Intestinal organoid isolation | 37 |
| 3.2.6 Determination of cell count and viability | 37 |
| 3.3 Molecular Biology Based Methods | 38 |
| 3.3.1 RNA isolation and determination | 38 |
| 3.3.2 Reverse transcription, cDNA synthesis | 38 |
| 3.3.3 Quantitative real time PCR | 38 |
| 3.3.4 DNA isolation and genotyping | 39 |
| 3.3.5 Agarose electrophoresis | 40 |
| 3.3.6 Protein extraction and determination | 40 |
| 3.3.7 Western blot | 41 |
| 3.3.8 Formalin-fixed and paraffin embedded tissue processing | 43 |

| | |
|--|-----------|
| 3.3.9 Immunohistochemistry..... | 44 |
| 3.4 Mouse Models | 45 |
| 3.4.1 Global deletion of <i>Il-4rα</i> : IL-4Rα ^{del/del} mice | 45 |
| 3.4.2 <i>Il-4rα</i> specific deletion in intestinal epithelial cells (IEC): IL-4Rα ^{ΔIEC} mice..... | 46 |
| 3.4.3 Global deletion of <i>Stat6</i> : Stat6 ^{-/-} mice | 48 |
| 3.4.4 AOM - DSS treatment protocols | 49 |
| 3.5 Statistics | 50 |
| 4 RESULTS..... | 51 |
| 4.1 IL-4Rα^{del/del} Mice..... | 51 |
| 4.1.1 Global deletion of <i>Il-4rα</i> does not cause any overt tumor-promoting phenotype in unchallenged mice..... | 51 |
| 4.1.2 IL-4Rα signaling promotes tumor formation and tumor growth | 51 |
| 4.2 IL-4Rα^{ΔIEC} Mice | 54 |
| 4.2.1 Specific IL-4Rα signaling in IEC promotes tumor growth with effects on tumor cell proliferation and STAT3 phosphorylation | 54 |
| 4.2.2 IEC-specific deletion of <i>Il-4rα</i> increases IEC apoptosis without affecting colonic epithelial regeneration at early events of AOM and DSS challenge | 55 |
| 4.3 Stat6^{-/-} Mice | 59 |
| 4.3.1 <i>Stat6</i> global deletion does not cause any overt phenotype in unchallenged mice | 59 |
| 4.3.2 <i>Stat6</i> expression during colitis-associated tumor model protects against tumor formation and tumor growth | 59 |
| 4.3.3 <i>Stat6</i> -deficient tumors present decreased P53 nuclear localization and reduced mRNA levels of <i>Mgmt</i> and <i>P21</i> genes | 62 |
| 4.3.4 <i>Stat6</i> -deficient enterocytes are the major contributors for increased colonic tumorigenesis in Stat6 ^{-/-} mice during colitis-associated tumor model | 63 |
| 4.3.5 Lack of <i>Stat6</i> increases IEC apoptosis in the early stages of tumorigenesis, leading to severe colitis in response to AOM/DSS challenge.... | 66 |
| 4.3.6 Acute effects of AOM on Stat6 ^{-/-} IEC leads to increased DNA double strand breaks and apoptosis | 69 |
| 5 DISCUSSION | 72 |
| 5.1 Global deletion of <i>Il-4rα</i> suppresses colorectal tumorigenesis by reducing STAT3 activity and inducing intestinal epithelial cell cycle arrest | 72 |
| 5.2 IEC-specific deletion of <i>Il-4rα</i> suppresses tumor development by inducing apoptosis of the initiated cells and by preventing epithelial hyperproliferation after DSS-induced colitis | 74 |
| 5.3 <i>Stat6</i> deletion promotes colorectal tumorigenesis by inducing aberrant overexpression of STAT3 during colitis-associated tumor..... | 76 |
| 5.4 DSS-induced colitis is exacerbated in Stat6 ^{-/-} mice..... | 79 |
| 5.5 <i>Stat6</i> expression protects IEC from AOM-induced DNA damage and apoptosis..... | 80 |
| REFERENCES..... | 82 |

| | |
|-------------------------------|------------|
| ABBREVIATIONS | 100 |
| ACKNOWLEDGEMENTS..... | ix |
| CURRICULUM VITAE | xi |
| APPENDIX..... | xii |
| Figure copyrights..... | xii |

“...Cada um tem o que merece, disse Jesus na cruz.”

ABSTRACT

Interleukin 4 (IL-4) signaling has been implicated in tumorigenesis in many types of malignancies including breast, lung, brain, renal and pancreatic cancer through different cell-intrinsic mechanisms. In order to understand how IL-4 signaling might affect inflammation-dependent colorectal tumor development and progression, this study aimed to investigate the most prominent components of this pathway: (i) interleukin 4 receptor alpha (IL-4R α) and (ii) signal transducer and activator of transcription 6 (STAT6). Taking advantage of genetically modified mice and a well-established colitis-associated cancer model functional relevance of IL-4R α and STAT6 in intestinal epithelial cells was evaluated. Employing the AOM/DSS tumor model mice with global deletion of IL-4R α developed fewer and smaller colonic tumors than WT mice. Additionally, IL-4R α loss during colitis-associated tumorigenesis reduced STAT3 activity in transformed colonocytes causing cell cycle arrest at G2-phase due to decreased CYCLIN B1 and CYCLIN E expression. Knowing that STAT6 is crucial to provide gene activation signals in the IL-4 pathway it was expected that *Stat6* ablation during colitis-associated tumorigenesis would generate similar results as the ones obtained with IL-4R α mice. Surprisingly, *Stat6* deficient animals showed enhanced susceptibility to chemically induced intestinal epithelial damage and subsequent colonic inflammation. A significant increase in tumor load and tumor size was observed in these animals followed by an increased STAT3 activation in tumors. STAT3 is known to influence colon cancer development and its compensatory upregulation could explain the phenotype observed in *Stat6* knockout mice. The findings here add further insights on STAT6 and IL-4R α signaling during intestinal tumorigenesis and stress that the loss of a single pathway component can exert dramatic influences for the phenotype of genetically modified mice and for the therapeutical use of inhibitors of signaling pathways. Moreover, considering that STAT6 is the most important known transcription factor downstream of IL-4 these data highlight unexpected IL-4-independent functions of STAT6.

ZUSAMMENFASSUNG

Der Interleukin-4 (IL-4) Signalweg wird über unterschiedliche Zell-intrinsische Mechanismen mit der Entstehung von Tumoren in verschiedenen Organen, wie Brust, Lunge, Gehirn, Niere und Pankreas, in Verbindung gebracht. Um zu verstehen, wie dieser Signalweg die Entwicklung von Tumoren des Dick- und Enddarms beeinflusst, wurden in dieser Studie die wichtigsten Komponenten des IL-4 Signalwegs untersucht: (i) Interleukin-Rezeptor 4 alpha (IL-4R α) und (ii) Signal-Transduktor und Transkriptions-Aktivator 6 (STAT6). Die funktionelle Bedeutung von IL-4R α und STAT6 in Darmepithelzellen wurde unter Verwendung von genetisch veränderten Mauslinien und einem etablierten Modell für Kolitis-assoziierte Darmkarzinome untersucht. Im AOM/DSS-Modell entwickelten Mäuse mit globaler Deletion von IL-4R α weniger und kleinere Dickdarmtumoren als Mäuse vom Wildtyp. Ergänzend dazu führte der Verlust von IL-4R α in diesem Modell zu einer reduzierten Aktivierung von STAT3 in transformierten Epithelzellen des Kolons und verursachte einen Stillstand im Zellzyklus in der G2-Phase durch verminderte Expression von Cyclin B1 und Cyclin E. Unter der Annahme, dass wichtige Aktivierungssignale für Gene im IL-4-Signalweg STAT6-abhängig vermittelt werden, erwarteten wir, dass die genetische Inaktivierung von STAT6 ähnliche Effekte in der Entwicklung von im Kolitis-assoziierten Darmkarzinomen zeigen würde wie Inaktivierung von IL-4R α . Überraschenderweise zeigen STAT6-defiziente Tiere erhöhte Anfälligkeit für chemisch-induzierte Schädigung der Darmschleimhaut und darauffolgende Entzündung. Eine signifikant erhöhte Tumorlast und -größe konnte im Zusammenhang mit verstärkter STAT3-Aktivierung in Tumoren beobachtet werden. STAT3 ist ein bekannter Einflussfaktor in der Entwicklung von Darmkarzinomen und seine kompensatorische Aktivierung könnte den Phänotyp der STAT6-defizienten Tiere erklären. Die hier erzielten Ergebnisse zeigen die Bedeutung des IL-4-Signalwegs für die Entwicklung von Darmtumoren aus entzündlichen Reaktionen der Schleimhaut. Unsere Beobachtung, dass die Manipulation einzelner Komponenten dieses Signalwegs unterschiedliche Auswirkungen auf das Endergebnis zeigen, hat

große Bedeutung für die eventuelle Entwicklung von Inhibitoren dieses Signalwegs für die klinische Anwendung. Darüberhinaus zeigen unsere Daten unerwartete, IL-4 unabhängige, Funktionen von STAT6 auf, gilt doch STAT6 als wichtigster IL-4 abhängiger Transkriptionsfaktor.

1. INTRODUCTION

1.1 The Large Intestine

1.1.1 Anatomy, structures and cell composition

The gastrointestinal tract (GI-tract) is the responsible organ for digestion and absorption of nutrients. Therefore, it is the largest mucosal surface of the body with 8,50 meters length in humans and 30 centimeters length in mice. Remarkable, up to 80% of its structure is comprised by the small intestine, which has an average length of six meters in an adult human. Both humans and mice digestive tracts share very close anatomical, histological, physiological and pathological similarities. Duodenum, jejunum, and ileum constitute the proximal to distal parts of the small intestine, whilst the large intestine being composed by caecum, colon, and rectum (Figure 1 and 2) [1, 2].

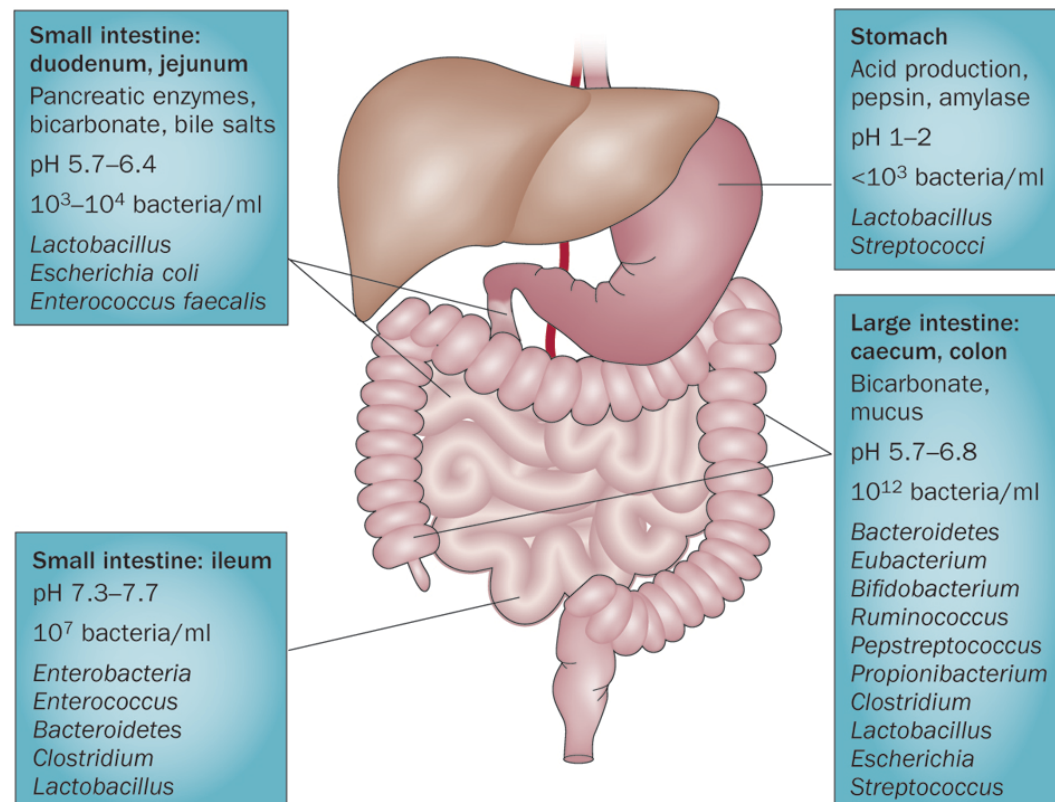


Figure 1. Characteristics of the normal human gastrointestinal tract. (Extracted and adapted by permission from Macmillan Publishers Ltd: Nature Reviews *Gastroenterology and Hepatology* 9, 590-598 [3]).

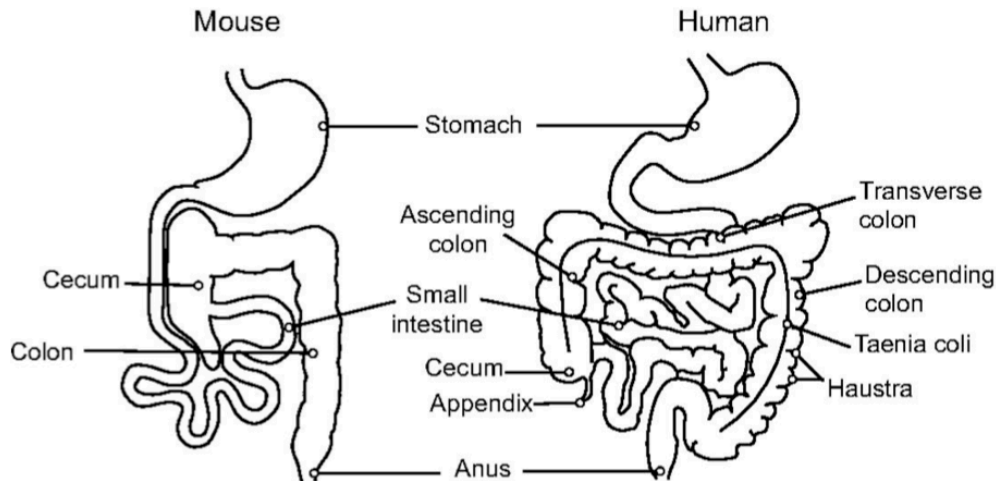


Figure 2. Gross anatomy of the human and murine gastrointestinal tract. (Extracted from *Thi Loan Anh Nguyen et al. Dis. Model. Mech. 2015;8:1-16 [4]*). The gastrointestinal segments can be directly compared between mice and humans. The main gross anatomic difference observed is the murine enlarged cecum and appendix.

The large intestine can be divided in 4 anatomic segments: the most proximal is the cecum with its vermiform appendix followed by the colon, the rectum and the anal canal, which is the most distal segment. In addition, the colon is subdivided into ascending colon, transverse colon, descending colon and sigmoid. The mucosa contains straight tubular glands, called crypts of Lieberkühn. They are the functional unit of the intestine and are present through its full thickness. These glands consist of simple columnar epithelium, which invaginate deep through the intestinal wall. At the microscopic level, examination of the luminal surface of the large intestine reveals the opening of the glands, which are arranged in an exceptionally organized pattern (Figure 3), [1].

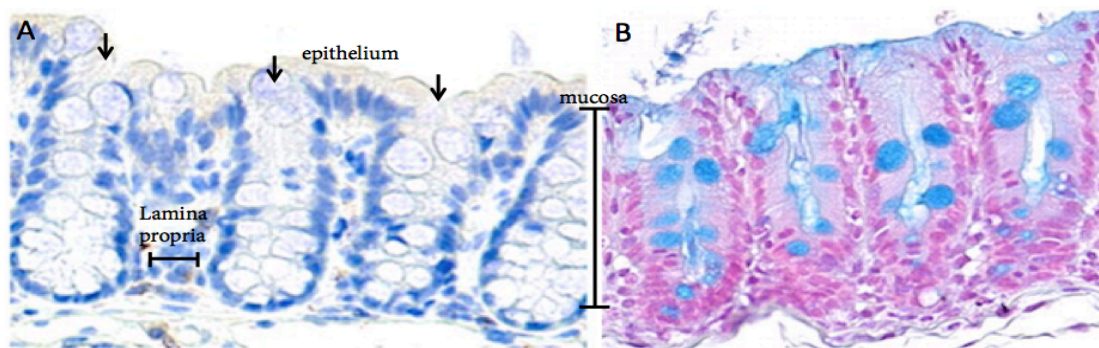


Figure 3. Histology of the large intestine mucosa. (Extracted and adapted with permission from *Disease Models & Mechanisms 2012 5: 107-114; doi: 10.1242/dmm.007591v [5]*). Hematoxylin and Eosin (A) of the mucosa and part of the submucosa. The surface of the epithelium is continuous and unbranched depicting the crypts of Lieberkühn arranged side-by-side. The arrows identify the openings of the crypts. The epithelial cells consist mainly in absorptive and goblet cells, which can be easily visualized by Alcian-Blue staining (B). The *lamina propria* contains numerous lymphocytes and other cells of the immune system.

Contrary to the small intestine, the large intestine lacks villi (finger-like protrusions that point towards the lumen and increase the absorptive area of the small intestine dramatically). Histologically, the colon is organized into three spatially distinct layers. The most exterior consists of several sheets of smooth muscle that in collaboration with the intramural enteric nervous system perform the rhythmic peristaltic movements of the intestine. The space between the outer muscle and the inner luminal epithelial layer is called submucosa. It is filled with connective tissue that contains numerous blood and lymphatic vessels, nerve fibers, and various cells of the immune system [6]. A simple single line of columnar epithelial cells that fold themselves into “finger-like invaginations” form the luminal surface of the intestine. These invaginations are further supported by the *lamina propria*, generating the so-called crypts of Lieberkühn (also often referred as colonic crypts) [7].

The mucosal epithelium of the large intestine holds the same cell types as the small intestine, with the exception of Paneth cells, that produce antimicrobial peptides which regulate the gut microbiota, as well as growth factors involved in the maintenance of the neighboring stem cells, and are usually absent in the colon of healthy humans and mice [8]. Four terminally differentiated epithelial cell lineages can be recognized in the colon luminal surface. Absorptive cells, goblet cells, endocrine cells, and tuft cells are found in the top middle-third of the crypt and are derived from stem cells located at the bottom of the crypt. These bottom-based stem cells undergo self-renewal by asymmetric division generating a population of transit amplifying cells (TA) that migrate towards the top of the crypt, proliferating and differentiating into one of the many epithelial cell types that compose the intestinal epithelium (Figure 4 and 5). Moreover, these proliferating intestinal crypts rely on paracrine signals (cell-to-cell signals) exchanged between the epithelium and the surrounding mesenchymal cells, such as fibroblasts. The maintenance and protection against the ectopic formation of crypts are controlled by a delicate balance between the expression of morphogenetic proteins and its antagonists (e.g. *noggin* and *gremlin*). Additionally, intestinal epithelial cell (IEC) differentiation towards secretory versus non-secretory lineages is highly influenced by the activation of Notch and WNT pathways, which can respectively promote stemness (maintain the self-renewal of stem cell

population at the bottom of the crypt) and induce proper differentiation of IEC at the top of the crypt [9-11].

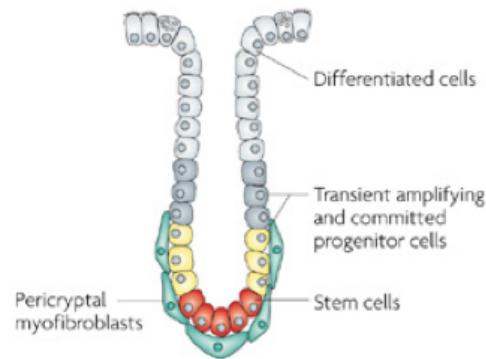


Figure 4. Diagrammatic representation of the colonic crypt. (Extracted and adapted by permission from Macmillan Publishers Ltd: *Nature Reviews Cancer* 8, 415-424 [12]). Intestinal stem cells (in red) are located in the base of the colonic crypt in close proximity with other crypt-niche cells, such as fibroblast (in green). Those form an outer layer and direct communicate by cellular signals with the stem cell niche. Transient amplifying and committed progenitor cells (in dark gray) can be found directly above, and will give rise to all different cell lineages.

In 2007, the Wnt target gene Leucine-rich repeat containing G protein-coupled receptor 5 (*Lgr5*) was identified as a marker of crypt base columnar cells. The study performed cellular lineage-tracing experiments identifying *Lgr5*⁺ cells as multipotent and self-renewing intestinal epithelial cells population [13]. Additionally, in the small intestine, cells located above the stem cell compartment (transient amplifying and committed progenitor cells zone) and expressing the Bmi1 polycomb ring finger oncogene (*Bmi1*) have been reported to have stem cell features, which partially overlap with *Lgr5* cells expression. [14].

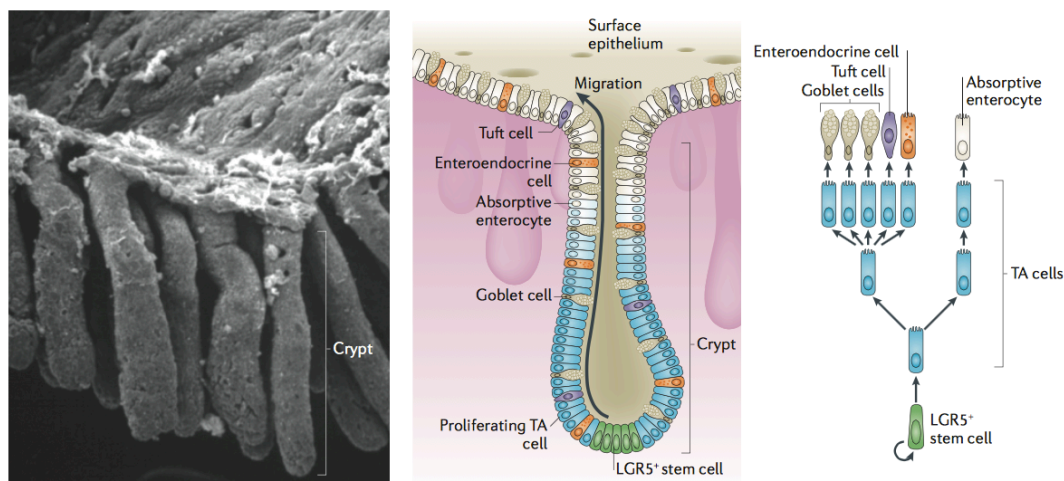


Figure 5. Electron micrograph and diagram colonic crypts. (Extracted and adapted by permission from Macmillan Publishers Ltd: *Nat Rev Mol Cell Biol.* 2014 Jan;15(1):19-33 [15]). The micrograph depicts the colonic crypt at its totality and the luminal linear surface of the intestinal colonic epithelium. The diagram exemplifies the localization of the different cell types inside the crypt highlighting the newly identified *Lgr5* stem cells (in green). Additionally, all different cell lineages originated by *Lgr5* stem cells are shown.

Although a lot of progress has been made regarding stem cell niche, most of the published studies have only addressed the niche components of the small intestine. Therefore, the colonic stem cell niche still needs better characterization not only about its cell composition but also about the signaling pathways involved in its maintenance. Addressing this issue, Rothenberg and colleagues [16] suggested that colonic cKIT-expressing goblet cells might support Lgr5⁺ cells secreting factors such as Notch ligands, TGF- α and WNT ligands, similar to what Paneth cells do at the small intestine. However, intestinal stem cell function and fate are still a major issue of investigation and debate.

Absorptive Cells – Enterocytes

The primary roles of the large intestine and its columnar absorptive cells are reabsorption of water, electrolytes, and compaction of the stool. The morphology of the absorptive cell - also called enterocyte - is similar throughout all of small and large intestine. Basically, they are tall columnar cells with a basally positioned nucleus. These cells have a striated border on its apical surface and junctional complexes that seal the lumen of the intestine from the lateral intracellular space (Figure 6), [17]. Reabsorption of water and electrolytes is accomplished by active transport systems like sodium pumps, which reduce the intracellular concentration of sodium by moving it through the cell into the extracellular space below the tight junction. The accumulation of sodium in the intercellular space makes with the intracellular water also moves there in order to reduce sodium levels. Once the sodium is pumped into the intercellular space water will always be absorbed at the surface of the colonic epithelium and redirected into the intercellular space by osmosis. Subsequently, the water and other electrolytes accumulated at the intercellular space will cross the basal membrane and will be diffused into the surrounding connective tissue, entering in capillaries and reaching the body blood circulation [17, 18].

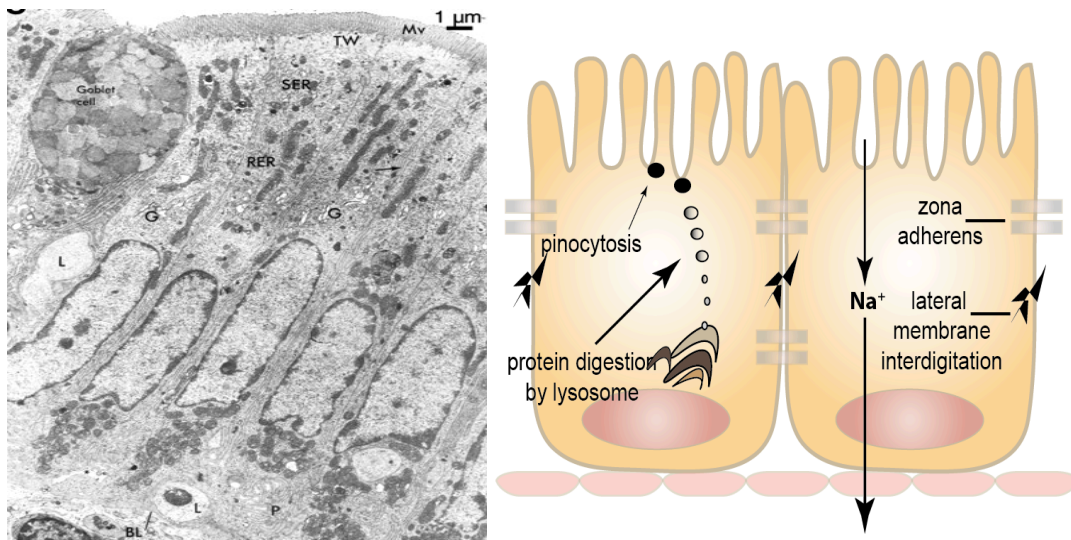


Figure 6. Electron micrography and diagram of an intestinal absorptive cell. (Micrograph extracted from *J Cell Biol* 34: 123–155, 1967 [19]). Micrography of a rat intestine shows several absorptive cells close to a goblet cell (top right). The nuclei of the absorptive cells are elongated and located basally, surrounded by cluster of mitochondria. Both the Golgi (G) and the rough endoplasmic reticulum (RER) can be visualized. The intestinal lumen is at the top. The diagram depicts two absorptive cells and their sodium pumps located at the lateral plasma membrane. The sodium flow through the cell to the extracellular space below the basal membrane is shown.

Goblet Cells

Goblet cells produce and secrete large amounts of mucus into the intestinal lumen facilitating the elimination of solid and semi-solid dietary residues. One of the main components of the secreted mucus are mucins, which not only lubricates the lumen of the intestine facilitating the excretion of the stool but also forms a mechanical barrier that protects the epithelium from potential harmful substances and microorganisms. Goblet cells are distributed among the other intestinal epithelial cells and are easily recognized by their morphology. As their own name says, they exhibit a chalice shape due to their distended theca, which is heavily packed with mucin granules (Figure 7), [20]. Anatomically, they are more numerous in the large intestine than in the small intestine, and the ratio of absorptive intestinal cells versus goblet cells decreases from the colon to the rectum, where the number of goblet cells is heavily increased [21]. From their generation at the bottom of the crypt until the point where they reach the intestinal epithelium surface, goblet cells produce and secrete not only mucins but also other bioactive factors, which are going to compose the mucus, such as cytokines that can act during intestinal inflammatory insults contributing to the restoration of epithelial homeostasis [22].

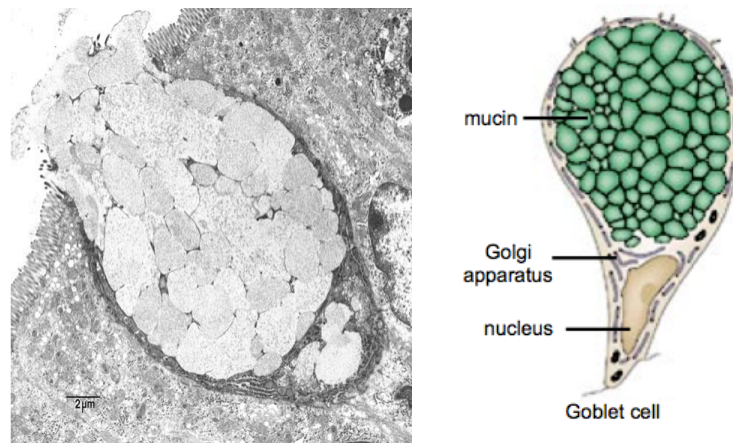


Figure 7. Electron micrography and diagram of mouse goblet cell between two intestinal absorptive cells. (Micrograph extracted by permission from the Electron Microscopy Research Laboratory, Kansas University, KUMC. Diagram adapted by permission from Macmillan Publishers Ltd: *Nature Reviews Genetics* 7, 349-359 [9]). Both in the micrography and in the diagram the presence of mucin at the apical surface of the cell can be easily observed over its basal cytoplasm.

From the secreted bioactive molecules, mucin 2 (MUC2) is by far the major goblet cell-derived mucin. Genetical experiments performed with *Muc2*-deficient mice showed that its ablation affects goblet cell morphology due to the collapse of the theca, although the continuous production of other goblet cell-factors is observed [20, 23]. Even more important than cellular morphological changes, inactivation of *Muc2* in different mouse models triggered colorectal tumorigenesis and spontaneous tumor formation without overt inflammatory insults. [23-26]. Therefore, the available literature demonstrates the importance of the goblet cells for the intestinal homeostasis and that a reduction in goblet cells and/or a reduction of the mucus layer produced by them has a significant impact on the promotion of colorectal tumorigenesis.

Along with the intestinal absorptive cells and goblet cells, other two important cell types can be identified in the colonic intestinal mucosa: (i) enteroendocrine cells; (ii) and tuft cells.

Enteroendocrine Cells

It has been already shown that the human digestive system is able to synthesize a vast diversity of hormones, being considered an important part of the endocrine system along with the thyroid, the adrenal glands, the reproductive system (ovary and testis) and the hypothalamus, to cite some.

This concept is firmly based on the function of the highly specialized enteroendocrine cells (EECs), which are diffusely distributed in the intestinal mucosa (Figure 8), [27, 28] [29]. Interestingly, the reason for this diffused distribution in the intestinal epithelium is due to the action of Notch signaling on these cells, which directly inhibits the nearby intestinal epithelial cell to differentiate into the enteroendocrine lineage [30]. EECs can be classified in more than 10 subtypes that may overlap in function, however three of these subtypes deserve special consideration: (i) enterochromaffin cells (also known as Kulchitsky cells), which are found mainly in the colon and rectum, secrete 5-hydroxytryptamine (5-HT) and are extremely important for the intestinal motility due to their direct interaction with the enteric nervous system [31]; (ii) L cells, which produce hormones including Glucagon-like peptide-1 (GLP-1) that are involved in insulin secretion and are found principally in the ileum and colon [32], and (iii) D cells, that are mainly known for their production of somatostatin, which regulates glucagon and insulin production. D cells are found in the small intestine and scarcely in the rest of the gut [33].

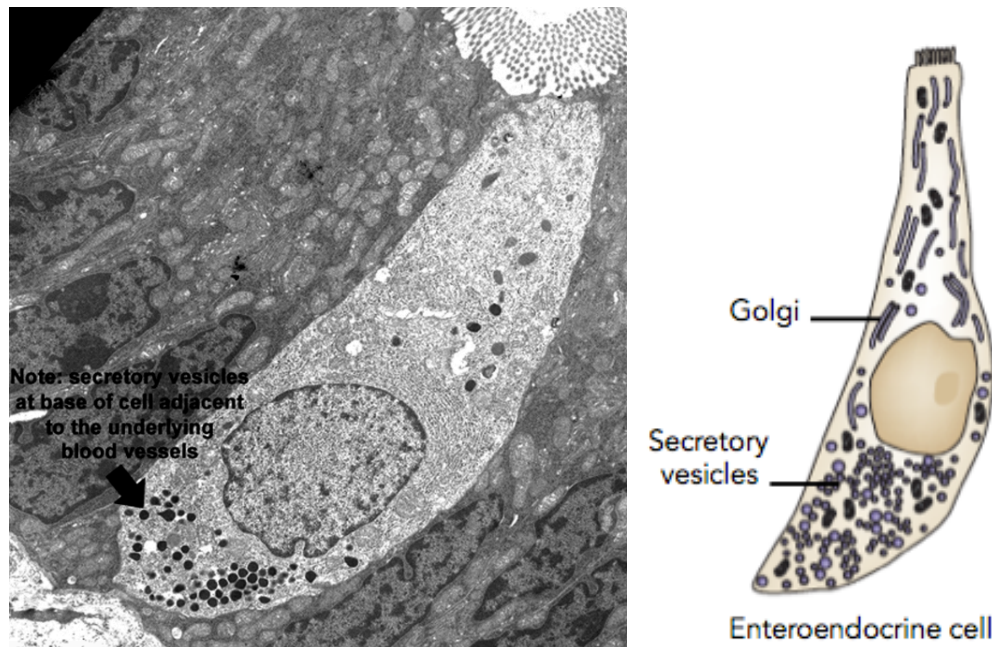


Figure 8. Enteroendocrine cell micrograph and diagram. (Micrograph extracted from *Electron Microscopy Research Laboratory, Kansas University, KUMC*. Diagram adapted by permission from Macmillan Publishers Ltd: *Nature Reviews Genetics* 7, 349-359 [9]). The existence of cytoplasmic secretory vesicles is one of the main features for enteroendocrine cells identification and characterization. Chromogranin A, synaptophysin, enolase and protein gene product 9.5 are often detected components [27, 34]. The secretory granules are marked with a black arrow at the micrography.

Tuft Cells

While migrating towards the top of the crypt, progenitor cells differentiate into perhaps the most distinct and less characterized cell type of the intestinal epithelium: the tuft cells.

Since their first identification in the rat trachea and mouse gastrointestinal tract in 1956 by Rhodin and Dalhamn [35] and Jarvi and Keyrilainen [36], tuft cells, also known as brush cells, have been confirmed in the respiratory tract [37-41] and the GI tract [42-49], of many other mammals including humans, rats, cats, pigs, cows, mice, rabbits, guinea pigs, and ferrets [50]. When compared to other intestinal epithelial cells, tuft cells exhibit a very distinct morphology due to their round and elongated microvilli, followed by a highly complex and specialized vesicular system composed of tubules and sacs, located over the cell nucleus (Figure 9). Tuft cells exact functions need to be better defined and are still under debate. Nevertheless, it was recently proposed that they might participate in the chemical sensation of antigens found in the gut's lumen [51, 52]. Taking this into consideration, it is possible that the recognition of parasitic infections is based on the ability described above, as intestinal worms alter the concentration of the intestinal luminal contents. Additionally, scientific data have demonstrated that tuft cells are also an important source of interleukin 25 (IL-25), a cytokine directly involved in the resolution of parasitic infections [53, 54].

Several markers have been proposed for tuft cells, such as *Dcamk1* [55] and *Atoh1* [51]. However, other intestinal epithelial cells also express these markers, so they cannot be fully recognized as tuft-cell specific. Therefore, tuft-cells precise identification must be made taking into account their unique, distinctive morphology and the expression of different molecular markers.

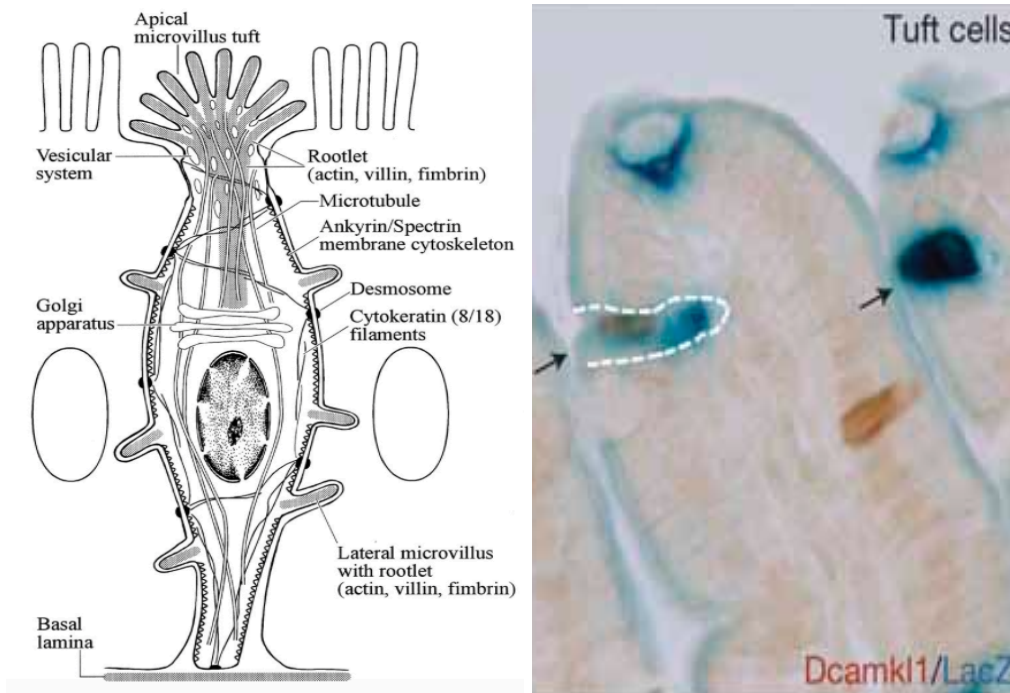


Figure 9. Tuft cell: histology and diagram. (Diagram extracted from *The American Physiological Society: Physiology*. 1 February 1999 Vol. 14 no. 1, 18-23 [56]. Histological figure extracted and adapted by permission from Macmillan Publishers Ltd: *Nature Cell Biology* 14, 1099–1104 (2012) [55]). The diagram shows the unique cellular morphology of the tuft cells and depicts their delicate tubule-vesicular system located in the supranuclear area. Interesting, the taste cells of the tongue exhibit similar cellular features such as abundant microtubules, long actin filaments and lateral villi associated with microvilli. Additionally, alpha-gustducin, a G protein found in taste receptors is identified in both cell types. On the right, the histological picture highlights the expression of Dcamk1, a proposed tuft cell marker.

1.1.2 Intestinal microbiota

Due to its fascinating capacity to host millions of microorganisms the gastrointestinal tract is considered the most significant of all mucosal barriers of the human body. It is estimated that the total microbial load existent in the GI-tract is between 10^{13} to 10^{14} microorganisms. That is proximally 100 times more than our genome [11, 57]. The amount and complexity of bacteria, fungi, viruses and archaea rises exponentially from the beginning to the end of our GI tract (Figure 10). Moreover, whilst in the proximal parts of the GI tract we observe mainly aerobic germs, at the distal parts they are outnumbered by anaerobic ones. Interestingly, although at an early age of life the human GI tract exhibits a significantly heterogeneous microbiome, during adulthood this diversity decreases and the microbiome becomes a more homogenous phylum, presumably due to environmental influences [58-60].

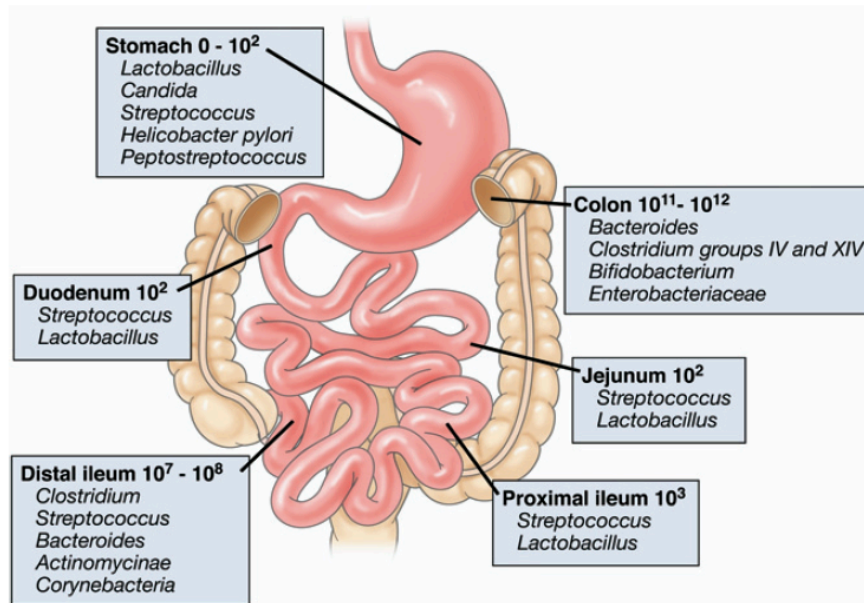


Figure 10. The gut microbiota and its localization. (Extracted and adapted from *GASTROENTEROLOGY* 2008;134:577–594 [58], with permission from Elsevier). Composition and luminal concentrations of main microbial species in various regions of the gastrointestinal tract.

The backbone of this extraordinary symbiotic relationship is the ability to maintain the distinction between host and microbial organisms, which is achieved mainly by two mechanisms: first by the gut motility (peristaltic movements) which prevents the long-term interaction between microbes and mucosal areas; second, by the luminal secretion of mucins and antimicrobial proteins, establishing a physical and biochemical barrier that restrains most bacteria, viruses, fungi and noxious substances from directly contacting the epithelial cell layer [20, 61, 62]. The potential damage caused by the translocation of germs into the mucosa and dissemination across the intestinal barrier is rewarded by their significant contribution to the host homeostasis. The microbiota existent in the intestinal tract is not only involved in the further digestion of the chyme, but also in many other complex processes such as the synthetisation of vitamins (mainly B and K), host metabolism, development of gut-associated lymphoid tissues and direct influence on host protection against opportunistic infections [63-74].

Notably, when the microbiota's composition or function gets disrupted a dysbiotic state is generated. In this scenario, the unbalanced gut microflora may disrupt the host-microbe homeostasis, which can have severe implications to the health of the host [75]. Recently, dysbiosis has been the

focus of innumerable scientific studies, and its correlation with the development of inflammatory bowel diseases (IBDs), such as Crohn's Disease (CD) and Ulcerative Colitis (UC) seems to be a relevant factor in the establishment and progression of these diseases (Figure 11) [76-81]. Additionally, quantitative and qualitative microbiological analysis of the intestinal luminal content of IBD patients revealed an increase in the levels of harmful pathogenic bacteria over the beneficial ones [82, 83].

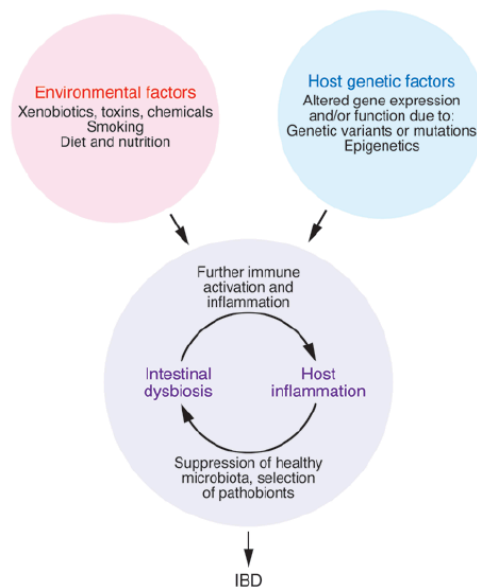


Figure 11. Dysbiosis and inflammatory bow diseases. (Extracted from *J Clin Invest.* 2014;124(10):4190–4196 [84], with permission of AMERICAN SOCIETY FOR CLINICAL INVESTIGATION in the format “Republish in a thesis/dissertation” via Copyright Clearance Center). IBDs are caused by a confluence of factors that perturb the balance between the environment, gut microbes, and host. IBDs are believed to arise from a “perfect storm” that involves the confluence of environmental and genetic factors tipping the balance between host immune and gut microbial factors and thus triggering disease in genetically susceptible individuals. IBDs are maintained by pathophysiological host processes and events that feed forward to promote a dysbiotic microbiota that can in turn worsen inflammation and create a vicious loop.

Although the precise risk rates for colorectal cancer development in patients with IBDs are still under debate, these patients present an apparent increased risk for malignant intestinal neoplasia, when compared with healthy individuals [85], therefore, a dysbiotic microflora might have a significant impact on intestinal tumorigenesis. The increase of harmful luminal bacteria can trigger mucosal inflammation, which in turn generates genotoxic stress on intestinal epithelial cells, which finally may give rise to cancer [86-89] (Figure 12).

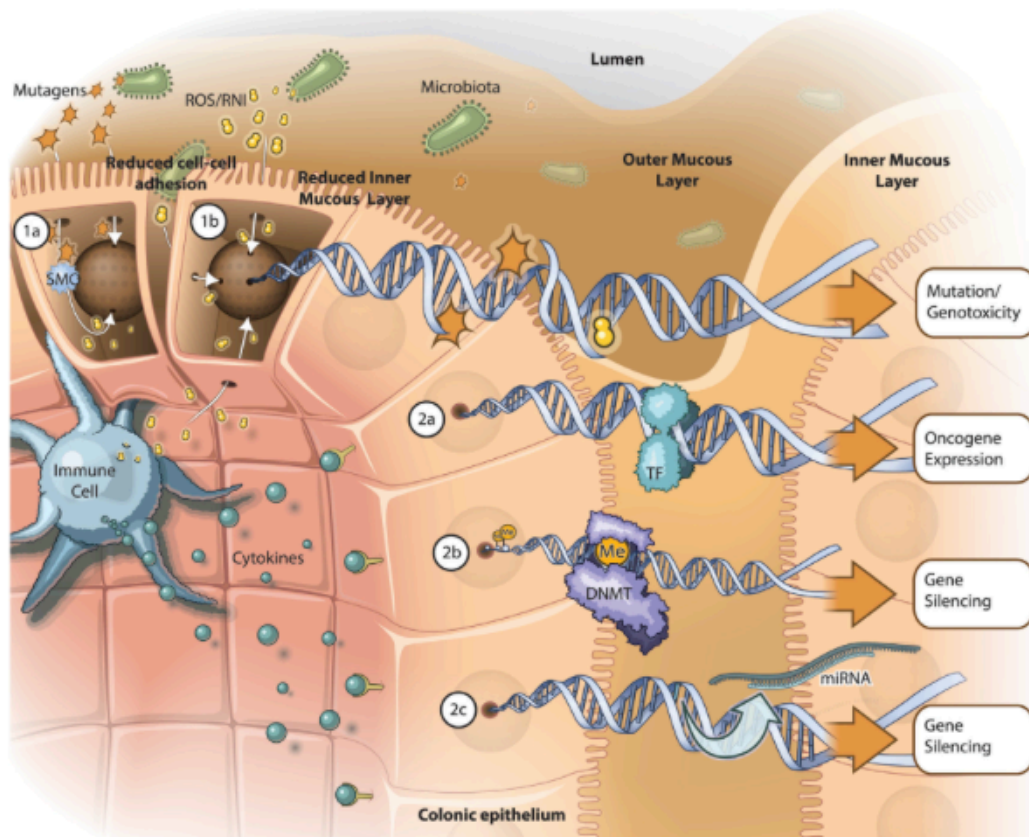


Figure 12. Inflammation-induced mechanisms of cancer development in the colon. (Extracted and adapted from *Molecular Cell* 54, April 24, 2014, [89]. with permission from Elsevier). (1a) Mutagens from food or excreted by the intestinal microbiota enter into the intestinal epithelial cell (IEC), causing DNA damage or inducing the production of reactive oxygen species (ROS). (1b) ROS and reactive nitrogen intermediates (RNI) species released by the microbiota or by immune cells are able to trigger genotoxicity in the IEC. (2a) The constant release of pro-inflammatory cytokines can deregulate the expression of genes involved in cell survival, proliferation, and angiogenesis, establishing a pro-tumorigenic intestinal environment. (2b) Pro-inflammatory cytokines, such as IL-6 and IL-1 β , might drive the expression of DNA methyltransferases (DNMT), resulting in the silence of tumor suppressor genes. (2c) The activation of other inflammatory signaling pathways can induce microRNA (miRNA) expression that can further silence the expression of tumor suppressor genes.

1.1.3 Immune cells

The symbiotic relationship between mammal hosts and microbes formed over millions of years of evolution is based on its benefits for both the host and the microbiome. Unfortunately, the microbiome has the ability to cause harm to the host by spreading from their gut luminal location to the intestinal submucosa and disseminating to other distant organs. In order to prevent and protect the host from such destructive threats, the intestinal tract is equipped with a highly complex and intrinsic immune system (Figure 13).

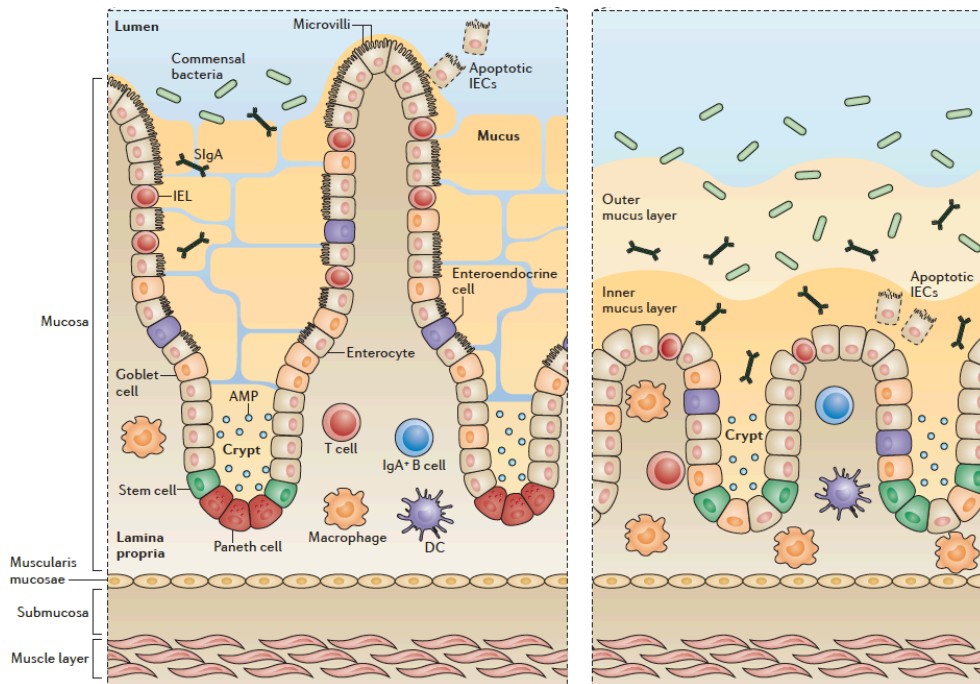


Figure 13. Anatomy of the intestinal mucosa and its immune apparatus. (Extracted and adapted by permission from Macmillan Publishers Ltd: *Nature Reviews Immunology* 14, 667–685 (2014)) [90]. Most of the intestinal immune cells are found in the *lamina propria*, with exception of the intraepithelial lymphocytes (IELs), which are located between intestinal epithelial cells. Reversely goblet and Paneth cells, IELs become less frequent progressing to the distal part of the small intestine, and are rare in the colon. Villi and Paneth cells are absent in the normal colon and the colonic crypts are smaller when compared with the crypts from the small intestine. DC, dendritic cell; SIgA, secretory immunoglobulin A.

Aside from all the already mentioned functions, the gastrointestinal tract is also considered a lymphoid organ, and the lymphoid tissue within it is referred to as the gut-associated lymphoid tissue. Directly under the intestinal epithelium – in the *lamina propria* – we find most of the intestinal immune cells and lymphoid structures that compose the gut-associated lymphoid tissue, such as lymphoid aggregates in the large intestine or Peyer's patches in the small intestine. [91, 92]. These both small and nodular lymphoid structures present on their surface a singular layer of follicle-associated epithelium (FAE), which hide underneath many different immune cell types [93, 94].

Strikingly, the FAE is not solely responsible for sheltering underneath innumerable immune cells, but also for harboring specialized antigen-sampling cells: Microfold or simply, M-cells. Microfold cells exhibit the extraordinary capability to sample intact intestinal luminal contents (transcytosis), such as soluble proteins, antigens, bacteria and viruses and directly present them to lymphocytes, dendritic cells and macrophages located in the *lamina propria* (Figure 14). Furthermore, germs opsonized by immunoglobulin A (IgA) can be abducted by microfold cells thanks to their IgA receptor expression,

redirecting them to immune cells [95-100].

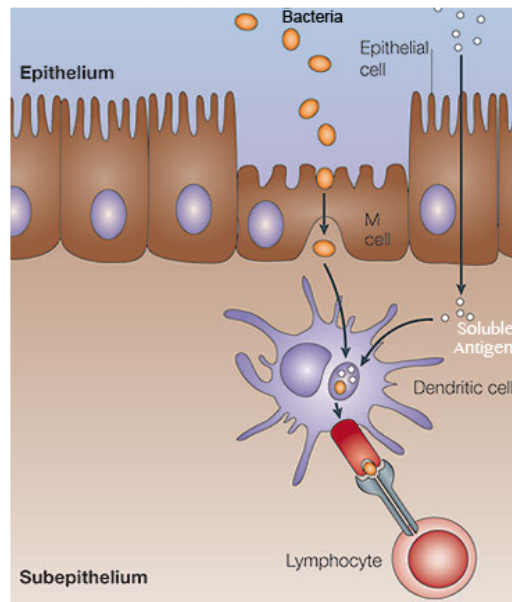


Figure 14. Diagram of an intestinal M cell. (Extracted and adapted by permission from Macmillan Publishers Ltd: *Nature Reviews Immunology* 5, 905-916 (December 2005) [101]). Particulate antigens are recognized by receptors at the surface of M cells and are presented to lymphocytes and macrophages. Soluble antigens, as well as small pathogens, can permeate the epithelium and be recognized by dendritic cells.

The extremely refined action of M cells in sampling the intestine is followed by a close interaction with immune cells residing in the *lamina propria*, such as macrophages and dendritic cells (DC). These both cell types make part of the innate immune system and can be considered the frontline defense against microbial infection. After activation, dendritic cells migrate to the mesenteric draining lymph nodes and further activate lymphocytes by presenting them with antigens captured directly, or given to them by M cells. This extremely coordinated process gives rise to the activation of our adaptive immunity and consecutively extra immune protection against pathogens [102-106].

Along with dendritic cells, macrophages are the most prevalent phagocytic cells in the intestine, and it is believed that the organ is the “largest reservoir” of these cells in the body [107, 108]. Different from dendritic cells, which are best known for being efficient antigen presenting cells (APCs), the macrophages exhibit extraordinary phagocytic capabilities to clear cellular debris, germs and foreign bodies (like pigments). Thus, their proper function is crucial for the gastrointestinal homeostasis [109, 110].

Unlike the cells of the innate immune system, which do not need previous activation (priming) to exert their immune functions, cells from the adaptive immune system require additional co-stimulation to generate proper effector responses. Notably, B and T lymphocytes are the main components of this system, and although they may need longer periods to undergo activation their responses against pathogens are extremely specific and continuous [111]. In the GI tract, most of the B and T lymphocytes are localized in lymphoid nodules, generally in a resting, naive state. Upon priming (generally by DCs), they undergo activation, proliferation and migrate to the sites of damage and infection to exert their effector functions, which in the case of the gut is usually the *lamina propria* [112]. Activated B cells will become plasma or memory B cells. The first will produce large amounts of immunoglobulins A and M and affinity antibodies against a specific antigen. The second, as its name describes will become a memory cell, providing fast antibody production in case of contact with an already known antigen [113].

Working in parallel with B lymphocytes to provide adaptive immunity another important cell population can be found: T lymphocytes. These cells, alike the B cells need co-stimulatory signals to acquire effector functions. They can be subdivided in CD8⁺ and CD4⁺ T cells. CD8⁺ T cells display robust cytotoxic capabilities towards infected, dysfunctional and transformed cells, being also known as a result of that as “T cytotoxic” cells. They exert their cytotoxicity through the release of cytolytic proteins, such as granzins and perforins or by the expression on their surfaces of FAS ligand. In both situations, the outcome will cause the apoptosis of the target cell [114]. Dissimilar, CD4⁺ T cells (also known as T helper or Th cells) are not recognized by their cytotoxic features, but by their ability to secrete regulatory and suppressive cytokines and chemokines. They can be characterized into at least four different subsets. In a simplistic overview, Th1 cells mainly produce interferon gamma (IFN γ), interleukin 2 (IL-2) and are directly involved in the defense against intracellular pathogens and eventually transformed cells; Th2 cells are mostly known for their production of IL-4 and IL-13, being involved in immune suppression, allergic reactions and in the resolution of parasitic infections. Th17 cells produce IL-17, IL-21, IL-22 and provide

protection against extracellular pathogens [115, 116]. Lastly, T regulatory cells (or Treg cells), express the transcription factor Foxp3 and produce large amounts of IL-10, which has a key role in the regulation of inflammatory signals being the major regulatory cell population in the GT tract of both humans and mice (Figure 15), [117, 118].

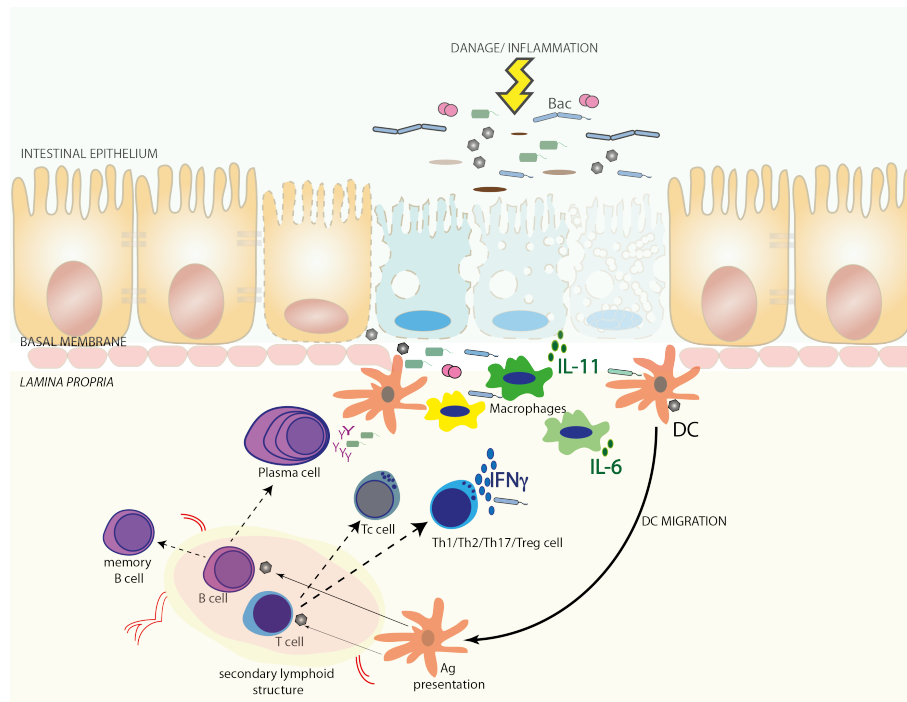


Figure 15. Adaptive immune system. The figure depicts cells from the adaptive immune system (T and B cells) becoming activated and exerting effector activities. Antigen presenting cells, like dendritic cells (DC), generally migrate to the secondary lymphoid structures activating resting, naïve B and T cells. Upon activation T and B cell differentiate into different subsets and migrate to the site of damage/ infection, mostly within the *lamina propria*.

1.2 The IL-4 Signaling Pathway

1.2.1 IL-4, IL-13, IL-4R α and Stat6

Maureen Howard and William E. Paul first described interleukin 4 (IL-4) in 1982, in "The Journal of Experimental Medicine". They identified a factor present in the supernatant of mouse thymoma cells that when applied on B cell cultures would lead to the sustained maintenance of the cultured B cells. They later called it "B cell growth factor" [119].

Since its discovery, the accurate functions that IL-4 can exert on cells are still not entirely known. The main reason for that is the abundant expression of IL-4 receptors in different tissues, and the evidence that different cell types exhibit distinct responses to IL-4 stimulation [120-122]. IL-4 and its receptor are believed to be the central components of the IL-4 pathway. However, other important molecules such as IL-13 (which has approximately 30% homology with IL-4 protein), and the signal transducer and activator of transcription 6 (STAT6) have already proven to be as much relevant and dynamic as IL-4 itself [123-126].

To date, IL-4 is still best known for being a Type 2 cytokine, produced by activated Th2 lymphocytes, but it is pertinent to mention that other immune cells like macrophages, γ/δ T cells, mast cells, natural killer T-cells, basophils, and eosinophils are also reported to produce IL-4 [127, 128]. Additionally to its effects on B cell differentiation, immunoglobulin production and survival, IL-4 (and in some instance IL-13) takes action on many other physiological processes. The most relevant and well-defined are: (i), inhibition of pro-inflammatory cytokine production in other immune cells [129]; (ii), upregulation of major histocompatibility complex class II on monocytes [130], (iii), wound healing, and (iv) resolution of parasitic infections [131, 132]. Nevertheless, perhaps the function that has attracted considerably more attention over the past years is the ability of IL-4 (and IL-13) to polarize macrophages in an alternative pathway, which clearly differ these cells from the IFN γ -mediated classical activation. Alternatively activated macrophages (AAM) assume a wound-healing/tissue repair phenotype, expressing large amounts of arginase, and anti-inflammatory molecules such as IL-4, IL-10, IL-13, Tumor Growth

Factor Beta (TGF- β) and Found in Inflammatory Zone 1 (FIZZ-1), between many others. AAM, contrarily to classically activated macrophages, lack major roles in type 1 response (Th1), such as killing intracellular pathogens (including fungi) and tumor resistance (Figure 16) [133, 134].

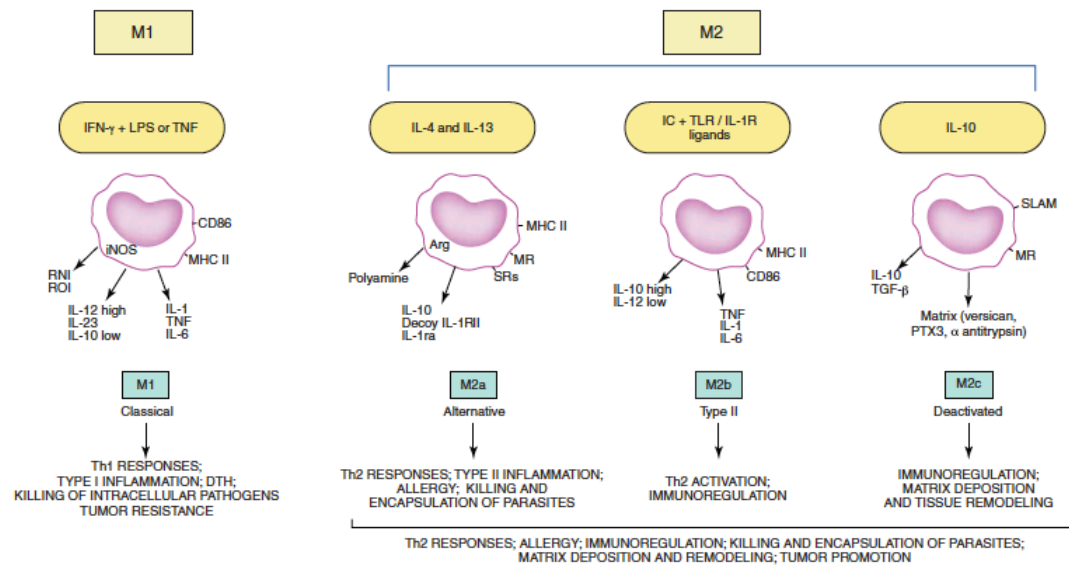


Figure 16. Classical versus alternative macrophage activation. (Diagram extracted from *F1000Prime Reports* 2014, 6:13 [134]). All copyrights reserved to Faculty of 1000 Limited. Mantovani and colleagues [135] proposed a M1-M2 macrophage model, in which M1 cells are polarized by IFN γ , lipopolysaccharide (LPS) or tumor necrosis factor alpha (TNF α); M2 cells were subdivided in three main groups accordingly its similarities and differences between IL-4 polarization (M2a), immune complexes and Toll-like receptor (TLR) ligands (M2b), and IL-10 and glucocorticoids (M2c).

As previously mentioned, the IL-4 signaling pathway mainly comprises the cytokine IL-4 and its receptors. IL-4 can signal through two different types of heterodimeric receptors: (i) type I receptor, formed by the IL-2R γ (also known by common gamma chain – “ γ c”) and IL-4R α , being this receptor conformation normally found in immune cells due to the expression pattern of γ c in cells of hematopoietic origin; (ii) type II receptor, formed by IL-4R α and IL-13R α 1, being not only found in immune cells but also in other cell types, such as epithelial cells and fibroblasts. Curiously, IL-4 is able to signal through both types of receptors (I and II), but IL-13 is restricted to receptor type II, or to its own receptor, IL13R α 2, whose role is still under debate due to its restricted signaling activity in limited conditions. Important to mention, IL-4 receptors do not present intrinsic kinase capabilities (Figure 17), [135-141].

The binding of IL-4 or IL-13 to their receptors initiates JAK-dependent tyrosine phosphorylation of IL-4R α and consequently of the downstream

transcription factor, Stat6. This action will lead to dimerization and translocation of Stat6 into the nucleus where it regulates the transcription of a number of IL-4-responsive genes [124, 142, 143]. IL-4 is considered to be the predominant cytokine to trigger STAT6 phosphorylation. Likewise, STAT6 is believed to be the IL-4 main transcriptional mediator.

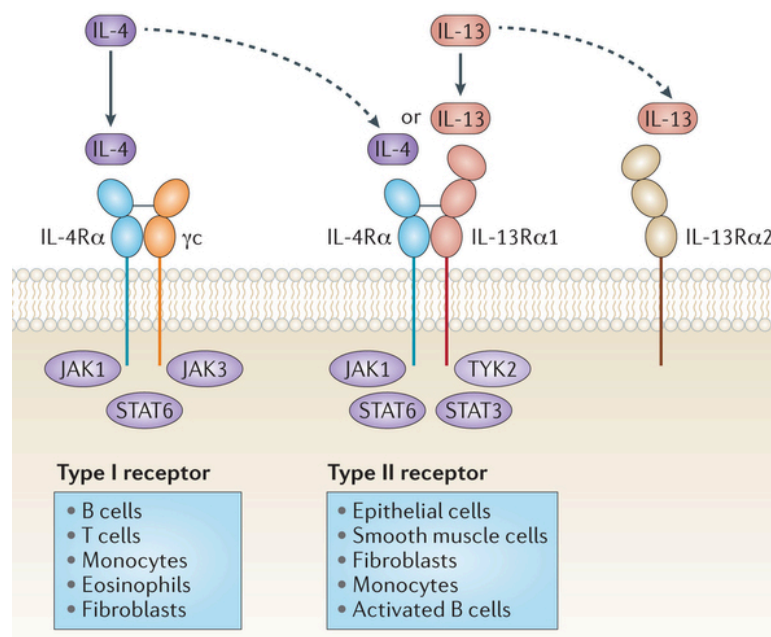


Figure 17. Receptor systems for IL-4 and IL-13. (Extracted and adapted by permission from Macmillan Publishers Ltd: *Nature Reviews Drug Discovery* 15, 35–50 (2016) [140]. The picture depicts the different IL-4 receptor conformations. The type I receptor, composed by IL-4Rα and the common cytokine receptor γ-chain (γc), only binds IL-4. The type II receptor complex, formed between IL-4Rα and IL-13Rα1, is the primary receptor for IL-13 but also binds IL-4. In addition, IL-13 will bind to a second receptor, IL-13Rα2.

Unlike most of the other members of the STAT family that recognize analogous DNA-binding sequences (STAT1, STAT3, STAT4, and STAT5) after nuclear translocation, STAT6 exhibits a distinct DNA-binding predisposition for palindromic sequences separated by four base pairs (bp) spacer (5'-TTCN4GAA-3', (N4 site)). Most relevant, binding to those sequences will activate a genetical program that can regulate in the target-cell differentiation, DNA replication and survival [144-148].

Significant progress has been achieved to understand the functions of IL-4 signaling mechanistically, but still little is known about STAT6 inducing gene expression in non-hematopoietic cells. To date, most of the performed studies have evaluated STAT6 functions exclusively in IL-4-driving conditions, without focusing on its direct relevance in epithelial cell homeostasis and

transformation. Regarding the intestinal tract, very limited data is available on its biological functions in the colonic epithelium, and the existing results on inflammation are conflicting depending on the model studied.

1.2.2 IL-4 signaling involvement in tumorigenesis

In addition to its well-established physiologic processes, IL-4 signaling has been demonstrated to be involved in a variety of pathological conditions, including cancer. IL-4 and IL-13 receptors were found overexpressed in different malignancies, such as brain, thyroid, breast, pancreas, lung, colon and bladder tumors [122, 149-158]. Moreover, the direct effects on tumor promotion of IL-4 and of IL-13 cytokines in the tumor microenvironment cells, such as tumor-associated macrophages (TAMs) and myeloid-derived suppressor cells (MDSC) have been already shown [159, 160].

Regarding colonic tumorigenesis, the contribution of IL-4 receptors in this process has been already investigated [151, 157]. Additionally, xenograft experiments have shown that colon cancer cells with constitutive STAT6 expression had significant growth advantages over STAT6-deficient cancer cells. Furthermore, mice bearing constitutive STAT6 expression had higher seric levels of IL-4, IL-5, and overexpression of CDK4 and CD44v6 in their tumor cells [161]. Then, these findings evidence that the expression of different components of the IL-4 signaling axis in colon cancer can create a scenario favoring tumor growth, survival and dissemination (Figure 18).

The direct involvement of IL-4R α in colonic tumorigenesis in a mouse model was accessed by Felicitas L. Koller and colleagues in 2010 [157]. Taking advantage of a colitis-associated tumor model, the investigators subjected WT mice or mice with global deletion of IL-4R α (IL-4R $\alpha^{\text{del/del}}$) to the pro-carcinogen azoxymethane (AOM) and two cycles of dextran sodium sulphate (DSS). Interestingly, IL-4R $\alpha^{\text{del/del}}$ mice exhibited significantly fewer and smaller tumors when compared with WT mice. Reduced tumorigenesis in these mice was associated with diminished proliferation and enhanced apoptosis of the tumor cells. The authors further showed that administration of a soluble chimeric receptor protein, which impairs IL-4 cytokine binding to IL-

4R α provided similar results on xenograft cecal implants of tumor cells, suggesting that IL-4R α could be a potential therapeutic target in colon cancer.

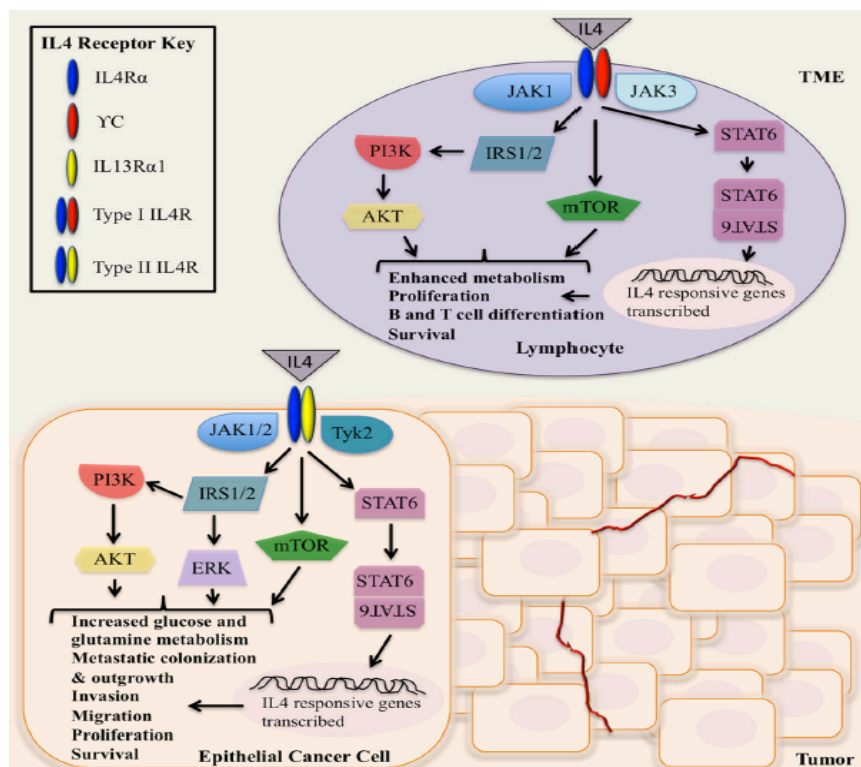


Figure 18. IL-4 signaling in epithelial cancer cells and hematopoietic cells of the tumor microenvironment (TME). (Extracted and adapted from *Clin Exp Metastasis* (2015) 32 (8): 847–856) [162], with permission of Springer. IL-4 binding to type I receptor results in receptor tyrosine residue phosphorylation and activation of Janus Kinases proteins (JAKs), which further causes STAT6 phosphorylation or activation of the IRS/PI3K/AKT pathway. Activation of both pathways in immune cells generally results in the expression of IL-4 responsive genes related with cell differentiation, proliferation and survival (top, “TME”). Additionally, in transformed non-hematopoietic cells (bottom, “Tumor”), such as epithelial cells, the IL-4 receptor type II can be found. In this scenario, IL-4 binding will not only induce cell growth and survival, but also might promote uncontrolled cell proliferation, resistance to apoptosis, cell invasion and metastatization.

Additionally, IL-4 signaling seems necessary for colon cancer stem cell (CSC) survival and chemotherapy resistance to apoptosis. Using human colorectal tumor spheroids, Matilde Todaro and colleagues showed that CD133 positive colon CSCs have an autocrine production of IL-4, which provides these cells with increased resistance to apoptosis, and protect them from chemotherapy-induced death. Furthermore, the authors demonstrated that systemic treatment with IL-4R α antagonist or anti-IL-4 neutralizing antibody potentiates chemotherapy efficiency in subcutaneous xenograft tumors in nude mice, leading to a significant reduction in tumor size [163]. Thus, although the participation of IL-4 signaling in colorectal tumorigenesis has been demonstrated, the exact underlying mechanisms that determine how IL-4R α and STAT6 dictate their biological responses and how these

molecules are regulated in colonic malignant transformation still require further detailed investigation.

1.3 Colonic Carcinogenesis

1.3.1 Colonic carcinogenesis

Colorectal cancer (CRC) is an important cause of mortality worldwide. It is the third most common incident malignancy in the western societies. When epidemiologically studied, Europe and Oceania share the highest rates while South America, Africa and the Caribbean the lowest [164]. Approximately 95% of malignant tumors are represented by adenocarcinomas and carcinomas, followed by a small fraction of lymphomas, leiomyosarcomas, carcinoids, histiocytomas, fibrous histiocytomas, hemangiosarcomas and melanomas [165]. Smoking, unbalanced or high-fat diet and sedentary lifestyle are all well-acknowledged risk factors for the development of the disease [166-168]. Colonic carcinogenesis is commonly classified as (i) sporadic (or non-hereditary), generally caused by somatic mutations in the WNT signaling, and being the vast majority of the cases (Figure 19a). Sporadic cases can be further linked to the presence or not of chronic colonic inflammation (so-called colitis-associated cancer - CAC); (ii) hereditary or familial cases, which are caused by inherited mutations, such as the ones found in hereditary non-polyposis colorectal cancer (HNPCC) syndrome, familial adenomatous polyposis (FAP) and Peutz-Jeghers syndrome [169, 170].

As previously mentioned, inflammatory bowel diseases (IBD) are another predisposing factor for colorectal cancer development as long-lasting inflammation increases the overall risk of developing colorectal carcinoma to approximately 18 % after 30 years of the setup of the condition [171]. The two most common entities are ulcerative colitis and Crohn's disease. Both have unknown etiology and are defined by persistent and recurrent inflammation of the gastrointestinal tract. Ulcerative colitis generally starts from the rectum and spreads across the whole mucosa till the proximal colon, while in Crohn's disease the transmural inflammation is observed predominantly in the ileum and proximal colon, with occasional involvement of other parts of the gastrointestinal tract, such as anus and mouth [172, 173]. A conception that a genetical susceptibility exists in patients afflicted by IBD is emphasized by the

knowledge that IBD-development is significantly increased in people who have a first-degree relative affected by these conditions [174, 175], (Figure 19b). Interestingly, although these patients exhibit an increased risk of CRC development, they just represent approximately 1 % of the new cancer cases, presumably, due to their frequent medical monitoring [175].

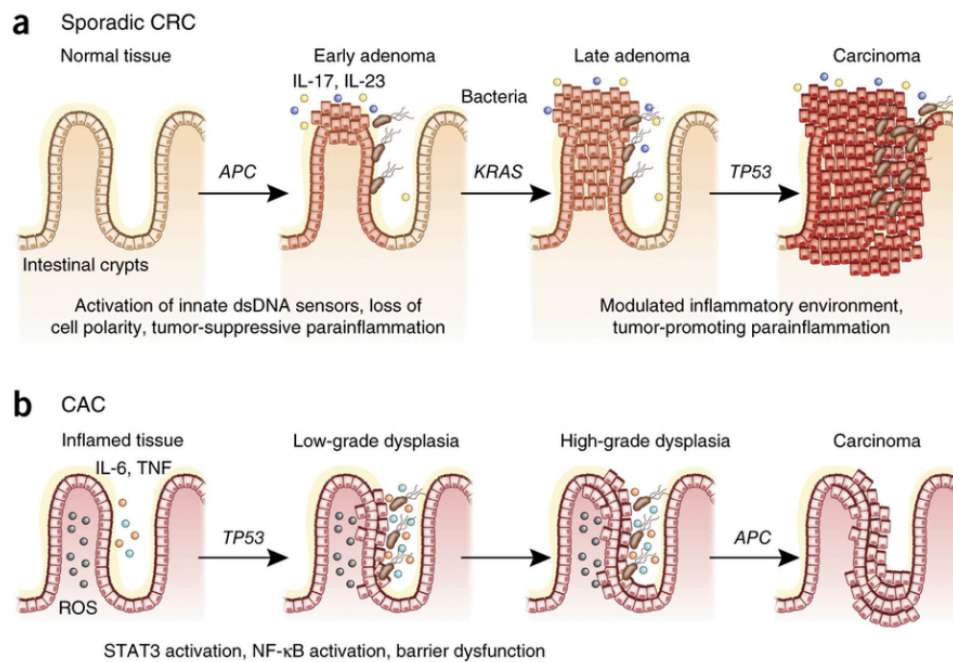


Figure 19. Inflammatory basis of sporadic CRC and CAC. (Extracted and adapted by permission from Macmillan Publishers Ltd: *Nature Immunology* 17, 230–240 (2016) [170]). (a) In sporadic CRC, the mutations in the Wnt signaling, commonly in the APC gene, along with loss of cellular polarity and loosening of tight junctions, promotes the translocation of the microbiota into the epithelium leading to the secretion pro-inflammatory cytokines such as IL-23 and IL-17 by immune cells, creating a pro-tumorigenic microenvironment. APC mutations are usually followed by KRAS and p53 mutations inducing the progression of the initial benign adenoma lesions to carcinoma. (b) In CAC, the chronic inflammation might induce mutation in tumor suppressor genes, such as p53. Additionally, constant activation of the NF-κB signaling pathway increases inflammation. As in the sporadic CRC situation, barrier defects will lead to microbiota translocation into the intestinal epithelium, generating genotoxic stress on the IECs, which can finally lead to mutations on APC and progression to carcinomas.

1.3.2 Molecular events of colonic carcinogenesis

Independent of its heredity or not, there are well-described molecular pathways leading to the development of colorectal cancer. The basic principle triggering colorectal carcinogenesis is generally a product of genomic instability, which leads to the inactivation of essential tumor suppressor genes, such as Adenomatous Polyposis Coli (*APC*). Inactivation of *APC* is found in approximately 80% of intestinal adenomas and carcinomas, being considered to be an early event in colorectal malignancies [176]. *APC* is a key tumor suppressor gene in CRC due to its exceptional ability to maintain tissue

homeostasis through the interaction with many important proteins, such as AXIN, RAC1, and β -CATENIN. APC activity controls the WNT signaling pathway by negatively regulating β -CATENIN, preventing its stabilization and constant nuclear translocation, which is known to have crucial effects on cell proliferation and induce oncogenic activity. Additionally, APC is able to bind to microtubules, promoting their stabilization and consequently a normal cellular architecture [177-180]. After APC inactivation, *KRAS* and *TP53* gene mutations are common successive events in the transformation of the intestinal epithelium (already dysplastic) to neoplasia. Moreover, both are products of genetical instability and are highly prevalent in colorectal tumors [181, 182], (Figure 20).

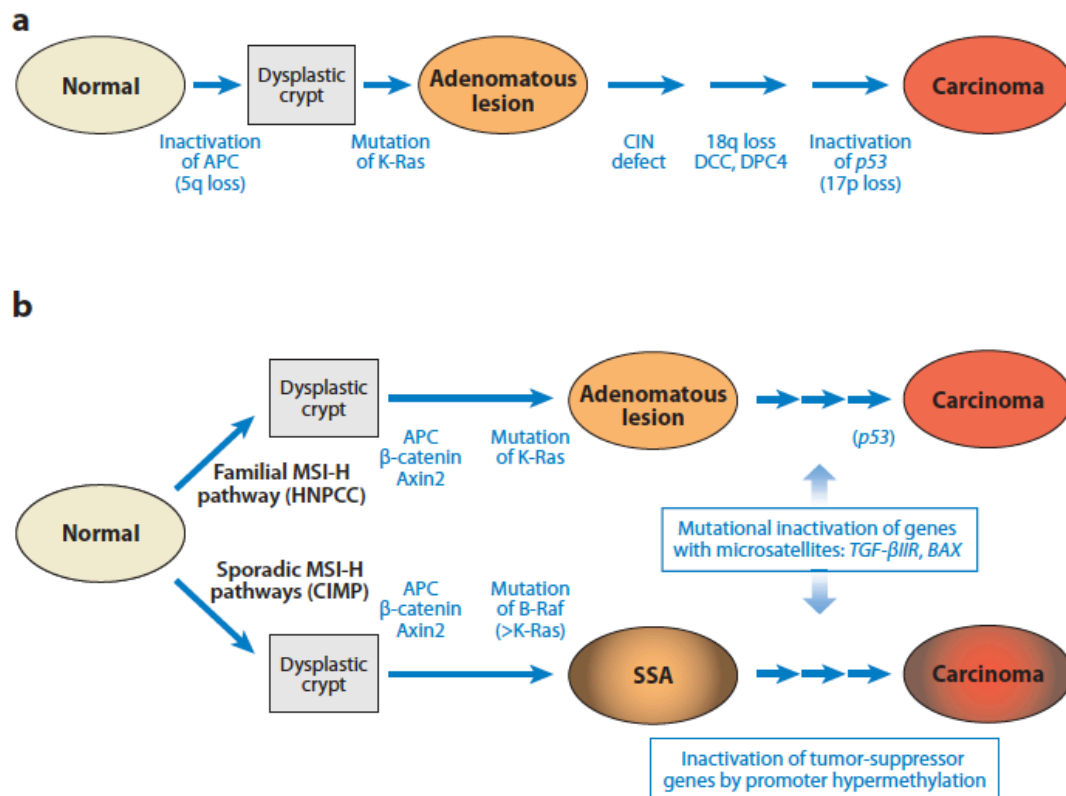


Figure 20. Genetic model of colorectal cancer (CRC). (Extracted from *Annu. Rev. Pathol. Mech. Dis.* 2011. 6:479–507 [176]. Copyright 2011 by Annual Reviews. All rights reserved) (a) Sporadic cases of CRC are believed to develop from benign adenomas driven by genetical events over the past of many years. The initial inactivation of APC is followed by additional somatic mutations in the *KRAS* gene, and later by inactivation of the tumor suppressor gene *P53* (b) In familial cases of CRC, patients already carry inherited somatic mutations, which can lead to the formation of adenomas. Additional acquired mutations, for example in mismatch repair genes generate a second hit to further malignant transformation. Commonly, in both cases (sporadic and familial) the microsatellite instability-drove tumors exhibit inactivation of *BAX* and *TGF β RII*.

Aberrant function or silencing of DNA mismatch repair (MMR) genes is another triggering-pathway to colorectal tumorigenesis. The MMR system is

composed of many different proteins (e.g. MSH2, MSH3, MHL1, PMS2), which detect and repair mismatched nucleotides in the genome [175, 183]. Malfunction of the MMR system might induce the formation of mutations (usually insertions and deletions) in microsatellite regions, causing microsatellite instability (MSI) [184, 185]. Thus, MSI can lead to frame shift mutations of tumor suppressor genes. Moreover, MSI is a regular feature of CRC found in approximately 15% of the sporadic cases of CRC and more than 95% in the cases of familial CRC [186]. Some examples of genes with mutations emerging in their microsatellite regions are *RAD50*, *BAX*, *TGF β RII*, *IGFRII* and *PTEN* [187].

An additional triggering-pathway in CRC is the hypermethylation of CpG islands. CpG islands are genomic regions with a high frequency of CpG sites, which are found throughout the genome, and are commonly methylated [188]. When these sites are located in the promoter regions of tumor suppressor genes, the methylation of CpG islands can lead to their silencing and complete loss of gene expression [189]. CRCs expressing these characteristics are classified as “CpG island methylator phenotype” or CIMP [190, 191]. Paradoxically, when methylation occurs outside gene promoter regions (gene body methylation), it might induce gene transcriptional activation [192, 193]. *CDKN2A* (P16), *CXCLC12* and *MLH1* are examples of genes found to be hypermethylated in CRC [194].

Finally, a common phenomenon through which the mechanisms mentioned above might be initiated and further supported is chronic intestinal inflammation [195-197]. Chronic inflammation has the ability to promote colorectal tumorigenesis without generating direct early mutations. A perfect example of this feature is the fact that activation of inflammatory pathways may trigger β -catenin nuclear translocation and accumulation independently *APC* mutations [196, 198-200]. This capacity to initiate colorectal carcinogenesis is mainly attributed to the expression of two critical pro-inflammatory proteins (i) signal transducer and activator of transcription 3 (STAT3) and (ii) nuclear factor- κ B (NF- κ B) [201-205].

STAT3 belongs to a group of transcription factors (STAT family, STAT1, STAT2, STAT4, STAT5a/b and STAT6), which intermediate cellular signals

usually generated at the cell cytoplasmic membrane to the nucleus. Therefore, its activation can be induced by a plethora of cytokines and growth factors, such as IL-6, IL-10, IL-11, leukemia inhibitory factor (LIF), platelet-derived growth factor (PDGF) and epidermal growth factor (EGF), to cite a few [203, 206-208]. The binding of STAT3-ligands to their cell-surface receptors can trigger STAT3 phosphorylation by Janus kinases and consecutively its dimerization. Dimerized, STAT3 translocates into the nucleus of the cell, where can initiate the transcription of innumerable STAT3-responsive genes – many of them involved in cellular proliferation and survival [175, 209]. Importantly, as most transformed cells (and also the tumor microenvironment) exhibit persistent activation of autocrine and paracrine signals, STAT3 may become constitutively active, further supporting colorectal tumorigenesis [208, 210-212].

STAT3 and NF- κ B do not fit in the typical oncogene definition as their activation mostly relies on paracrine stimuli. However, upon activation both molecules can govern the expression of relevant genes, becoming important mediators to tumorigenesis [202, 210, 213-215]. Regarding NF- κ B, the five-member of this transcription factor family are *RelA* (P65), *RelB*, *cRel*, P105/P50 (*NF κ B1*), and P100/P52 (*NF κ B2*). When inactive, NF- κ B, family members are cytoplasmic found in dimeric conformation (homo/heterodimers) linked to a member of the I κ B inhibitory family. NF- κ B activation happens when paracrine or autocrine signals induce the phosphorylation of the I κ B element by I κ B kinase (I κ K), which leads to I κ B degradation and consequently release of NF- κ B dimers. Free, nuclear translocated NF- κ B will bind to promoter regions, and as STAT3, start the transcription of genes implicated in cell survival, proliferation, and differentiation [216-218]. Similarly to STAT3, NF- κ B activation is triggered by cytokines and growth factors, such as IL-1 β , TNF α , and EGF. Moreover, constitutive NF- κ B activation is observed in many tumor entities, including CRC [219-223], in which NF- κ B ablation reduced tumor incidence [201].

1.3.3 Mouse models of colonic carcinogenesis

The possibility to evaluate colorectal tumorigenesis through the continued accumulation of mutations in vivo is only possible due to the existence of animal models, in particularly mouse models. Mouse models are powerful tools to recapitulate and study the many different aspects involved in colitis-associated colon cancer. Nevertheless, due to CRC heterogeneity, the available mouse models do not recreate the process of malignant transformation in its totality, being necessary to use different models to fully understand the mechanisms involved in CRC development and progression [224, 225].

As a result of this heterogeneity, several different genetically engineered mice (GEM) and scientific animal protocols have been developed to evaluate the genetical, morphological and clinical aspects of CRC (Table 1). Basically, these different mouse models can be divided into three categories: (i) genetically engineered mice, which exhibit contrasting tumorigenic features and allow the study of intestinal tumorigenesis from its benign initiation to its malignant transformation (e.g. *MMR* system-deficient mice, *APC*^{Min/Δ} mice, *IL-10* and *MUC2* deficient mice, β -CATENIN-transgenic mice); (ii) xenograft mouse models, which are mainly useful to evaluate tumor growth, metastasis and the efficiency of new therapeutic compounds, but as generally make use of immune-deficient animals leave the contribution of the immune system to tumorigenesis or therapy response unaddressed; (iii) chemically induced mouse models, which use of pro- and carcinogenic drugs to induce cellular transformation [226, 227]

Regarding chemically induced models, one of the most used mutagenic drugs is azoxymethane (AOM). AOM is a pro-carcinogen that when injected intraperitoneally in rodents is fast metabolized to methylazoxymethanol (MAM) leading to the formation of O⁶-methylguanine and consequently DNA damage. [228, 229]. When combined with the administration of dextran sodium sulphate (DSS) in the drinking water a synergism between these two drugs is observed inducing the rapid growth of intestinal tumors (approximately 12 weeks) in mice [226, 230]. DSS is toxic to

the IECs, causing their death and consecutively the destruction of the intestinal epithelial layer. The direct contact of the microbiota and dietary products with the mucosa and *lamina propria* result in strong immune cell activation and inflammatory response, with the release of cytokines and massive generation of genotoxic stress on IEC. These effects can further promote intestinal transformation and CRC [88, 89, 231]. AOM/DSS-induced tumors display similar histopathological and molecular characteristics as observed in human intestinal neoplasms. They usually express β -CATENIN nuclear accumulation, *Kras* mutations and in a lower frequency *APC* mutations [232-234]. Mutations in *P53* are rarely observed, and the tendency to distant metastatization is very low or absent. [235, 236].

Table 1. Most Common Mouse Models of CRC

| Human disease | Mouse model | Advantages and disadvantages |
|------------------------------|--|--|
| FAP | <i>Apc</i> mutants or β -catenin transgenic mice | Mimic APC mutation in human. However, most tumors located in the small intestine. Tumors are not metastatic. |
| HNPCC | <i>Msh2</i> ^{-/-} , <i>Msh6</i> ^{-/-} , and <i>Mlh1</i> ^{-/-} mice | Mimic MMR deficiency in human. However, MMR-deficient mice develop tumors in other organs. The colonic tumors are not metastatic. |
| Inflammation-related | DSS-induced mouse models | Easy and reproducible. Tumor incidence is low. AOM/DSS combination produces more tumors at earlier time point. |
| | <i>IL10</i> ^{-/-} , <i>IL2</i> ^{-/-} , T-cell receptor ^{-/-} / <i>p53</i> ^{-/-} or <i>TGF-1</i> ^{-/-} / <i>Rag-2</i> ^{-/-} | Tumor incidence is low. Requires the involvement of enteric microflora. |
| | <i>Muc2</i> ^{-/-} | High incidence of colon and rectal tumors. Early development of rectal prolapse reduces life span. |
| Sporadic colorectal cancer | Carcinogen-induced mouse model | Easy and reproducible. DMH/AOM/MAM have relatively high colorectal tumor incidence. IQ, PhIP, DMAB, MNNG or MNU target multiple organs and exhibit a low tumor incidence. The tumors are not metastatic. |
| | Cre adenovirus-mediated <i>Apc</i> inactivation | Require surgical procedures. Results are reproducible. Develop metastasis in ~20% of animals. |
| Metastatic colorectal cancer | Orthotopic inoculation model | Mimics colon tumor invasion, vascular spread, and metastasis to distal organ. Metastasis rates depend on cell lines and rodent strains. |
| | Intrasplenic inoculation model | Reproducible and mimics vascular spread of colorectal cancer. Metastasis rates depend on cell lines and rodent strains. |
| | Intraportal inoculation model | Mimics vascular spread of colorectal cancer metastasis and theoretically limits tumor growth predominantly to the liver. Metastasis rates depend on cell lines and rodent strains. |
| | Intrahepatic inoculation model | Model is reproducible but does not mimic the generally accepted hypothesis of hematogenous spread of colorectal cancer. |

(Extracted from *J Carcinog.* 2011; 10: 9 [226]. All copyrights reserved to *Journal of Carcinogenesis*)

FAP, familial adenomatous polyposis; HNPCC, hereditary nonpolyposis colorectal cancer; MMR, mismatch repair; DSS, dextran sulfate sodium; MAM, methylazoxymethanol; DMH, 1,2-dimethylhydrazine; AOM, azoxymethane; PhIP, 2-amino-1-methyl-6-phenylimidazo[4,5-b]pyridine; IQ, 2-amino-3-methylimidazo [4,5-f] quinoline; DMAB, 3,2'-dimethyl-4-aminobiphenyl; MNU, methylnitrosourea; MNNG, N-methyl-N'-nitro-N-nitrosoguanidine.

2 AIM

Interleukin 4 signaling has been involved in crucial homeostatic and pathologic events, including tissue repair, allergy and cancer. It is well known for exerting resistance to apoptosis and to promote immune suppression, which favors tumor development. Nevertheless, the effects of IL-4 signaling cascade on colorectal carcinogenesis are still poorly understood and need further characterization. The aim of this study was to evaluate the cell type specific contribution of IL-4 signaling axis components IL-4R α and STAT6 to colorectal carcinogenesis using mouse models of colitis-associated tumorigenesis to elucidate the molecular mechanisms governing this process.

3 MATERIAL AND METHODS

3.1 Materials

3.1.1 Chemicals, reagents and kits

Chemicals, reagents and kits used are listed in table 3.1.

Table 3.1 List of Chemicals, Reagents and Kits

| Chemical/Reagent/Kit | Company |
|--|------------------------------|
| Acrilamide | Merck |
| Ammonium Persulfate | Sigma |
| Antigen Unmasking Solution | Vector Laboratories |
| Avidin/Biotin Blocking Kit | Vector Laboratories |
| Ciprobay 500mg | Bayer |
| Dextran Sulfate Sodium Salt (36.000-50.000 M.Wt) | MP Biomedicals |
| dNTP mix | Carl Roth |
| DTT | Invitrogen |
| Ethanol 99.8% purity | Carl Roth |
| LPS | Sigma |
| Methanol | Carl Roth |
| Oligo (dT) primer | Invitrogen |
| Paraformaldehyde 16% | Electron Microscopy Sciences |
| PBS 10X | Invitrogen |
| Poly I:C | Sigma |
| PVDF membrane | Millipore |
| QIAshredder Kit | Qiagen |
| Recombinant mouse IL-4 | PeptoTech |
| RNaseOUT | Invitrogen |
| RNeasy Mini Kit | Qiagen |
| SDS Ultra Pure | Sigma |
| SuperSignal West Femto Substrate | Thermo Scientific |
| SuperSignal West Pico Substrate | Thermo Scientific |
| TEMED | Sigma |
| Golgi Plug | BD |
| Phorbol 12-myristate 13-acetate (PMA) | Sigma |
| Ionomycin | Sigma |
| RPMI medium | Invitrogen |
| Trypan Blue | Sigma |
| FBS | Gibco |
| β -mercaptoethanol | Sigma |

3.1.2 Oligonucleotides

The following oligonucleotides were used for Quantitative Real Time PCR.

Table 3.2 Quantitative Real Time PCR Primer List

| Gene | Foward Primer | Reverse Primer |
|--------------------------------|--------------------------|-----------------------------|
| <i>Bax</i> | AAACTGGTGCTCAAGGCCCT | AGCAGCCGCTCACGGAG |
| <i>Cox-2</i> | CAGCCAGGCAGCAAATCCT | CTTATACTGGTCAAATCCTGTGCTCA |
| <i>Cyclophilin</i> | ATGGTCAACCCACCGTGT | TTCTGCTGTCTTTGGAACTTTGTCT |
| <i>Il-1β</i> | AGCAGGATGGAGAATTACAGGAAC | TGTGGCCTGCTTGGGC |
| <i>Il-10</i> | GGTTGCCAAGCCTTATCGGA | ACCTGCTCCACTGCCTTGCT |
| <i>Il-11</i> | CTGCACAGAGAGAGACAAATTCC | GAAGCTGCAAAGATCCCAATG |
| <i>Il-6</i> | ATGGTACTCCAGAAGACCAGAGGA | GATGAACAACGATGATGCATTG |
| <i>Kc (Cxcl-1)</i> | GCCAATGAGCTGCGCTGT | CCTCAAGCTCTGGATGTTCTTG |
| <i>Mannose receptor</i> | TTGGTGGCAATTCACGAGAG | GGGAAGGGTCAGTCTGTGTTTG |
| <i>Mcp-1</i> | CAGCCAGATGCAGTTAACGC | AGCCTACTATTGGGATCATCTTG |
| <i>Mdm2</i> | AATCCTCCCCTTCCATCACACT | GATTTCACCTTTATCTTTCCCCTTATC |
| <i>Mgmt</i> | CGTGCACTAGGAGGAGCAATG | GAACCAACCTGTGGCAGG |
| <i>Mip-2</i> | ATCCAGAGCTTGAGTGTGACGC | AAGGCAAACCTTTTGACCGCC |
| <i>Noxa</i> | CTCCAGGAAGGAAGTTCCG | CGAGCGTTTCTCCTATCACATC |
| <i>p21</i> | ATTCAGAGCCACAGGCACCAT | TCTCCGTGACGAAGTCAAAGTT |
| <i>Puma</i> | ACGACCTCAACGCGCAGT | GTGAGGGTCGGTGTGCATG |
| <i>TNF-α</i> | ACTCCAGGCGGTGCCTATG | GAGCGTGGTGGCCCT |

The following oligonucleotides were used for mice genotyping.

Table 3.2.1 Oligonucleotides Used for Genotyping

| Gene | Forward Primer | Reverse Primer |
|--|---------------------------|----------------------|
| IL-4Rα Global Deletion Mice | | |
| Common | CAGGGAACAGCCCAGAAAAG | |
| WT allele | TGTGGGCTCAGAGTGACCAT | |
| Mutant | CCAGACTGCCTTGGGAAAAG | |
| IL-4R Floxed Mice | | |
| WT allele | CCCTTCCTGGCCCTGAATTT | GTTTCCTCCTACCGCTGATT |
| knockout allele | GGCTGCTGACCTGGAATAACC | |
| Stat6 mice | | |
| Mutant | AATCCATCTTGTTCAATGGCCGATC | |
| WT allele | AAGTGGGTCCCCTTCACTCT | |
| Common | ACTCCGAAAGCCTCATCTT | |

Villin-Cre**Recombinase** ACCTGAAGATGTTTCGCGATTATCT ACCGTCAGTACGTGAGATATCTT**3.1.3 Antibodies**

The antibodies used are listed in table 3.3.

Table 3.3 Antibody List

| Antibody | Company | Reference | Condition |
|------------------------|-----------------|------------------|------------------|
| BCL-2 | BD Biosciences | 610539 | WB 1:1000 |
| | Santa Cruz | | |
| BAD | Biotec | Sc-8044 | WB 1:500 |
| BCL-XL | BD Biosciences | 556499 | WB 1:800 |
| BrdU | Serotec | MCA2060 | IHC 1:400 |
| Cleaved CASPASE-3 | Cell Signaling | #9661 | ICH 1:400 |
| | Santa Cruz | | |
| CYCLIN B1 | Biotec. | Sc-752 | WB 1:500 |
| CYCLIN D2 | BD Biosciences | 554200 | WB 1:500 |
| E-CADHERIN | BD Biosciences | 610182 | WB 1:2000 |
| phospho-P53 | Abnova | PAB12640 | IHC 1:500 |
| P53 | Novocastra | NCL-p53-CM5p | IHC 1:500 |
| phospho-ERK | Cell Signaling | #9101 | WB 1:1000 |
| phospho-H2AX | Cell Signaling | #2577 | IHC 1:1000 |
| phospho- HISTONE H3 | Cell Signalling | #9701 | IHC 1:200 |
| phospho-STAT3 Y705 | Cell Signaling | #9131 | IHC 1:200 |
| phospho-STAT3 Y705 | Cell Signaling | #9131 | WB 1:1000 |
| phospho-STAT6 | Abcam | Ab54461 | WB 1:800 |
| SOCS-3 | Abcam | Ab16030 | WB 1:1000 |
| t-STAT3 | BD Biosciences | 610190 | WB 1:1000 |
| | Santa Cruz | | |
| t-STAT6 | Biotec. | Sc-981 | WB 1:500 |
| t-ERK | Cell Signaling | #9102 | WB 1:1000 |
| VIMENTIN | Abcam | Ab92547 | WB 1:1000 |
| β-ACTIN | Sigma | A4700 | WB 1:5000 |

3.2 Cell Culture-Based Methods**3.2.1 Extraction and stimulation of mouse bone marrow derived macrophages (BMDM)**

Mice were sacrificed and the femur and tibia were isolated. Bone marrow cells were flushed out with sterile 1X PBS using a 25 G needle. Afterwards, cells were homogenized by pipetting, filtered through a 70 μ m mash and centrifuged at 500 rcf for 10 minutes (4°C). Finally, cells were resuspended in RPMI medium (with glutamine) supplemented with 10% FBS, 1% penicillin/streptomycin, 10% L929 cells supernatant, plated into 10 cm Petri dishes (day one) and kept in humidified cell incubator at 37°C, 5% CO₂. On day four medium was exchanged and cells were allowed to differentiate till day seven.

To stimulate, approximately 2×10^6 BMDM were plated per well into 6-well uncoated-plates in 1ml of serum-free RPMI supplemented with 1% penicillin/streptomycin. The following compounds were used at time points of 6 and 24 hours (table 3.4):

Table 3.4 Compounds Used for Stimulation

| Compound | Concentration |
|-------------------------------|--------------------|
| Recombinant mouse IL-4 | 10 ng/ml |
| Recombinant mouse IFNg | 5 ng/ml or 100U/ml |
| LPS | 100 ng/ml |
| Poly I:C | 100 ng/ml |
| H ₂ O ₂ | 100 μ M/ml |

3.2.2 Extraction and stimulation of mouse peritoneal macrophages

To obtain peritoneal macrophages each mouse was intraperitoneally injected using a 25 G needle with 3 ml of 3% thioglycolate medium. After three days mice were sacrificed, disinfected with 70% ethanol and eight ml of ice-cold sterile 1X PBS injected IP with a 27 G needle. To withdraw any attached macrophage into the PBS a gently abdominal massage was performed for one minute. Using forceps and scissors the skin was cut and pulled off, exposing the peritoneal wall. Carefully, a 10 ml syringe attached to a 21 G needle was inserted and all intra abdominal fluid was aspirated. The cell suspension was passed through a 40 μ m mash, centrifuged at 200 rcf for 10 minutes (4°C), resuspended with RPMI medium (with glutamine) supplemented with 10% FBS and 1% penicillin/streptomycin. Approximately

2×10^6 cells were plated per well into 6-well uncoated-plates and incubated over night in humidified cell incubator at 37°C, 5% CO₂ for attachment.

To stimulate, cells were brought to serum-free RPMI supplemented with 1% penicillin/streptomycin and the same stimulation conditions of section 2.2.1 was applied.

3.2.3 Intestinal epithelial cell isolation

To extract intestinal epithelial cells (IEC), first the intestine segment was cleaned from feces with ice-cold 1X PBS and cut-open longitudinally. Next, the intestine was cut in small pieces and incubated in 10 ml of pre-warmed HBSS medium supplemented with 5 mM EDTA (Roth) and 2mM DTT (Sigma). Samples were gently shaking (80 rpm) for 10 minutes at 37°C. After, the 50 ml conic tube containing the tissue was vortexed for 30 seconds and put to rest on ice for more 30 seconds to allow the *lamina propria* to precipitate whilst IEC remained in the supernatant. The supernatant was carefully transferred to a new 50 ml conic tube passing through a 70 µm mash and further centrifuged for 5 minutes at 500G at 4°C. The obtained pellet was resuspended with 3 ml of ice-cold 1X PBS and divided in 2 to 3 1.5 ml eppendorf tubes. These were further centrifuged for 5 minutes at 2000 rpm at 4°C. The clean washouts were discarded and the pelleted IEC were immediately frozen in liquid nitrogen. Finally, samples were stored at -80°C until use.

3.2.4 Intestinal fibroblast isolation

The intestinal fibroblast isolation was performed as described in [237], with minor modifications. Basically, the intestinal segment (colon) was enzymatically digested and the single cell suspension plated in 10 cm culture plates. Cells were used at the 5th passage and stimulation with recombinant mouse IL-4 was done in complete medium.

3.2.5 Intestinal organoid isolation

The colon was harvested and flushed 3X with ice-cold 1X PBS to remove the feces. Next, the intestine was cut-open longitudinally, minced in small pieces and transferred to a 50 ml conic tube containing 1X PBS supplemented with 1% Penicillin/Streptomycin and 50 µg/ml of Gentamicin (both Invitrogen). Tissue was pipetted up-and-down 10 times, the supernatant discarded and replaced by fresh supplemented PBS. This procedure was repeated 15 times until the supernatant become clear. Next, the 15th washout was discarded and the tissue was resuspended with 25 ml of 1X PBS containing 2mM EDTA (Roth) and left on ice for 30 minutes with constant shaking (80rpm). After the incubation with EDTA the tissue was allowed to settle down and the supernatant removed. Then, 10 ml of 1X PBS containing 10% FBS was added and pipetted up-and-down 5 times. Tissue was allowed to settle down and the first supernatant discarded due to the high amount of debris. This step was repeated more 4 times and the supernatant collected passing through a 70 µm mash placed on a 50 ml conic tube. Cells were then centrifuged at 1200 rpm for 5 minutes at 4°C. The pellet was further resuspended with ERN culture medium (F-12 advanced DMEN/F-12 medium, Invitrogen) supplemented with 1% 1M HEPES, 1% Penicillin/ Streptomycin (Invitrogen), 1% Glutamine (Invitrogen), 20% Noggin (in-house made), 10% R-Spondin (in-house made), 1X N2 (Invitrogen), 80 µM n-Acetylcysteine - NAC (Sigma), 1X B27 supplement (Invitrogen), 200 ng/ml mEGF, 3.4 µg/ml Rock inhibitor - Y (Sigma), 10mM Nicotinamid (Sigma), 5µM CHIR (Axon), 500 nM A83-01 (Tocris) and transferred to a 15 ml conic tube. After 5 minutes centrifugation at 800 rpm at 4°C the supernatant was carefully removed and matrigel (BD) added to the pellet (generally between 150 to 300 µl). 25 µl drops of matrigel-containing cells were plated in 48 well-plates (Sarsted) and covered with 250 µl ERN culture medium. Medium was changed every 3 days, and organoids passaged at a 1:3 ratio once a week. Stimulation with recombinant IL-4 was performed in complete medium.

3.2.6 Determination of cell count and viability

Single-cells suspensions were obtained directly or by harvesting with 0,25% Trypsin/EDTA and counted with a hemocytometer in the presence of 1% trypan blue. Trypan blue negative cells were considered as viable cells.

3.3 Molecular Biology Based Methods

3.3.1 RNA isolation and determination

RNA isolation was performed using RNeasy Mini Kit (Qiagen). Cells, whole intestinal mucosa or tumor tissues were lysed with RTL buffer containing 1% β -mercaptoethanol. Complete tissue disruption and homogenization was achieved by using the Precellys 24 tissue lyser (Bertin Technologies), followed by QIAshredder Column Kit (Qiagen). The remaining steps were performed according to the manufacturer's protocol. RNA concentration and purity was determined by NanoDrop 2000 Spectrophotometer (Thermo Scientific). RNA was either directly subjected to cDNA synthesis or stored at -80°C.

3.3.2 Reverse transcription, cDNA synthesis

For cDNA synthesis, generally 1 μ g of RNA was used. The reaction was performed in a final volume of 20 μ l. First, 1 μ g RNA, 2.5 μ M OligodT (Invitrogen) and 0.5 mM dNTP-mix (Invitrogen) were incubated at 65°C for 5 minutes. The mixture was cooled down on ice for approximately 2 minutes and mixed with 1X reaction buffer (Invitrogen), 5 mM DTT, 0.5 U RNaseOUT (Invitrogen) and 10 U Superscript II reverse transcriptase (Invitrogen). Next, the reaction was performed at 42°C, for 60 minutes followed by reaction inactivation, achieved by heating the samples up to 70°C for 15 minutes. Finally cDNA was diluted 1:4 with DNA-RNase free water and stored at -80°C.

3.3.3 Quantitative real time PCR

Quantitative PCR analysis was performed using gene specific primers

designed for the gene of interest (table 3.2). For the reaction mix volume of 20 μ l, 1 μ l of cDNA, 1X SYBR-Green Master Mix (Roche), 2 mM forward primer and 2 mM reverse primer were used. The reaction was carried out in the StepOnePlus Real Time PCR system (Applied Biosystems) using the conditions in table 3.5. The expression levels were normalized to the housekeeping gene *Cyclophilin* (Relative Expression = $\text{POWER } 2^{(\text{CT}_{\text{housekeeping gene}} - \text{CT}_{\text{target gene}})}$).

Table 3.5 Quantitative PCR Program

| Cycles | Temperature °C | Time (seconds) |
|----------------------|----------------|----------------|
| Holding once | 50 | 60 |
| Holding once | 95 | 600 |
| Cycling 40X | 95 | 30 |
| Cycling \leftarrow | 60 | 60 |

3.3.4 DNA isolation and genotyping

In order to genotype the mice DNA was isolated by tail or ear sampling and lysed overnight in 95 μ l tail lysis buffer (table 3.6) supplemented with 5 μ l Proteinase K (Qiagen) at 60°C. The enzymatic digestion was stopped by heat inactivation at 95°C for 10 min. DNA samples were diluted with distilled water 1:10 and centrifuged for 5 min at 10000 rpm to remove insoluble parts. All supernatants were directly subjected to polymerase chain reaction (PCR) (table 3.7).

Table 3.6 Tail Lysis Buffer

| Compound | Concentration |
|----------------|---------------|
| Tris (pH8.5) | 1,5M |
| NaCl | 200mM |
| SDS Ultra Pure | 0,2% (w/v) |
| EDTA | 5mM |

Table 3.7 General PCR Reaction

| Reagent | Amount |
|-----------------------------|-------------|
| 10X PCR Buffer (Invitrogen) | 2 μ l |
| 50 mM MgCl (Invitrogen) | 0,8 μ l |
| 100 mM dNTP mix (Carl Roth) | 0,4 μ l |

| | |
|-------------------------------------|----------|
| 20 pM Forward Primer | 0,5 µl |
| 20 pM Reverse Primer | 0,5 µl |
| TAQ Polymerase 5 U/ µl (Invitrogen) | 0,15 µl |
| Destilled Water | 14,15 µl |
| DNA sample | 1.5 µl |

3.3.5 Agarose electrophoresis

Agarose gel was prepared by mixing 1X TAE buffer (table 3.8) with 1-2% (w/v) agarose and by boiling the mixture in a microwave oven at 600W for four minutes. The gel was left to cool-down to approximately 60°C for the addition of ethidium bromide (0.005%). The gel was poured into the tray to cast and appropriate combs were placed for the formation of wells. Concomitantly, DNA samples were prepared by mixing 5X loading dye (Fermentas). Once the gel had polymerized, combs were removed and the gel was put into electrophoresis chamber, submerge in 1X TAE buffer. 1kb loading marker (Invitrogen) was used and gel was run at 120V for 30-60 minutes. The DNA bands were observed under UV-light and they were photographed by using Gel Doc XR imaging system (Biorad).

Table 3.8 50X TAE Buffer

| Compound | Concentration |
|-------------|---------------|
| Tris | 2M |
| Acetic Acid | 5,7% |
| EDTA | 5mM |

3.3.6 Protein extraction and determination

Frozen intestinal epithelial cells, whole intestinal mucosa or tumor tissues were lysed with freshly prepared lysis buffer (table 2.9) containing protease and phosphatase inhibitors. Tissue disruption and homogenization was achieved by using the Precellys 24 tissue lyser (Bertin Technologies). Homogenized samples were let stand on ice for complete lysis for 15 minutes.

For cell cultures, cells grown on culture plates were washed twice with ice-cold 1X PBS. Sufficient amount of lysis buffer containing protease and phosphatase inhibitors was directly added, cells were scrapped from the plates and collected into microcentrifuge tubes and lysed on ice for 15

minutes. When kept in suspension, cells were first transferred to a conic 15 ml tube, centrifuged 5 minutes, 500G at 4°C to pellet, washed once with ice-cold 1X PBS and then transferred to microcentrifuge tubes to be lysed. Complete homogenization was achieved by hydrodynamic shearing (21 G needle), for a minute on ice.

In all situations cell debris was removed by centrifugation 10 min, 13.000 rpm at 4°C and supernatants containing total protein lysates collected. If not directly used, proteins were stored at -80°C.

Table 3.9. Protein Lysis Buffer

| Compound | Concentration |
|-----------------------------------|-------------------|
| Tris | 50mM (pH 7.8) |
| NaCl | 250mM |
| EDTA | 30mM |
| EGTA | 30mM |
| Sodium-pyrophosphate | 25mM |
| Triton X 100 | 1% |
| NP-40 | 0,5% |
| Glycerol | 10% |
| DTT | 1mM |
| β-glycerophosphate | 50mM |
| Sodium fluoride | 25mM |
| Sodium Orthovanadate | 5mM |
| PMSF | 2nM |
| Roche Complete protease inhibitor | 1 tablet to 50 ml |

3.3.7 Western blot

Protein lysates from tumors, colonic mucosa, intestinal epithelial cells or immune cells were subjected to SDS-PAGE in order to evaluate the expression of several molecules. The running gel percentage was chosen and prepared accordingly to the protein molecular weight of interest (tables 3.10; 3.11; 3.12; 3.13 and 3.14 provide the composition of running/stacking gels and gel buffers). Gel electrophoresis was generally performed at 80 volts, for 90 minutes in 1X running buffer.

Table 3.10 Western Blot Running Gel Composition

| Gel Percentage | Bis-acrylamide 40% (ml) | Running Gel Buffer (ml) | Distilled Water (ml) | 10% APS (µl) | TEMED (µl) |
|-----------------------|--------------------------------|--------------------------------|-----------------------------|---------------------|-------------------|
| 08% | 2 | 2,5 | 5,5 | 50 | 7 |
| 10% | 2,5 | 2,5 | 5 | 50 | 7 |
| 12% | 3 | 2,5 | 4,4 | 50 | 7 |
| 15% | 3,75 | 2,5 | 3,65 | 50 | 7 |

Table 3.11 Western Blot Running Gel Buffer Composition

| Compound | Concentration |
|-----------------|----------------------|
| Tris-HCL pH 8,8 | 1,5M |
| SDS | 0,4% |

Table 3.12 Western Blot Stacking Gel Composition

| Gel Percentage | Bisacrylamide 40% (ml) | Stacking Gel Buffer (ml) | Distilled Water (ml) | 10% APS (µl) | TEMED (µl) |
|-----------------------|-------------------------------|---------------------------------|-----------------------------|---------------------|-------------------|
| 05% | 0,713 | 950 | 4,6 | 62,5 | 15 |

Table 3.13 Western Blot Stacking Gel Buffer Composition

| Compound | Concentration |
|-----------------|----------------------|
| Tris-HCL pH 6,8 | 0,5M |
| SDS | 0,4% |

Table 3.14 Western Blot Electrophoresis Running Buffer Composition (10X)

| Compound | Concentration |
|-----------------|----------------------|
| Tris | 250mM |
| Glycine | 2M |
| SDS | 1% |

After electrophoresis, samples were transferred to PVDF membranes by wet blotting, using 1X transfer buffer (table 3.15) applying 300 mA during 90 minutes, on ice. For proteins larger than 100 KDa the transfer time was increased to 120-150 minutes. PVDF membranes were further blocked with 3% skim milk in PBST for 30 minutes. Antibody incubation was performed overnight at 4°C. Phosphorylated antibodies were diluted in 3% BSA/PBST

instead of 3% skim milk. Secondary HRP-conjugated antibodies were diluted in 3% skim milk in PBST during 30 minutes at room temperature. Detection was done by chemiluminescent reaction (SuperSignal West Pico Substrate, Thermo Scientific).

Table 3.15 Western Blot Transfer Buffer Composition (10X)

| Compound | Concentration |
|----------|---------------|
| Tris | 12mM |
| Glycine | 96mM |

* Add 20% methanol to the final volume to obtain 1X transfer Buffer

3.3.8 Formalin-fixed and paraffin embedded tissue processing

Immediately after sacrifice all necessary organs were harvested and fixed overnight in 4% PFA at 4°C. The following day, samples were transferred to 70% ethanol and processed by Leica Dehydrator Tissue Processor ASP 300S, according to manufacture's protocol (table 3.16). After dehydration tissues were embedded in paraffin blocks and stored at RT.

Table 3.16 Tissue Dehydration Protocol

| Reagent | Incubation Time (min) |
|--------------|-----------------------|
| Ethanol 70% | 45 |
| Ethanol 86% | 45 |
| Ethanol 96% | 45 |
| Ethanol 96% | 60 |
| Ethanol 100% | 60 |
| Ethanol 100% | 60 |
| Ethanol 100% | 60 |
| Xylene | 45 |
| Xylene | 70 |
| Xylene | 75 |
| Paraffin | 60 |
| Paraffin | 60 |
| Paraffin | 60 |

For histological staining, 2-4 μ m sections were cut with Leica Microtome RM 2235, transferred to 46°C water bath and fixed on SuperFrost (Thermo) glass slides. Before histological staining, sections were deparaffinized and rehydrated using the protocol described below (table 3.17).

Table 3.17 Deparaffinization and Rehydration Protocol

| Reagent | Incubation Time (min) |
|--------------|-----------------------|
| Xylene | 5 |
| Xylene | 5 |
| Ethanol 100% | 2 |
| Ethanol 100% | 2 |
| Ethanol 96% | 2 |
| Ethanol 96% | 2 |
| Ethanol 80% | 2 |
| Ethanol 80% | 2 |
| Ethanol 70% | 2 |
| Ethanol 70% | 2 |
| Ethanol 50% | 2 |
| Ethanol 50% | 2 |
| PBS | 5 |

3.3.9 Immunohistochemistry

For immunohistochemistry staining, sections were deparaffinized and rehydrated (table 3.17). After, antigen retrieval was performed. For surface markers tissues were incubated in 0.3% Triton 10-20 minutes at 4°C. For nuclear or cytoplasmic stainings, sections were microwaved (approximately 400 watts) in 1X low pH antigen unmasking solution (Vector Laboratories) for 15 minutes, cooled down to RT and washed with PBS for 5 minutes. In order to block endogenous peroxidases the sections were further incubated in 3% H₂O₂ solution for 10 minutes. To avoid unspecific binding of antibody the sections were blocked for 30 minutes at RT with 3% BSA/PBS with streptavidin (Vector Laboratories). After blocking, the primary antibody was applied in the proper concentration (table 3.3) diluted in 3% BSA/PBS with biotin (Vector Laboratories), overnight at 4°C. The next day sections were washed with 1X PBS for 10 minutes and incubated with the appropriate biotin conjugated secondary antibody for 30 minutes at RT.

After washing twice with 1X PBS for 5 minutes, the slides were incubated for 30 minutes at RT with ABC complex (Vector Laboratories). For visualization color reaction DAB kit (Vector Laboratories) was freshly prepared and used on the sections. The reaction was stopped submerging the slides in distilled water after the visualization of the color reaction under Leica Primo Star microscope. The sections were then stained with Mayer's hematoxylin

(Merck) for counter-staining. After washing 3 times with distilled water, for 5 minutes each, the sections were dehydrated according to the protocol in table 3.18 and covered with mounting medium (Vector Laboratories) and a glass cover slide.

Table 3.18 Dehydration Protocol

| Reagent | Incubation Time (min) |
|--------------|-----------------------|
| Ethanol 50% | 3 |
| Ethanol 70% | 3 |
| Ethanol 80% | 3 |
| Ethanol 96% | 3 |
| Ethanol 100% | 5 |
| Xylene | 5 |
| Xylene | 5 |

3.4 Mouse Models

3.4.1 Global deletion of *IL-4Rα*: *IL-4Rα*^{-/-} mice

Interleukin 4 receptor alpha deficient (*IL-4Rα*^{-/-}) mouse was generated and described by Dr. Nancy Noben-Trauth and colleagues in *Proc Natl Acad Sci U S A.* 1997 Sep 30; 94(20): 10838–10843 [238].

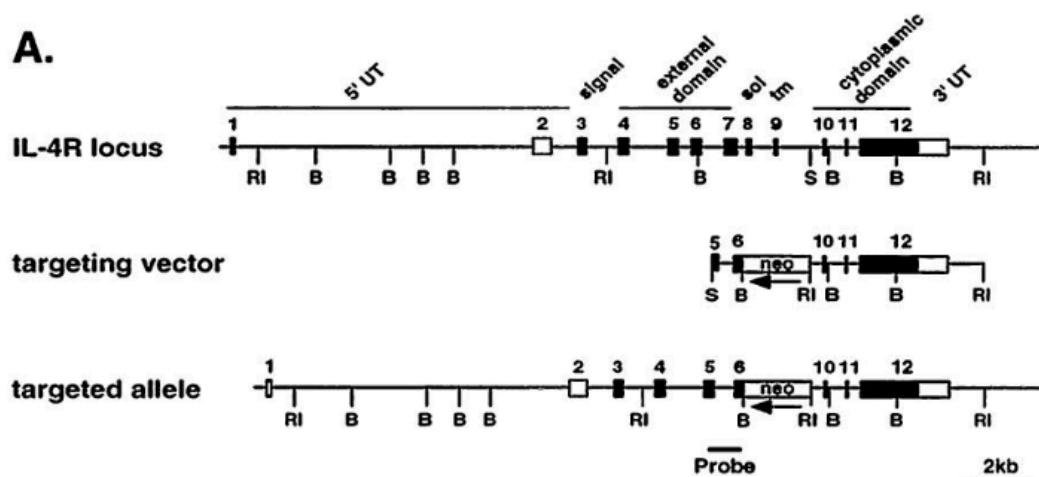


Figure 21. Targeting of *IL-4Rα*. (Extracted from *Proc Natl Acad Sci U S A.* 1997 Sep 30; 94(20): 10838–10843 [238]. Copyright 1997 © by the National Academy of Sciences). The disruption of the *IL-4Rα* locus. (A) After homologous recombination exons 7 to 9 were exchanged by a PGKneogene in a anti-parallel orientation to the *IL-4Rα* gene. The targeting vector used had a 6.3 kb homology with *IL-4Rα* gene.

Briefly, a targeting vector carrying a neomycin-resistant cassette was inserted between exons 7 to 9 into Balb/c mouse embryonic stem cells disrupting the *Il-4rα* locus (Figure 21). Complete *Il-4rα* deletion was obtained by intercrossing heterozygous offspring. Homozygous IL-4Rα knockout mice show no apparent phenotypic abnormalities, but exhibit a loss of IL-4 signal transduction. This results in a diminished TH2 helper T cell response demonstrated both *in vitro* and *in vivo*. The strain was donated to The JAX Laboratories (Bar Harbor, Maine, USA) in a Balb/c background, and is commercially available under the stock number 003514.

3.4.2 *Il-4rα* specific deletion in intestinal epithelial cells (IEC): IL-4Rα^{ΔIEC} mice

To achieve intestinal epithelial cell-specific deletion of *Il-4rα*, *Il-4rα loxP* flanked-mice were crossed (IL-4Rα^{flox/flox}) with mice expressing *Cre* recombinase gene downstream the *villin* gene promoter (*Villin-Cre*).

IL-4Rα^{flox/flox} mice were generated and kindly provided by Dr. Frank Brombacher (University of Cape Town, Health Sciences Faculty, South Africa) and described at Immunity, Vol. 20, 623–635, 2004 [239]. Concisely, a neomycin resistance/thymidine kinase cassette flanked by *loxP* sites was inserted into exon 7 and an additional *loxP* site was inserted into exon 10 of the *Il-4rα* gene. *Cre* expression in mouse embryonic stem cells bearing the construct causes the removal of the selection cassette and joining of the *loxP* sites, flanking exons 7–9 (Figure 22). The intercross between the *floxed* strain with a *villin* *Cre*-recombinase-bearing strain [240] generated the intestinal epithelial cell-specific IL-4Rα-deficient mice.

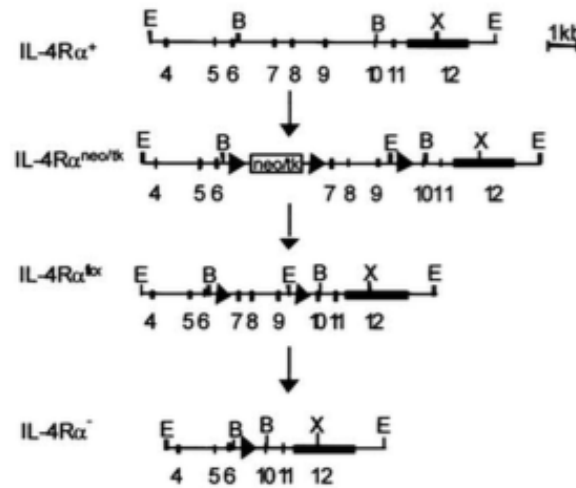


Figure 22. *IL-4Rα* gene locus and targeted deletion. (Extracted and adapted with permission from Elsevier: *Immunity*, Vol. 20, 623–635, May, 2004 [239]). Introduction of (neo/tk) selection cassette flanked by two loxP sites (arrowhead), and one loxP site 5 of exon 10 resulted in the generation of the conditional “floxed” mouse (exons 7 and 10) after gene targeting in Balb/c ES cells and transient Cre-mediated recombination. Numbers indicate exons of the *IL-4Rα* gene; B, E, and X, restriction site for *Bam*HI, *Eco*RI, and *Xho*I respectively.

Transgenic *Villin-Cre* mice have the mouse villin (*Vil-1*) promoter controlling the expression of *Cre* recombinase in villus and crypts of the small and large intestines. When these mice are bred with another strain containing loxP site sequences, specific deletion of the target gene may be obtained. Thus, they are a useful tool for studying intestinal development, functioning and its disorders (Figure 23). Villin Cre-recombinase mice were developed and first described by Dr. Blair B. Madison and colleagues at J Biol Chem. 2002 Sep 6;277(36):33275-83 [240]. The strain was later on donated by Dr. Deborah L. Gumucio (University of Michigan), to the JAX Laboratories (Bar Harbor, Maine, USA). It is commercially available at the stock number 021504.

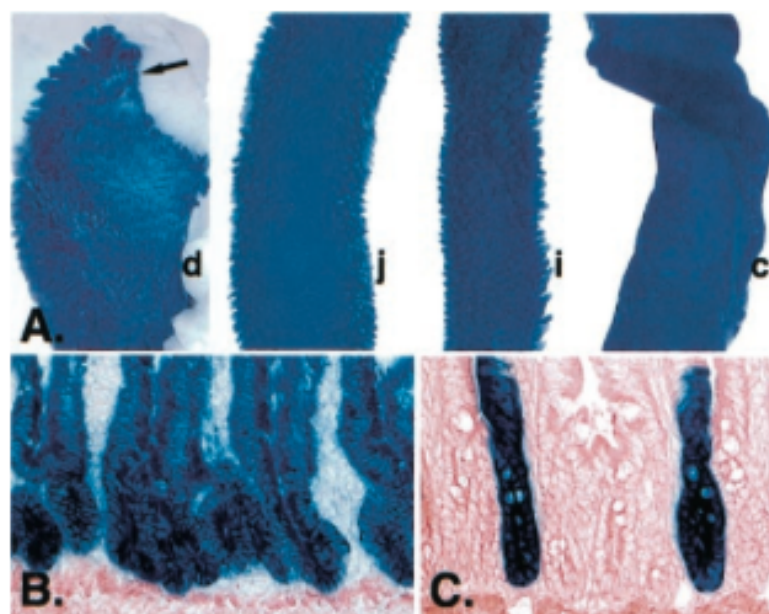


Figure 23. Villin Cre-recombinase mouse. (Extracted and adapted with permission by American Society for Biochemistry and Molecular Biology from *J Biol Chem.* 2002 Sep 6;277(36):33275-83 [240]). (A), B-galactosidase expression due to Cre recombinase activity obtained by crossing hemizygous transgenic Cre mice with homozygous Rosa26 report mice. Expression is observed in duodenum (A d), jejunum (A j), ileum (A i) and colon (A c). The duodenum-stomach border is depicted by the arrow (A d). (B) The expression of B-galactosidase was observed in all regions of the intestine; note that submucosa tissue do not express B-galactosidase. (C) Mice exhibiting mosaic expression.

3.4.3 Global deletion of *Stat6*: *Stat6*^{-/-} mice

Stat6-deleted mouse was generated in the Department of Cancer Biology, Harvard School of Public Health Boston, Massachusetts USA, under the supervision of Dr. Michael J. Grusby, and published by Mark H. Kaplan and colleagues at Immunity, Vol. 4, 313–319, March, 1996 [142]. Briefly, a neomycin resistance gene cassette replaced the exons containing the amino acids 505 to 584 of the *Stat6* gene (region of the SH2 domain required to dimerization). Next, murine D3 embryonic stem cells were transduced by electroporation with the construct, and the G418-resistant clones that had undergone homologous recombination at the *Stat6* locus were selected. Chimeras were generated injecting the construct into Balb/c blastocysts. Finally, heterozygous animals were intercrossed to generate mice homozygous for the *Stat6* mutation (Figure 24). Homozygous mice are viable, fertile and with no behavioral abnormalities. Phenotypically, *Stat6*-deficient lymphocytes do not proliferate in response to IL-4, and exhibit a deficient IgE response upon *in vivo* immunization with anti-IgD. *Stat6* knockout-derived

splenocytes have normal Th1 differentiation, and produce normal levels of IFN γ compared with WT. However, Th2 cell differentiation is strongly reduced upon *in vitro* stimulation with IL-4 or IL-13. No other phenotypes are described in unchallenged Stat6^{-/-} mice.

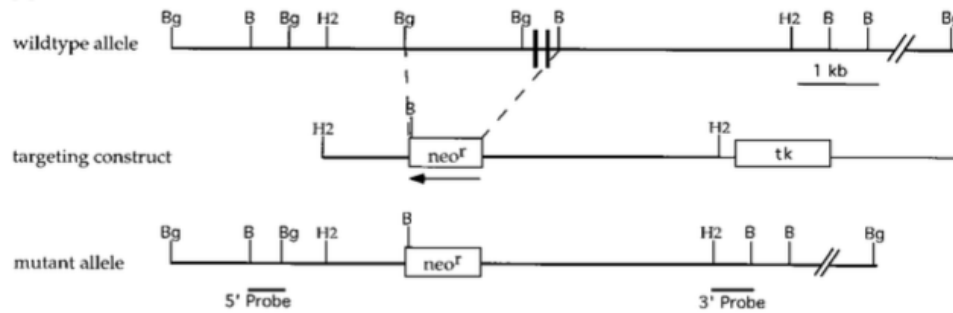


Figure 24. Generation of Stat6^{-/-} Mice. (Extracted and adapted with permission from Elsevier: *Immunity*, Vol. 4, 313–319, March, 1996 [142]). A neomycin-resistant cassette was inserted into the exon regions responsible for STAT6 dimerization upon activation (SH2 domain). This strategy assured that any mutant protein produced would be unfunctional. Restriction enzymes sites B, BamHI; Bg, BglI; H2, HindII.

The strain was donated to The JAX Laboratories (Bar Harbor, Maine, USA) in a C57BL/6 background, and is commercially available under the stock number 005977.

3.4.4 AOM - DSS treatment protocols

To study tumor development and progression driven by colitis mice were subjected to two intraperitoneal injections of AOM at concentration of 10mg/kg of body weight, followed by three cycles of DSS in the drinking water, for five days. The animals were sacrificed and the organs harvested 84 days after the beginning of the experiment. Figure 25 depicts the protocol used in the study. The DSS concentration in the drinking water varied accordingly to the mouse strain ranging from 2.0% w/v to 2.5% w/v. Stat6^{-/-} mice and mice that were subjected to adoptive transfer had to be sacrificed at an earlier time point due to severe anal hemorrhage and strong weight loss.

To evaluate the early molecular events of carcinogenesis mice were subjected to a single intraperitoneal injection of AOM (10mg/kg of body weight) followed by one cycle of DSS in the drinking water, during five days. The DSS concentration in the drinking water varied accordingly mouse strains

ranging from 2.0% w/v to 2.5% w/v. After 15 days animals were sacrificed and the colon harvested.

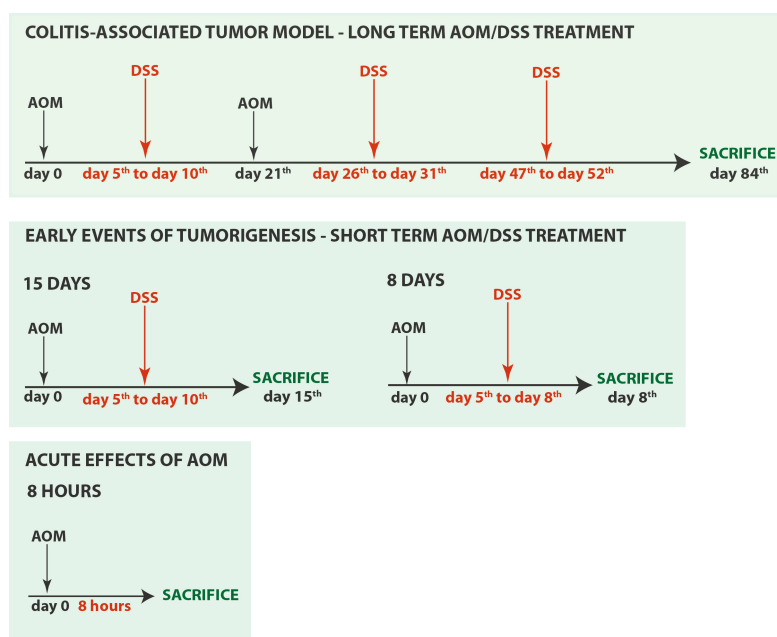


Figure 25. Azoxymethane (AOM) and dextran sodium sulphate (DSS) protocol diagrams.

Alternatively, to closer observe the affects of AOM/DSS on IEC death, mice were subjected to a single intraperitoneal injection of AOM (10mg/kg of body weight) followed by one cycle of DSS in the drinking water, during 3 days. At day eight, (3 days after the beginning of the DSS treatment) animals were sacrificed and the colon harvested. The DSS concentration in the drinking water was 2.0% w/v.

Finally, to evaluate the acute effects of AOM on IEC, mice were intraperitoneally injected with AOM (10mg/kg of body weigh) and sacrificed 8 hours after for tissue harvesting.

3.5 Statistics

Results were calculated using GraphPad Prisma 6 software. The p-values were considered significant when ≤ 0.05 , by Student's T-test analysis.

4 RESULTS

4.1 IL-4R α ^{-/-} Mice

4.1.1 Global deletion of *Il-4r α* does not cause any overt tumor-promoting phenotype in unchallenged mice

First, to determine whether global *Il-4r α* deletion would influence homeostasis and promote tumorigenesis in the colonic epithelium of unchallenged mice, the colons of wild-type (WT) mice and mice with global deletion of *Il-4r α* (IL-4R α ^{-/-} mice) were histologically analyzed at two different time points: at 1.5 and 18 months old (n≥4). Animals from both ages did not present any apparent spontaneous abnormalities in the colonic epithelium, showing no differences in intestinal development and with similar numbers of cells per colonic crypt (Figure 26 A, B). These results indicate that IL-4R α is dispensable for colon homeostasis in steady state conditions.

4.1.2 IL-4R α signaling promotes tumor formation and tumor growth

The lack of detailed information about IL-4 signaling and its influence on the underlying mechanisms of colorectal malignant transformation raises the question of how IL-4R α loss would affect colitis-associated colon carcinogenesis. In order to address this issue, WT and IL-4R α ^{-/-} mice (both on Balb/c background) were exposed to two intraperitoneal injections of AOM and three cycles of 2% DSS in the drinking water (Figure 26 C). From the beginning of the treatment, it was observed that IL-4R α ^{-/-} mice were less susceptible to weight loss than their WT counterparts, with significant differences at the end of the experiment (p≤0.05), (Figure 26 C). In response to AOM/DSS challenge, IL-4R α ^{-/-} mice showed reduced tumor formation (p≤0.01) and reduced tumor growth than their WT controls (p=0.0674), (Figure D, E). Tumors from both genotypes displayed a classical tubular morphology and were exclusively located in the colon, both typical characteristics of AOM/DSS-induced tumors (Figure 26 D) [230]. To examine the reasons for

the observed differences in tumor load and size, the intratumoral proliferation rate was determined by staining FFPE tumor sections for BrdU incorporation and phospho-Histone H3 expression. Surprisingly, no changes in BrdU incorporation were observed. However, transformed epithelial cells from IL-4R α ^{-/-} mice showed a significant reduction in phosphorylated Histone H3 expression, whereas WT mice exhibited an increase of approximately 40% compared to the proliferation rate determined for IL-4R α ^{-/-} mice

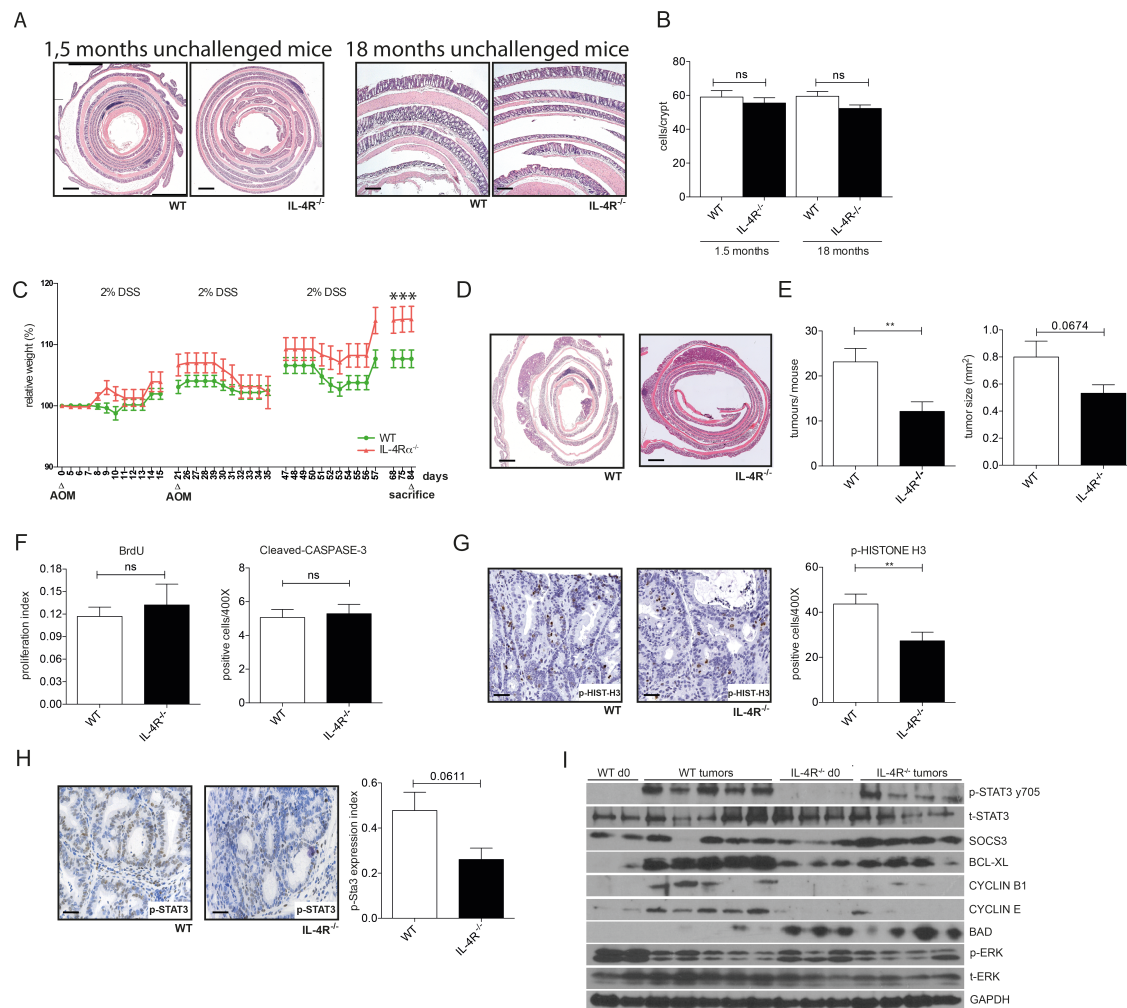


Figure 26. IL-4R α ^{-/-} mice show reduced tumorigenesis in colitis-associated tumor model (A-H). Global deletion of IL-4R α does not cause any overt tumor-promoting phenotype in the colon of unchallenged mice at 1,5 and after 18 months, when compared with respective-age controls, (n \geq 4), (A, B); colitis-associated tumor model performed with WT (Balb/c) and IL-4R α ^{-/-} mice (n \geq 07), (C-I); mice were subjected to two IP injections of AOM and exposed to 3 cycles of 2% DSS in the drinking water, for 5 days. After 84 days animals were sacrificed, colons collected and fixed in 4%PFA and further stained with H&E for tumor counting and tumor measurement (D); IL-4R α ^{-/-} mice showed reduced tumor formation (p \leq 0.01) and tumor growth (p=0.0611), (E); immunohistochemical analysis of tumors from IL-4R α ^{-/-} mice do not show any differences in BrdU incorporation or cleaved-Caspase 3; however, express lower levels of phospho-Histone H3 (p \leq 0.01), (F, G), and phospho-Stat3 Y705 (p=0.0611), (H); immunoblot analysis of tumor lysates from IL-4R α ^{-/-} mice at day 84 confirmed decreased Stat3 phosphorylation at tyrosine residue 705, followed by deregulated levels of SOCS3, decreased Bcl-xL, decreased Cyclins B1 and E, and increased Bad; no alterations in Erk phosphorylation was observed, although its total levels are decreased in IL-4R α ^{del/de} tumors (I). A, D – H&E; G, H – hematoxylin as co-staining. Scale bars: A, 1.5 months 1 mm, 18 months 0.2 mm; D, 1 mm; G, H, 0.05 mm. Data are mean \pm SEM.

(Figure 26 F, G). In contrast, immunohistochemistry for cleaved-Caspase 3 to access apoptosis, performed with FFPE tumor sections did not reveal any alterations (Figure 26 F).

Additionally, the expression of signal transducer and activator of transcription 3 (STAT3), which has been proved to be a supportive molecule in colonic carcinogenesis [203] was checked in tumors from WT and IL-4R $\alpha^{\text{del/del}}$ mice. Immunohistochemical analysis revealed a specific nuclear localization of phosphorylated tyrosine 705 (active) of Stat3 (p-STAT3 Y705) in transformed enterocytes of WT mice, and this signal was decreased in transformed enterocytes from the colons of IL-4R $\alpha^{-/-}$ mice, (Figure 26 H). This finding was later confirmed by immunoblot analysis of tumor lysates from WT and IL-4R $\alpha^{-/-}$ mice (Figure 26 I, top panel).

Furthermore, STAT3 target molecules suppressor of cytokine signaling 3 (SOCS3) and B-cell lymphoma-extra large (BCL-XL) were differentially regulated in IL-4R $\alpha^{-/-}$ tumors. SOCS3 expression, which is apparently increased in IL-4R $\alpha^{-/-}$ tumors, has the ability to act as a negative regulator of STAT3 activity; BCL-XL, an important anti-apoptotic molecule from the Bcl2 family, is found strongly reduced (Figure 26 I). In accordance to the reduced tumorigenic phenotype observed in the IL-4R $\alpha^{-/-}$ mice, decreased expression of CYCLIN B1 and CYCLIN E, followed by strong upregulation of pro-apoptotic molecule Bcl-2-antagonist of cell death (BAD), was also observed in IL-4R $\alpha^{-/-}$ tumors (Figure 26 I, middle panel). MAP kinase P44/42 (also known as ERK) phosphorylation did not show clear differences between genotypes. Interestingly, the total levels of ERK are decreased in IL-4R $\alpha^{-/-}$ tumors (Figure 26 I, bottom panel).

Collectively, these results indicate that *Il-4r α* ablation reduces colonic neoplastic transformation during colitis-associated tumor model with direct effects on cell proliferation and survival. Decreased STAT3 activity, altered expression of apoptosis-related molecules BCL-XL and BAD, followed by decreased CYCLIN B1 and CYCLIN E expression account for the phenotype observed in AOM/DSS-challenged IL-4R $\alpha^{-/-}$ mice.

4.2 IL-4R $\alpha^{\Delta IEC}$ Mice

4.2.1 Specific IL-4R α signaling in IEC promotes tumor growth with effects on tumor cell proliferation and STAT3 phosphorylation

To investigate the role of IL-4R α signaling specifically in intestinal epithelial cells (IEC) during colitis-associated tumorigenesis, IL-4R α floxed (IL-4R α^{floxed}) mice [239] were crossed to villin *Cre* transgenic mice [240], generating IL-4R $\alpha^{\Delta IEC}$ mice. The crossing results in excision of exons seven to nine of the *Il-4r α* gene, thus abrogating the transcription of functional IL-4R α mRNA (Figure 22). Based on the observations made using IL-4R $\alpha^{-/-}$ mice, was hypothesized that deletion of *Il-4r α* specifically in enterocytes would not induce any apparent tumor-promoting phenotype. Indeed, histological analysis of one and 18 months old unchallenged mice ($n \geq 5$) demonstrated that animals from both genotypes and ages did not develop any spontaneous colonic tumors (Figure 27 A). Notably, histological examination of the colons from IL-4R $\alpha^{\Delta IEC}$ mice at 18 months revealed the presence of scattered areas showing signs of mild immune cells infiltration into the colonic mucosa and the area around the crypts, which were absent in WT mice. The adjacent epithelium did not show altered morphology or signs of transformation (Figure 27 A, 200X and 400X magnifications).

Next, to better understand the effects of *Il-4r α* deletion on IEC during colitis-associated tumor, IL-4R α^{floxed} (WT littermates) and IL-4R $\alpha^{\Delta IEC}$ mice were exposed to two intraperitoneal injections of AOM and three cycles of 2% DSS in the drinking water, (Figure 27 B). During the entire treatment with AOM and DSS, no significant differences in weight loss between genotypes were observed (Figure 27 B). In response to the challenge, IL-4R $\alpha^{\Delta IEC}$ mice presented significantly reduced tumor growth ($p \leq 0.05$) but no effects on tumor incidence (Figure 27 C, D). Tumors of both genotypes had a classical tubular morphology and were exclusively located in the colon (Figure 27 C). To clarify the reasons for tumor size differences, the intratumoral proliferation rate was determined by staining FFPE tumor sections for BrdU incorporation and phosphorylated Histone H3 expression. A reduction in BrdU incorporation in

transformed epithelial cells of the IL-4R $\alpha^{\Delta\text{IEC}}$ mice was observed ($p \leq 0.05$), whereas WT mice exhibited an increase of approximately 50% compared to the proliferation rate determined for IL-4R $\alpha^{\Delta\text{IEC}}$ mice (Figure 27 E). In line with IL-4R $\alpha^{-/-}$ mice results, Histone H3 phosphorylation was also found significantly reduced ($p \leq 0.001$), (Figure 27 F). Interestingly, immunohistochemistry staining for cleaved-Caspase 3 using tumor sections did not reveal significant alterations in apoptosis between groups at this time point (84 days), (Figure 27 G).

To examine whether STAT3 expression was affected in IL-4R α -deficient transformed intestinal epithelia, immunohistochemical analysis with tumors from WT and IL-4R $\alpha^{\Delta\text{IEC}}$ mice was performed. Notably, as formerly identified in IL-4R $\alpha^{-/-}$ mice tumors, a specific nuclear staining was observed in transformed enterocytes of WT mice, and this signal was approximately 4.5-fold decreased in transformed enterocytes from IL-4R $\alpha^{\Delta\text{IEC}}$ mice ($p \leq 0.05$), (Figure 27 H).

Collectively, these results provide evidence that IL-4R α signaling specifically in IEC has tumor-growth promoting effects during colitis-associated tumorigenesis, and that IL-4R α loss caused reduced cell proliferation and decreased STAT3 activity in the colonic epithelium.

4.2.2 IEC-specific deletion of *Il-4r α* increases IEC apoptosis without affecting colonic epithelial regeneration at early events of AOM and DSS challenge

AOM/DSS administration initially leads to enterocyte DNA damage followed by DSS-induced apoptosis causing the disruption of the intestinal epithelial layer with translocation of microorganisms into the *lamina propria*. The presence of pathogens in the *lamina propria* triggers strong inflammatory response, which upon DSS-withdrawal starts to resolve and allow epithelial regeneration. This regeneration is widely promoted by immune cell-derived secreted cytokines, which induce IEC proliferation reconstructing tissue architecture. Homeostasis will be reached when the intestinal epithelial layer is re-established. At this time point usually, the expression of anti-

inflammatory cytokines, such as IL-4 and IL-10 are found increased [175, 241, 242]. As evidenced by the results here described, and by other elegant studies, IL-4/IL-4R α signaling axis has crucial effects on cell survival and apoptosis in both normal and transformed epithelial cells [162]. Therefore,

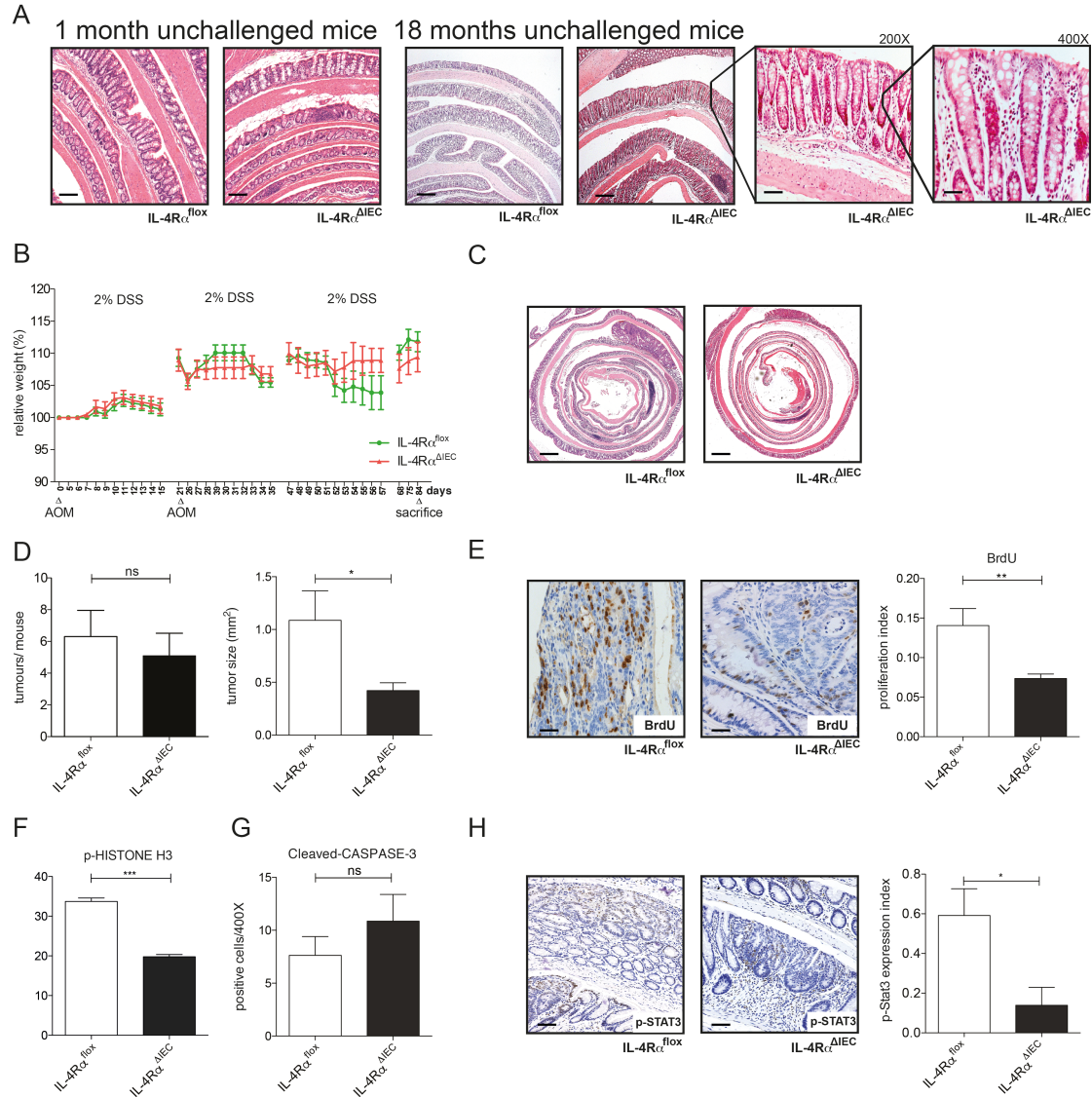


Figure 27. IL-4R α ^{ΔIEC} mice show reduced tumorigenesis in colitis-associated tumor model (A-H). Colonic histological analysis of unchallenged IL-4R α ^{ΔIEC} mice does not show any tumor-promoting phenotype in mice at 1 and 18 months of age, when compared with respective-age controls (n \geq 5), (A); 18 months of age IL-4R α ^{ΔIEC} mice display increased mucosal infiltration of immune cells (A, 200X and 400X magnifications); colitis-associated tumor model performed with WT littermates (IL-4R α ^{flx}) and IL-4R α ^{ΔIEC} mice (n=10), (B-H); mice were subjected to two IP injections of AOM and exposed to 3 cycles of 2% DSS in the drinking water, for 5 days. After 84 days animals were sacrificed, colons collected and fixed in 4% PFA and further stained with H&E for tumor counting and tumor measurement (C-D); IL-4R α ^{ΔIEC} mice showed reduced tumor growth (p \leq 0.05), without significant changes in tumor formation (D); IHC showed that tumors from IL-4R α ^{ΔIEC} mice exhibited lower BrdU incorporation (p \leq 0.01), compared with WT (n \geq 5), (E), and lower phospho-Histone H3 expression (n \geq 3) (F); immunohistochemical analysis for cleaved-Caspase 3 did not reveal any significant difference between treated groups (G); IL-4R α ^{ΔIEC} mice tumors expressed significant lower levels of phospho-STAT3 Y705 (n \geq 4), (p \leq 0.05), (H). A, C – H&E; E, H – hematoxylin as co-staining. Scale bars: A, 0,2 mm – 200X and 400X magnifications: 0,1 mm and 0,05 mm, respectively; C, 1 mm; E, 0,05 mm; H, 0,1 mm. Data are mean \pm SEM.

to evaluate the effects of IL-4R α loss on DSS-induced apoptotic response,

WT and IL-4R $\alpha^{\Delta IEC}$ mice were treated with one IP injection of AOM and exposed to 2% DSS in the drinking water for three days, being sacrificed and analyzed eight days after the beginning of the challenge (Figure 28 A). Efficient induction of apoptosis was confirmed by immunohistochemical staining performed on FFPE colon sections for cleaved-Caspase 3 (Figure 28 B). Increased apoptosis in the epithelium of IL-4R $\alpha^{\Delta IEC}$ mice ($p \leq 0.01$) was accompanied by a distinct reduction in BCL2 expression in lysates of isolated IEC at the 8th day of the regime (d8). No differences between unchallenged IEC lysates (d0) were observed (Figure 28 C, immunoblot analysis). Expression of the pro-apoptotic molecule BAD was not altered between treated groups (d8) but slightly increased in unchallenged IEC lysates (d0) (Figure 28 C). These findings are in agreement with the hypothesis that IL-4/IL-4R α signaling is involved in the regulation of apoptotic-related molecules in epithelial cells.

Next, to evaluate inflammatory response, epithelial damage and regeneration in the early events of tumorigenesis, WT and IL-4R $\alpha^{\Delta IEC}$ mice were injected IP with AOM and exposed for five days to 2% DSS in the drinking water, followed by a five days recovery phase on normal water (Figure 28 D). It was hypothesized that IL-4R $\alpha^{\Delta IEC}$ mice would experience stronger colitis based on the increased DSS-induced apoptotic response, and given the central role of IL-4R α for IL-4 signaling, a strong immune-suppressive pathway. Unexpectedly, histological analysis of inflammatory response, epithelial damage and regeneration did not reveal differences between treated groups, in spite of IL-4R $\alpha^{\Delta IEC}$ mice exhibiting reduced BrdU incorporation at the 15th day of the analysis (Figure 28 E, F, K).

Corroborating the immune-histological findings, RT-PCR analysis of inflammatory and chemoattractant genes, performed with whole colonic mucosal samples from WT and IL-4R $\alpha^{\Delta IEC}$ mice did not show any significant alterations in mRNA expression between treated (d15) and untreated mice (d0), (Figure 28 G-I). Finally, immunoblot analysis performed with lysates of isolated IEC at the 15th day of the regime showed reduced phosphorylation of STAT3 at Y705, followed by decreased expression of CYCLINS D2 and B1, both relevant cell cycle regulatory proteins, (Figure 28 J). Interestingly,

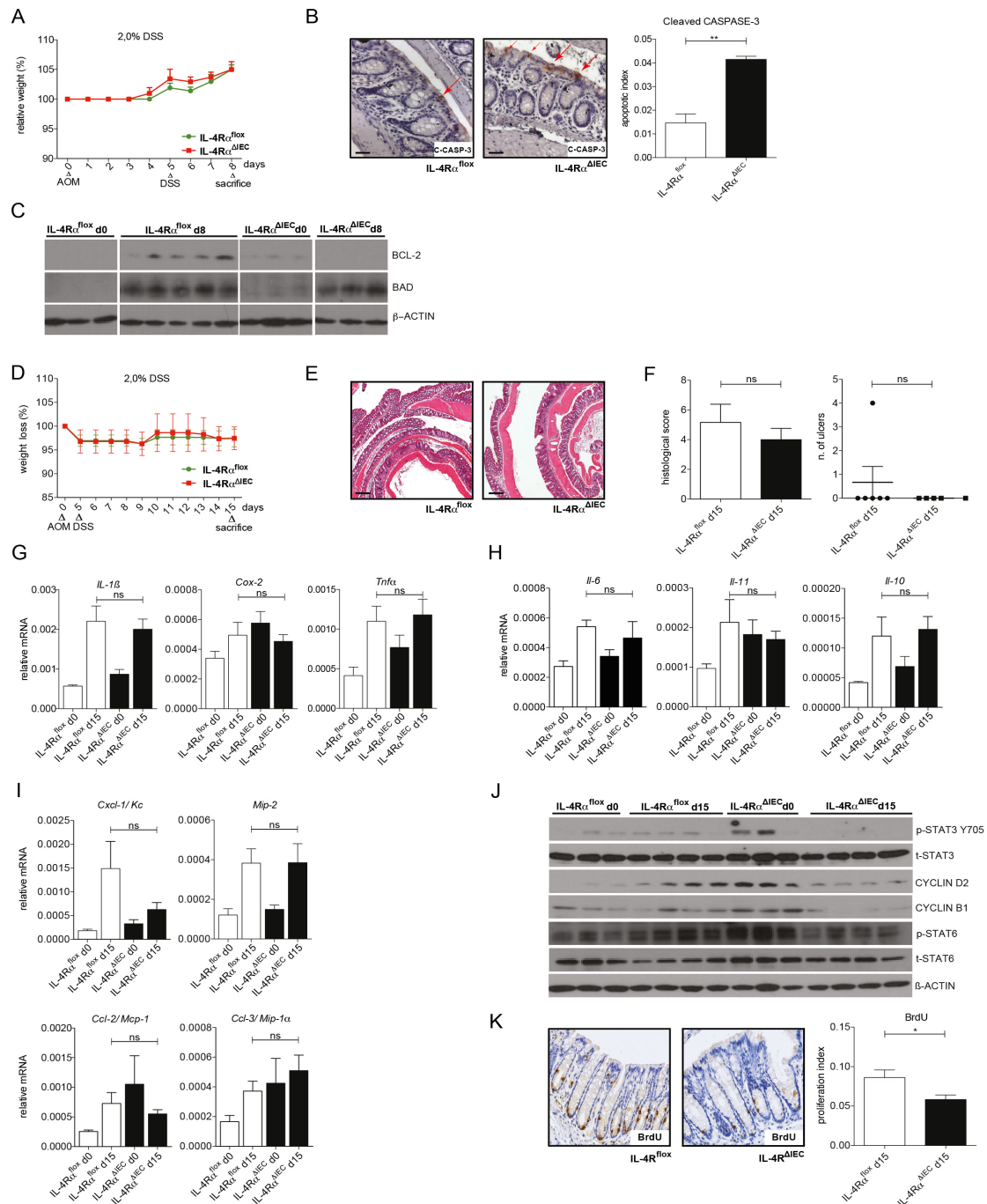


Figure 28. IL-4R α deletion in intestinal epithelial cells sensitizes enterocytes to apoptosis, without affecting tissue regeneration after AOM and DSS administration (A-K). To determine the apoptotic response to AOM/DSS, WT and IL-4R $\alpha^{\Delta IEC}$ mice were treated with one IP injection of AOM and exposed to 2% DSS in the drinking water for 3 days, being sacrificed 8 days after the beginning of the challenge (n=5), (A); IHC for cleaved-Caspase 3 performed with FFPE colonic sections from WT and IL-4R $\alpha^{\Delta IEC}$ mice showed enhanced apoptosis in the epithelium of IL-4R $\alpha^{\Delta IEC}$ mice compared with WT controls, (p<0.01), (B); immunoblot performed with IEC lysates from WT and IL-4R $\alpha^{\Delta IEC}$ mice reveals decreased BCL2 expression at day 8 in IL-4R α -deleted IEC when compared with WT IEC. BAD expression is unmodified (C); to determine inflammatory response, epithelial damage and regeneration after AOM/DSS treatment, animals were treated as previously, but 2% DSS was administered for 5 days in the drinking water followed by a 5 days recovery phase on normal drinking water. Mice were sacrificed and analyzed on day 15 of the beginning of the challenge (n≥5) (D); histological analysis of inflammatory response, damage and ulceration did not reveal differences between groups (E, F); RT-PCR analysis of whole colonic mucosa samples for inflammatory markers and chemoattractants at day 15 did not evidence significant changes in mRNA expression between treated and untreated groups (G-I); Immunoblot analysis showed decreased expression of p-STAT3 Y705, CYCLIN D2, CYCLIN B1 and p-STAT6 in IL-4R α -deficient IEC lysates extracted at day 15, when compared with WT (J). IHC staining for BrdU incorporation at day 15 indicates decreased IEC proliferation in IL-4R $\alpha^{\Delta IEC}$ mice compared with WT, (p<0.05), (K). Scale bars: B, 0,05 mm; E, 0,2 mm; K, 0,05 mm; (B, K), hematoxylin as co-staining. (E) H&E; Data are mean \pm SEM.

phosphorylation of STAT6, the most important transcription factor downstream IL-4/IL-4R α was still observed in IL-4R α -deficient IEC at day 15 (Figure 28J).

Taken together, these findings indicate that during the early events of carcinogenesis, IL-4R α deletion in IEC affects the apoptotic response caused by AOM-DSS treatment. Additionally, loss of *Il-4r α* in IEC reduced epithelial cell hyperproliferation in the regenerative phase of the colitis, evidenced by lower BrdU incorporation caused by decreased CYCLIN D2 and CYCLIN B1 expression. Strikingly, the enhanced apoptotic rate and reduced STAT3 activity found in *Il-4r α* -deficient IEC must be compensated by other molecules not detected by our analysis, as we did not observe differences in tissue regeneration at the end of the treatment with AOM/DSS. Finally, the unexpected observation that STAT6 phosphorylation was still present in *Il-4r α* -deficient IEC suggests IL-4-independent functions of STAT6.

4.3 Stat6^{-/-} Mice

4.3.1 Stat6 global deletion does not cause any overt phenotype in unchallenged mice

To elucidate whether global *Stat6* deletion would influence homeostasis or promote tumorigenesis in the colonic epithelium of unchallenged mice, the colons of WT mice and mice with global deletion of the *Stat6* gene (Stat6^{-/-} mice) were histologically analyzed at 1.5 and 18 months of age. Animals from both genotypes and ages did not present any apparent abnormalities in the colonic epithelium, showing no differences in intestine development (Figure 29 A).

4.3.2 Stat6 expression during colitis-associated tumor model protects against tumor formation and tumor growth

To further clarify the role of IL-4 signaling during colitis-associated tumorigenesis WT and Stat6^{-/-} mice were subjected to AOM/DSS treatment. It was hypothesized that being STAT6 one of the main components of the IL-4

pathway and a downstream target of the IL-4R α , the effects of its loss during colitis-associated tumor model would be similar to the ones obtained with IL-4R $\alpha^{-/-}$ and IL-4R $\alpha^{\Delta IEC}$ mice. To address this issue, WT and Stat6 $^{-/-}$ mice (both on a C57BL/6 background) were exposed to two intraperitoneal injections of AOM and three cycles of 2% DSS in the drinking water ($n \geq 8$), (Figure 29 B). From the second cycle of the treatment, it was observed that Stat6 $^{-/-}$ mice were significantly more susceptible to weight loss than WT counterparts, with significant differences until the end of the experiment (respectively, $p \leq 0.05$ and $p \leq 0.01$). Due to intense anal hemorrhage and weight loss, animals had to be sacrificed and tissues collected at an earlier time point, 57 days after the beginning of the treatment (Figure 29 B).

Surprisingly, and in disagreement with the initial hypothesis, Stat6 $^{-/-}$ mice showed increased tumor formation and tumor growth compared to WT controls ($p \leq 0.001$), (Figure 29 C, D). Tumors from both genotypes had a classical tubular morphology and were exclusively located in the colon (Figure 29 C). To elucidate the differences in tumor formation and growth, the intratumoral proliferation and apoptotic rates were determined by staining FFPE tumor sections from both genotypes for BrdU incorporation and cleaved-Caspase 3. Intriguingly, at this time point (57 days), no differences were detected in any of the genotypes in both parameters (Figure 29 E). Next, knowing that IL-4 signaling disruption during colitis-associated tumorigenesis was able to alter STAT3 activity in enterocytes, tumor sections from WT and Stat6 $^{-/-}$ mice were immunohistochemically analyzed for STAT3 phosphorylation. Interestingly, it was observed that Stat6-deficient tumors presented increased STAT3 phosphorylation at Y705 by 3-fold, when compared with WT tumors ($n \geq 3$), (Figure 29 F);

To further identify the molecular mechanisms that could be involved in the phenotype obtained, the lysates of unchallenged colons (d0) and tumors from WT and Stat6 $^{-/-}$ mice were analyzed by immunoblot. Endorsing the IHC results, increased STAT3 phosphorylation at Y705 in Stat6 $^{-/-}$ tumors, was re-confirmed when compared to WT tumors (Figure 29 G, top); this was followed by deregulated SOCS3 expression in the tumor samples from Stat6 $^{-/-}$ mice (Figure 29 G). Additionally, an increase in the expression of CYCLIN B1 in

Stat6^{-/-} mice was detected, not only in tumors but also in unchallenged colons (Figure 29 G). This finding was followed by increased expression of anti-apoptotic protein BCL-XL (Figure 29 G).

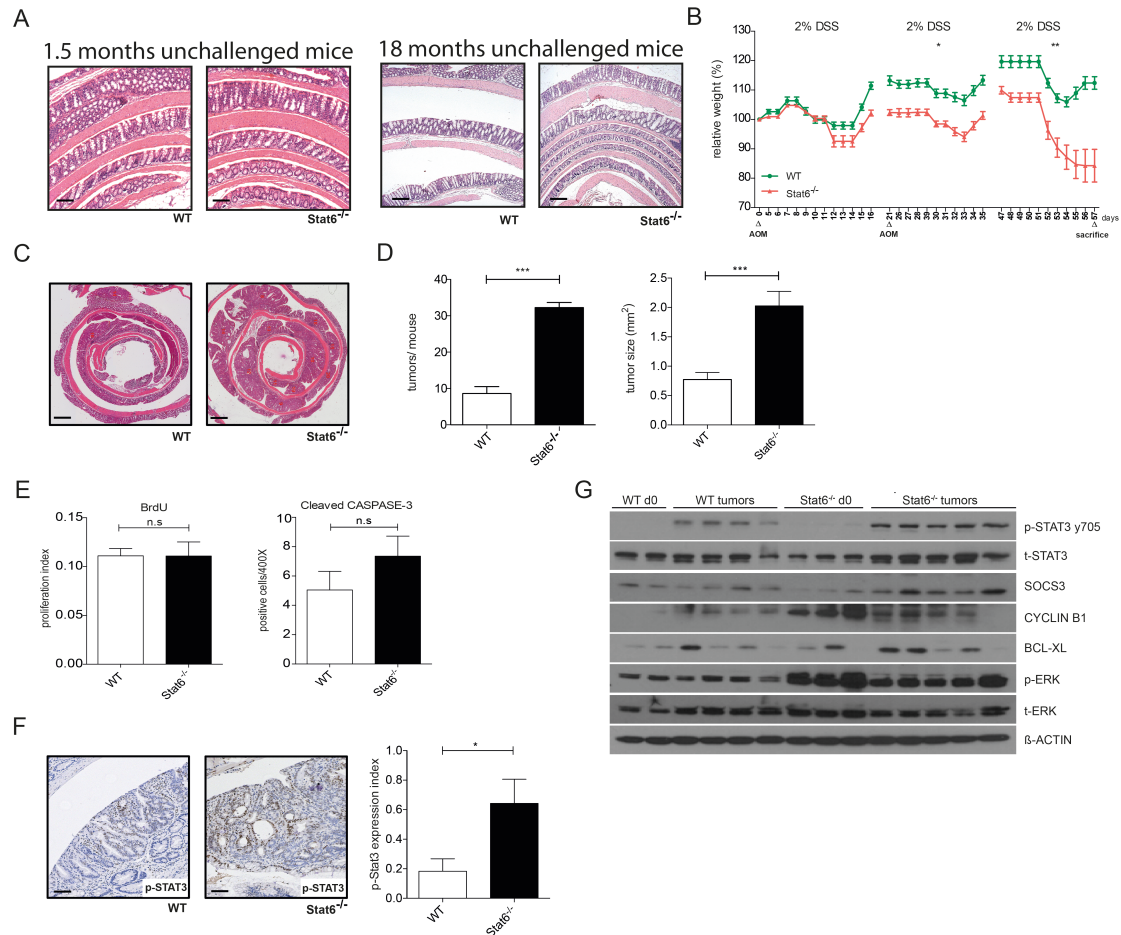


Figure 29. *Stat6* expression during colitis-associated tumor model protects against tumor formation and tumor growth (A-G). Histological analysis of the colon of unchallenged *Stat6*^{-/-} mice do not reveal any apparent tumor-promoting phenotype at 1.5 and 18 months of age, when compared with respective age-controls (n \geq 4), (A); colitis-associated tumor model performed with WT and *Stat6*^{-/-} mice (n \geq 8), (B-G); mice were subjected to two IP injections of AOM and exposed to three cycles of 2% DSS in the drinking water, during five days; due to severe weight loss and anal hemorrhage, animals were sacrificed and tissues collected 57 days after the beginning of the treatment (B); colons were fixed in 4% PFA and stained with H&E for tumor counting and measurement (C); *Stat6*^{-/-} mice presented increased tumor formation and tumor growth when compared with WT controls (p \leq 0.005) (D); BrdU incorporation and cleaved Caspase-3 expression evaluation by immunohistochemistry do not show any significant differences between groups at 57 days (E); immunohistochemical analysis of FFPE tumor sections from *Stat6*^{-/-} and WT mice showed enhanced STAT3 phosphorylation at Y705 in *Stat6*^{-/-} mice (p \leq 0.05), (F); immunoblot analysis performed with unchallenged colons and tumor-lysates from WT and *Stat6*^{-/-} mice asserts increased STAT3 activity in *Stat6*-deficient tumors, followed by deregulated expression of STAT3-target molecule SOCS3, (G); upregulated expression of CYCLIN B1, BCL-XL and phosphorylated ERK in *Stat6*^{-/-} tumors, when compared with tumors from WT; CYCLIN B1 and phosphorylated-ERK expressions were also found increased in unchallenged colon-lysates of *Stat6*^{-/-} mice, when compared with unchallenged WT colon lysates (G). Scale bars: A, 0.2 mm; C, 1 mm; F, 0.1 mm; (A, C), H&E staining; (F) hematoxylin as co-staining. Data are mean \pm SEM.

Finally, supporting the above findings, the ERK MAPK pathway, which is critical for cellular growth, was found to be dramatically upregulated in all *Stat6*^{-/-} samples, notably, not only in tumors but also in unchallenged colons (Figure 29 G, bottom). Thus, these results clearly indicate that *Stat6*

expression during colitis-associated tumor model protects against tumor formation and tumor growth, with direct effects on STAT3 activity and STAT3-regulated molecules.

4.3.3 *Stat6*-deficient tumors present decreased P53 nuclear localization and reduced mRNA levels of *Mgmt* and *P21* genes

The transcription factor P53 is regarded to be one of the most important tumor suppressors not only for colorectal carcinogenesis but also for nearly all malignancies. Under cellular stress, P53 activation occurs (due to post-translational modifications, such as phosphorylation) leading to its rapid nuclear translocation and accumulation. In the nucleus, P53 can initiate the expression of innumerable stress-response genes, which generally might result in three different outcomes: DNA repair, cell cycle arrest or apoptosis [243, 244]. Therefore, it was asked whether *Stat6* ablation during colitis-associated tumorigenesis would influence P53 cellular expression or localization. To answer this question, immunohistochemical analysis for P53 activity was performed using FFPE tumor sections from WT and *Stat6*^{-/-} mice. As a result, a 3-fold decrease in nuclear localization of P53 in transformed enterocytes from *Stat6*^{-/-} mice tumors was observed when compared to WT tumors (p≤0.01), (Figure 30 A). In agreement with the immunohistochemical analysis, the mRNA level of O⁶-methylguanine DNA methyltransferase (*Mgmt*) gene, whose expression is regulated by P53 was found to be diminished in *Stat6*^{-/-} tumors, as was the mRNA levels of the cell cycle regulator *P21* gene, whose expression is also tightly controlled by P53 (RT-PCR; Figure 30 B). Expression levels of *Mdm2* (a P53 negative regulator gene), or *Noxa* (a pro-apoptotic P53-inducible gene), were not altered (RT-PCR; Figure 30 B).

Taken together, these data indicate that STAT6 activation during colitis-associated tumorigenesis provides tumor suppressive functions. Mechanistically, *Stat6* ablation promotes *Stat3* activation. Subsequently, *Stat3* activity might affect molecules involved in cell cycle regulation and cellular growth such as CYCLIN B1 and ERK, as well as tumor suppressor gene *P53* and its targets, *Mgmt* and *P21*.

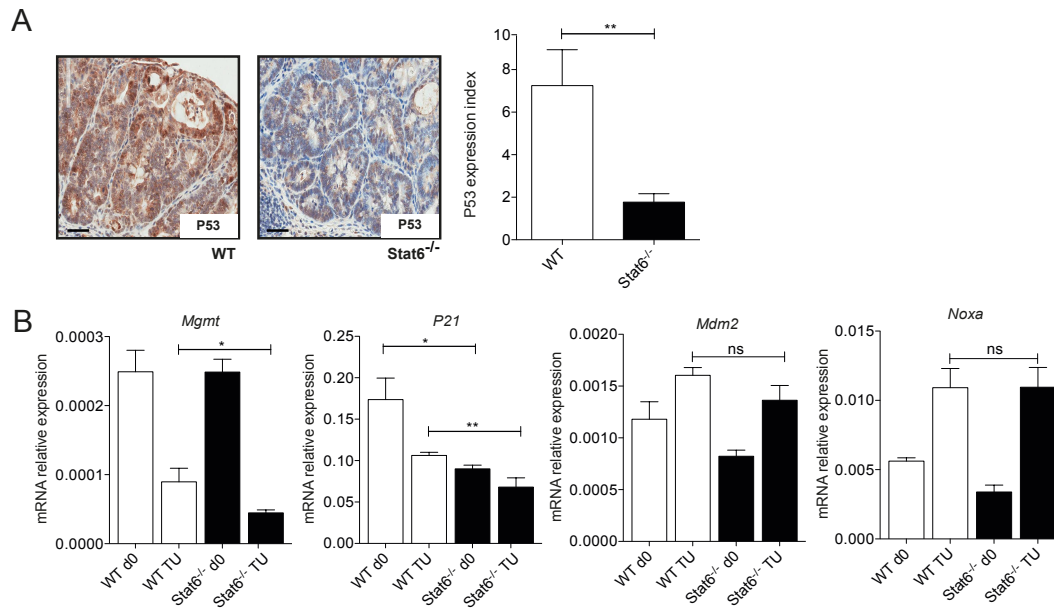


Figure 30. STAT6 expression affects P53 nuclear localization during colitis-associated tumor model (A-B). Immunohistochemical analysis of P53 activity reveals a 3-fold decrease in nuclear localization in Stat6^{-/-} tumors ($p \leq 0.01$, ($n \geq 3$), (A); decreased mRNA levels of P53 target genes *Mgmt* and *P21*, by RT-PCR analysis in Stat6^{-/-} tumors ($p \leq 0.05$ and $p \leq 0.01$, respectively), (B); *P21* mRNA expression is also found decreased in the colon of unchallenged Stat6^{-/-} mice ($p \leq 0.01$), (B); mRNA expression of *Mdm2* and *Noxa* genes, in the tumors of WT and Stat6^{-/-} mice did not reveal any alterations. Scale bars: A, 0,05 mm; (A) hematoxylin as co-staining. Data are mean \pm SEM.

4.3.4 Stat6-deficient enterocytes are the major contributors for increased colonic tumorigenesis in Stat6^{-/-} mice during colitis-associated tumor model

Considering that *Stat6* deletion was global (whole-body), it was not possible to discriminate which cell population was responsible for the increased tumorigenic phenotype observed in these animals during colitis-associated tumor model. Thus, to address the contribution of *Stat6* loss in immune cells during tumorigenesis, adoptive transfer experiments were performed with either WT (C57BL/6 controls) or *Stat6*-deficient bone marrows (Figure 31 A). Eight weeks after the transplantation, WT mice, which received *Stat6*-deficient bone marrow (Stat6^{-/-} BM \rightarrow WT), and Stat6^{-/-} mice that received WT bone marrow (WT BM \rightarrow Stat6^{-/-}), were subjected to AOM/DSS challenge. However, during the second administration of 2% DSS, WT BM \rightarrow Stat6^{-/-} mice started to lose weight dramatically followed by strong anal hemorrhage, being necessary to terminate the experiment 54 days after the first AOM injection (Figure 31 B). In response to the challenge, WT BM \rightarrow

Stat6^{-/-} mice presented a 6-fold increase in tumor formation ($p \leq 0.05$) when compared to Stat6^{-/-} BM \rightarrow WT mice (Figure 31 C, D). WT BM \rightarrow Stat6^{-/-} mice tumors were also larger but failed to reach statistical significance. Tumors from both genotypes had a classical tubular morphology and were exclusively located in the colon (Figure 31 C). Interestingly, similarly to untransplanted Stat6^{-/-} mice subjected to colitis-associated tumor model (Figure 29), IHC quantification for BrdU incorporation and cleaved-Caspase 3 expression did not reveal alterations in proliferation or apoptosis between groups, at 54 days (Figure 31 E).

To examine whether STAT3 expression was affected in transformed enterocytes, immunohistochemical analysis with tumors from WT BM \rightarrow Stat6^{-/-} and Stat6^{-/-} BM \rightarrow WT mice was performed. As formerly observed in untransplanted Stat6^{-/-} mice tumors, a specific nuclear staining was detected in transformed enterocytes of WT BM \rightarrow Stat6^{-/-} mice, and this signal was 2.5-fold reduced in transformed enterocytes from Stat6^{-/-} BM \rightarrow WT mice ($p \leq 0.05$), (Figure 31 F).

In addition to IEC and immune cells, vascular cells and fibroblasts are also components of the tumor milieu. Fibroblasts are one of the largest cell populations present in the tumor microenvironment, and many elegant studies have already shown that these cells can exert important features on intestinal transformed epithelial cells, promoting tumor development, growth and even metastasis [237, 245-247]. Thus, to evaluate the potential influence of colonic fibroblast in the phenotype obtained with WT BM \rightarrow Stat6^{-/-} mice, WT fibroblasts and colonic organoids were extracted and stimulated *in vitro* with recombinant mouse IL-4 and analyzed after 30 and 60 minutes. Immunoblot analysis performed with lysates from WT colonic organoids and fibroblasts depicts clear STAT6 phosphorylation at Y641 in organoids at 30 and 60 minutes after stimulation with recombinant IL-4 (Figure 31 G). However, STAT6 phosphorylation was completely absent at any time point in colonic fibroblasts, which also failed to express total levels of STAT6 (Figure 31 G). To assure the epithelial and mesenchymal origin of the samples, the immunoblot membrane was further incubated with anti-E-cadherin and anti-Vimentin antibodies (Figure 31 G).

Altogether, these results indicate that the non-hematopoietic system, primarily the *Stat6*-deficient enterocytes, are the major cells involved in increased tumor formation and tumor growth in *Stat6*^{-/-} mice during the colitis-associated tumor model. Moreover, deletion of *Stat6* in enterocytes renders these cells more susceptible to STAT3 upregulation in response to inflammatory insults. STAT3 overexpression provides enterocytes with strong tumor-promoting features during colorectal tumorigenesis.

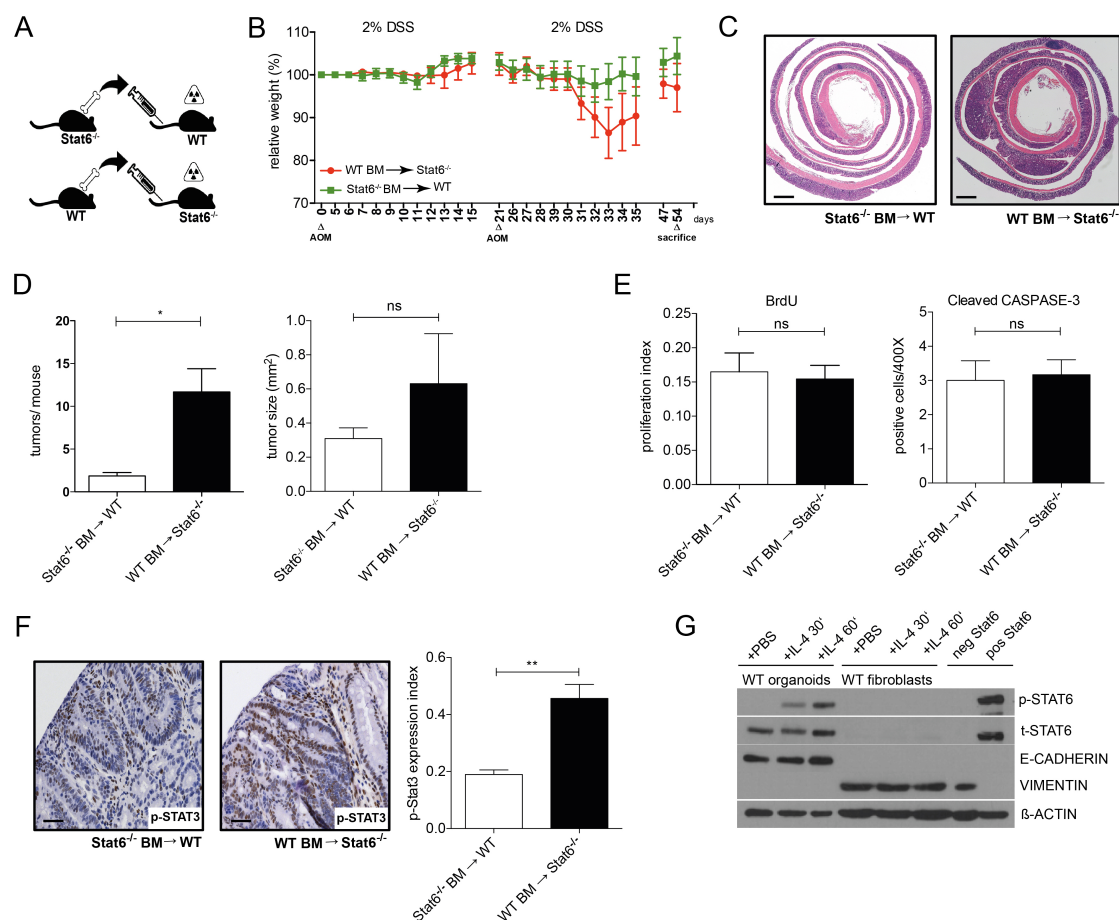


Figure 31. Adoptive transfer experiments with *Stat6*-deficient and *Stat6*-proficient bone marrow (A-G). 9.5 Gy-irradiated WT and *Stat6*^{-/-} mice received either STAT6-deficient or WT bone marrow (A), and 8-weeks after the transplantation were subjected to two IP injections of AOM and two cycles of 2% DSS (n≥6). Due to severe weight loss and anal hemorrhage in the group of *Stat6*^{-/-} mice which received WT bone marrow, animals had to be sacrificed and colons collected in 4% PFA 54 days after the beginning of the AOM/DSS treatment (B); *Stat6*^{-/-} mice which received WT bone marrow showed 6-fold increase in tumor formation (p≤0.05), and larger tumors (C, D); immunohistochemical analysis of FFPE tumor sections from *Stat6*^{-/-} and WT transplanted mice showed enhanced STAT3 phosphorylation at Y705 in *Stat6*^{-/-} mice which received WT bone marrow (p≤0.01), (n≥3) (F); immunoblot analysis with lysates from WT colonic organoids and fibroblasts depicts STAT6 phosphorylation at Y641 in organoids after 30 and 60 minutes stimulation with recombinant mouse IL-4 (10ng/ml). However, this phosphorylation was complete absent at any time point in colonic fibroblasts, which failed to express total levels of STAT6 (G). To assure the epithelial and mesenchymal origin of the samples membranes were blotted with anti-E-CADHERIN and anti-VIMENTIN antibodies (G); *Stat6*-deleted splenocytes, stimulated eight hours with recombinant mouse IFNγ (5ng/ml) were used as negative control (neg. Stat6); WT abdominal macrophages, stimulated two hours with recombinant mouse IL-4 (10 ng/ml) were used as positive control (pos. Stat6). Scale bars: C, 1 mm; F, 0.05 mm; (C), H&E staining; (F), hematoxylin as co-staining; Data are mean ± SEM.

4.3.5 Lack of *Stat6* increases IEC apoptosis in the early stages of tumorigenesis, leading to severe colitis in response to AOM/DSS challenge

Interleukin 4 and IL-13 binding to IL-4R α trigger STAT6 phosphorylation by JAK kinases and its nuclear translocation, which then may initiate the transcription of IL-4/IL-13 signaling-related genes. It is known that the activation of this pathway influences wound healing, cell survival and is able to exert anti-inflammatory effects [132, 136, 248]. Therefore, to determine by which mechanisms *Stat6* loss affects colorectal tumorigenesis during AOM/DSS treatment, animals from both WT and *Stat6*^{-/-} genotypes at the early stages of tumor development were examined, on day eight and 15 of the colitis-associated tumor model.

First, to determine the epithelial apoptotic response to DSS, WT and *Stat6*^{-/-} mice were injected with AOM and sacrificed three days after the starting of DSS administration (Figure 32 A). As observed previously in IL-4R α ^{Δ IEC} mice, immunohistochemical analysis of cleaved-Caspase 3 revealed a 3-fold induction of apoptosis in *Stat6*^{-/-} mice compared to WT ($p \leq 0.01$), (Figure 32 B). This result raised the question whether the increase in apoptosis detected at the 8th day of the colitis-associated tumor model would induce a stronger colitis in *Stat6*^{-/-} mice. To address this issue, animals were treated as previously, but 2% DSS was administrated in the drinking water during five days followed by a five-day recovery phase on normal drinking water. This approach allowed the evaluation of inflammatory response, epithelial damage, and tissue regeneration. Throughout the treatment, the weight loss was similar between the genotypes (Figure 32 C). However, histological analysis of the colons at day 15 of the AOM/DSS challenge revealed that *Stat6*^{-/-} mice suffered from more severe colitis than the WT counterparts ($p \leq 0.001$) (Figure 32 D). STAT6-deficient mice clearly showed a delay in induction of the healing phase with extensive damage to the colonic architecture, which was replaced by massive immune cell infiltration and ulcerations (Figure 32 D, E).

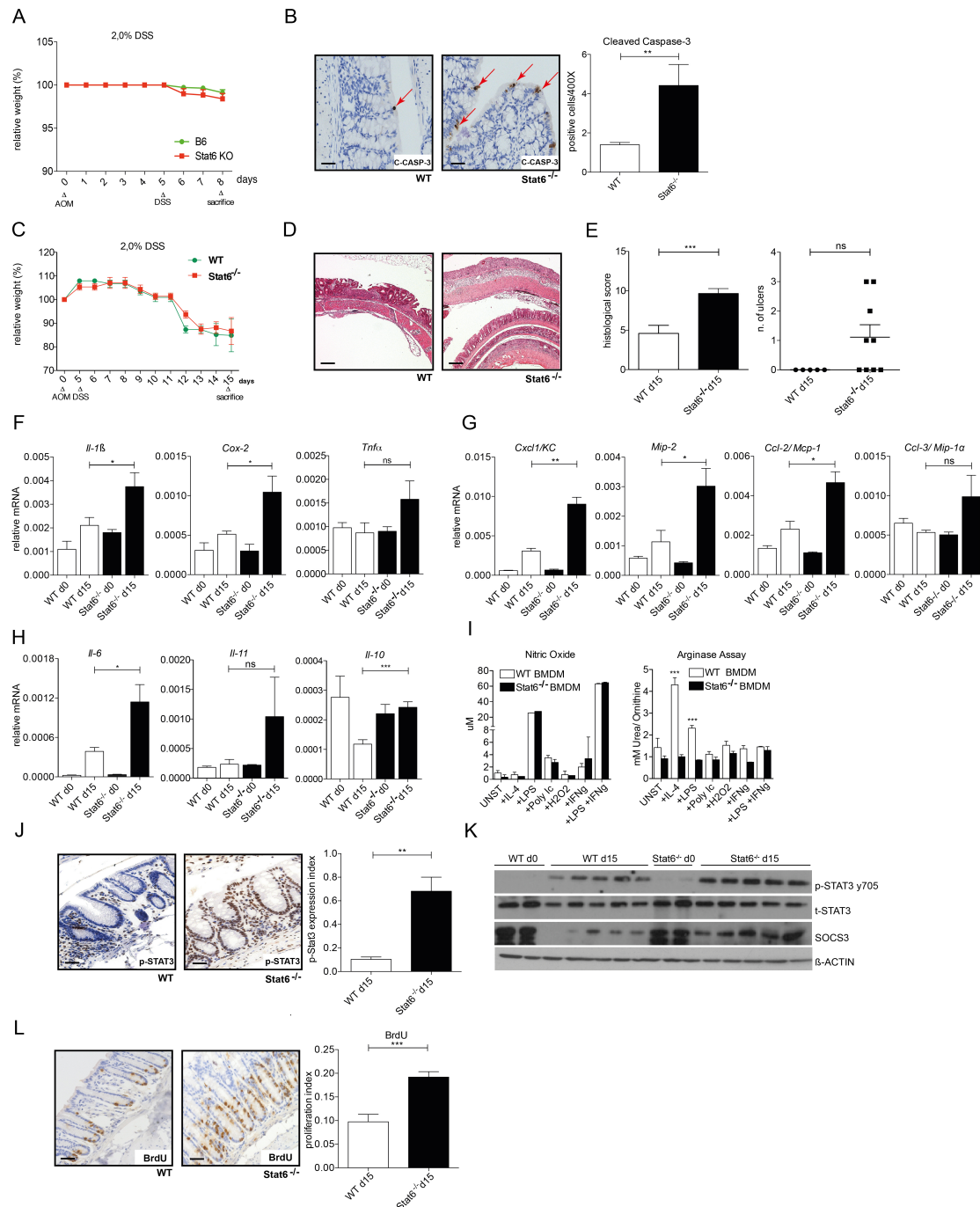


Figure 32. Stat6-deficient colonocytes display increased susceptibility to DSS-induced apoptosis in early stages of tumorigenesis, resulting in severe colitis upon AOM/DSS treatment (A-L). WT and Stat6^{-/-} mice were treated with 1 IP injection of AOM and exposed to 2% DSS in the drinking water for 3 days, being sacrificed 8 days after the beginning of the challenge (n=5), (A); immunohistochemistry for cleaved-Caspase 3 performed on FFPE colon sections from WT and Stat6^{-/-} mice at day 8 showed enhanced apoptosis in colonocytes from Stat6^{-/-} mice (p<0.01), (B); WT and Stat6^{-/-} mice were treated as previously (A), but 2% DSS was administrated for 5 days in the drinking water, followed by a 5 days recovery phase on normal drinking water. Animals were sacrificed at day 15 of the beginning of the challenge, (n≥5), (C); histological analysis of WT and Stat6^{-/-} colons revealed increased inflammatory response and tissue damage in Stat6^{-/-} mice, compared to WT, (p<0.001), (D, E); RT-PCR analysis for inflammation-related and chemoattractant genes, performed with colonic mucosal samples at day 15, displayed mRNA upregulation for all tested genes in Stat6^{-/-} mice at day 15 (F-H); Griess assay performed with supernatants of stimulated BMDM do not show any difference in NO production between groups (I); arginase assay performed with BMDM lysates stimulated with recombinant IL-4 and LPS showed reduced conversion of arginine to ornithine and urea in BMDM from Stat6^{-/-} mice (I); immunohistochemical analysis of FFPE colon sections show increased STAT3 phosphorylation at Y705 (p<0.01) and BrdU incorporation (p<0.001) in colons from Stat6^{-/-} mice (J, L); immunoblot performed with unchallenged (d0) and AOM/DSS treated colon lysates from WT and Stat6^{-/-} mice revealed stronger STAT3 activity in Stat6^{-/-} samples at day 15 (d15) (K); SOCS3 expression is deregulated between WT and Stat6^{-/-} samples at day 15 (K). Scale bars: B, 0,05 mm; D, 0,2 mm; J, L, 0,05 mm. D, H&E staining. B, J, L, hematoxylin as co-staining. Data are mean ± SEM.

Supporting the histological findings, RT-PCR analysis of whole colonic mucosal samples for inflammatory and chemoattractants-related genes, revealed significantly increased mRNA expression of the genes encoding *Il-1 β* , *Cox-2*, *Kc*, *Mip-2*, *Ccl-2*, *Il-6* and *Il-10* in *Stat6*^{-/-} mice at day 15. No differences between unchallenged animals were found (d0), (Figure 32 F-H).

Previously, John Elrod and colleagues speculated that *Stat6* loss might render myeloid cells with enhanced nitric oxide (NO) cytotoxicity towards microbes, regulating colitis severity [249]. Therefore, to verify whether this reactive metabolite was increased in BMDM from *Stat6*^{-/-} mice during inflammatory responses, BMDM were stimulated with different compounds. However, no differences were detected in NO release between genotypes, as depicted in Figure 32 I. Additionally, to check whether the ability to convert L-arginine to urea and ornithine was altered in *Stat6*^{-/-} mice - as IL-4 signaling controls arginase activity [250], which in turn modulates NO production - an arginase assay was performed. Upon IL-4 stimulation *Stat6*^{-/-} BMDM failed to generate urea and ornithine, evidencing that arginase levels are dependent on STAT6 *in vitro* (Figure 32 I).

Because the previous results showed that disruption of the IL-4 signaling during colitis-associated tumor model affected STAT3 activity, and considering that secretion of IL-6, IL-11 and IL-10 are known to influence its expression, STAT3 phosphorylation at Y705 was checked on day 15 in both genotypes. Immunohistochemistry detected a 6-fold stronger signal in *Stat6*^{-/-} enterocytes, which was greatly decreased in WT enterocytes, ($p \leq 0.001$), (Figure 32 J). Moreover, immunoblot analysis performed with unchallenged (d0) and 15 days treated colon lysates confirmed STAT3 enhanced activation and SOCS3 overexpression in *Stat6*-deficient colon lysates (Figure 32 K). Finally, it was hypothesized that the intense inflammatory response followed by the robust STAT3 activation would alter the process of mucosal regeneration, which involves epithelial cell hyperproliferation. Indeed, immunohistochemical analysis for BrdU incorporation revealed a significant increase in proliferation in enterocytes from *Stat6*^{-/-} mice at day 15 ($p \leq 0.001$), (Figure 32 L).

Collectively, these data show that *Stat6* deficiency affects IEC susceptibility to DSS-induced apoptosis, which leads to severe colitis. The extensive tissue damage found in *Stat6*^{-/-} mice induces massive immune cell infiltration and cytokine release into the colonic mucosa, triggering strong STAT3 activation in *Stat6*-deficient enterocytes. During the regenerative phase, overexpression of STAT3 leads to aberrant epithelial proliferation, thus promoting colorectal tumorigenesis.

4.3.6 Acute effects of AOM on *Stat6*^{-/-} IEC leads to increased DNA double strand breaks and apoptosis

AOM has been widely used for more than 40 years to study the molecular mechanisms involved in colorectal carcinogenesis. Upon its administration, AOM is hepatic metabolized by cytochrome P450 generating MAM. MAM is further degraded into 2 other metabolites, formaldehyde and reactive alkylating species, both highly toxic agents that can cause DNA damage and initiate tumorigenesis [251-253]. Acutely, the DNA alkylation and formation of O6-methylguanine lead to DNA damage and to the activation of several intracellular signaling pathways related to DNA damage response. Phosphorylation of Histone H2AX (γ -H2AX) at DNA double strand breaks (DSB) is one of the initial signals upon DNA damage and it is generally followed by P53 phosphorylation at serine 15 (Ser15), which in mouse corresponds to serine 18. P53 activation can result in DNA repair, cell cycle arrest, senescence and/or apoptosis. The last generally triggered via transcriptional induction of genes that encode pro-apoptotic factors, such as *Bax* and *Puma* [228, 254, 255].

To observe the acute carcinogenic effects of AOM on IEC and better understand the underlying mechanisms for increased tumorigenesis in *Stat6*^{-/-} mice, animals were subjected to one IP injection of AOM and sacrificed eight hours later (Figure 33 A). It was initially hypothesized that upon AOM administration STAT6-deficient IEC would be more susceptible to DNA damage with reduced P53 activation, which later would lead to increased acquisition of mutations, promoting colorectal tumor development. Indeed, immunohistochemical analysis for Histone H2AX phosphorylation using FFPE

Finally, knowing that the alkylating hit produced by AOM administration also induces IEC apoptosis, and this effect is generally mediated by P53 activity, the apoptotic response in enterocytes from WT and Stat6^{-/-} mice was evaluated. It was predicted that apoptotic rates would be reduced in Stat6^{-/-} IEC due to diminished P53 phosphorylation and unaltered expression of its target genes *Puma* and *Bax*, after DNA damage. Surprisingly, 8 hours after AOM treatment, Stat6^{-/-} mice showed enhanced cleaved-CASPASE 3 expression by IHC staining, when compared to WT mice ($p \leq 0.01$), (Figure 33 E). Furthermore, unchallenged Stat6^{-/-} mice also presented enhanced apoptosis rates than WT mice ($p \leq 0.05$), (Figure 33 E).

Thus, these results indicate that STAT6-deficient IEC are more susceptible to DNA damage produced by alkylating agents, such as AOM. Furthermore, they show that *Stat6* loss influences P53 activation, evidenced by reduced P53 phosphorylation. Unexpectedly, we observed that Stat6 signaling in enterocytes protects these cells from apoptosis, as both unchallenged and AOM-treated Stat6^{-/-} mice show increased expression of cleaved-CASPASE 3. Intriguingly, this event seems to be independent of P53 activity.

5 DISCUSSION

The aim of the current work was to determine the contribution of IL-4 signaling molecules IL-4R α and STAT6 to colorectal tumor development in a mouse model of colitis-associated tumorigenesis. The findings revealed that the role of IL-4 signaling differs dramatically depending on the signaling component analyzed. It was demonstrated that both IL-4R α and STAT6 exert specific cell-intrinsic functions affecting IEC cell survival and proliferation during colitis-associated tumorigenesis. Above all, it was shown that despite IL-4R α and STAT6 make part of the same signaling axis, their loss during the initial events of tumor development lead to remarkably opposite outcomes. This work provides further evidence for the underlying mechanisms of IL-4 signaling in colorectal carcinogenesis and demonstrates the importance of dismembering cellular signaling pathways in order to comprehend their regulatory complexities better.

5.1 Global deletion of *Il-4r α* suppresses colorectal tumorigenesis by reducing STAT3 activity and inducing intestinal epithelial cell cycle arrest

The lack of detailed information about IL-4R α , a component of the IL-4 signaling, in colorectal malignant transformation prompted the investigation of which would be the effects of *Il-4r α* loss during colitis-associated tumorigenesis. Making use of the AOM/DSS tumor model, it was shown that mice with global deletion of *Il-4r α* had fewer and smaller colonic tumors when compared to WT mice. These findings are partially in accordance with a preliminary report by Felicitas Koller and colleagues [157], where the authors suggested that *Il-4r α* loss during AOM/DSS treatment reduces tumorigenesis by inhibiting proliferation and enhancing apoptosis of transformed cells. However, in the present analysis, no differences in apoptosis in tumors were found. One possible explanation could be the differences in the adopted AOM/DSS protocol. Unlike in the study of Felicitas Koller and colleagues, that sacrificed animals approximately 40 days after the beginning of the treatment,

the currently experimental set up consisted in exposing the mice to two IP injections of AOM and three cycles of DSS, sacrificing animals 84 days after the beginning of the experiment. It is possible that at this later time point differences in cleaved-CASPASE 3 expression are not any longer detected.

Additionally, it was reported that global deletion of *Il-4r α* during colitis-associated tumor model reduces STAT3 activity in transformed colonocytes. In normal and untransformed cells, the levels of activated STAT3 remain transient; however, STAT3 remains constitutively active in approximately 70% of solid human tumors [256]. Its constitutive activation regulates the expressions of many target genes, such as, *Cyclin B1*, *Cyclin D1*, *c-Myc*, *Bcl-xl*, and *Survivin*, which are closely involved in tumorigenesis and tumor survival [257-262]. The importance of epithelial *Stat3* expression to IEC survival and cell cycle progression has been already proven by many elegant studies [175, 203, 263-265]. The reduction in STAT3 activity after the *Il-4r α* loss could explain why pre-neoplastic lesions from IL-4R $\alpha^{\text{del/del}}$ mice display similar rates of BrdU incorporation, an established S-phase marker, but show reduced proliferation by the M-phase marker phospho-Histone H3. Whereas transformed WT colonocytes progress to cell division, most IL-4R α -deficient cells stay in cell-cycle arrest at G2. It was shown that the reduction in proliferation observed in the tumors of IL-4R $\alpha^{\text{del/del}}$ mice was caused by decreased expression of CYCLIN E and CYCLIN B1 – the last, a crucial molecule for adequate cell cycle progression from G2 to the M-phase and known to be also regulated by STAT3 [266, 267]. Overexpression of CYCLIN B1 is observed in several malignancies including laryngeal and esophageal squamous cell carcinoma and colorectal carcinomas [268-271]. Therefore, CYCLIN B1 downregulation in *Il-4r α* -deficient mice could also be directly involved in the reduced neoplastic transformation and consequently in tumorigenesis.

Although immunohistochemical analysis of tumors from WT and IL-4R $\alpha^{\text{del/del}}$ mice at the 84th day of the AOM/DSS regime did not detect differences in cleaved-CASPASE 3 expression, it was demonstrated that IL-4R $\alpha^{\text{del/del}}$ mice tumors distinctly express reduced levels of the anti-apoptotic protein BCL-XL and increased expression of the pro-apoptotic protein BAD.

Whereas BCL-XL may be directly regulated by STAT3 activity [203, 264], BAD expression could be controlled through IL-4 signaling, as binding of IL-4/IL-13 to IL-4R α also induces the phosphorylation of insulin receptor substrate 1/2 (IRS 1/2) activating the PI3K/AKT pathway. When active, AKT is able to phosphorylate BAD, suppressing BAD expression and its antagonistic functions against anti-apoptotic proteins. In line, pharmacologic inhibitors and dominant inhibitory forms of PI3K and AKT abolish the anti-apoptotic effects of IL-4 [272]. Thus, *Il-4r α* deletion could cause a reduction in the PI3K/AKT pathway activity, explaining the increase in BAD expression.

5.2 IEC-specific deletion of *Il-4r α* suppresses tumor development by inducing apoptosis of the initiated cells and by preventing epithelial hyperproliferation after DSS-induced colitis

Since both tumor and stromal cells were deficient in IL-4R α in the IL-4R $\alpha^{\text{del/del}}$ mice, the contribution of *Il-4r α* loss on IEC to the obtained phenotype during colitis-associated tumorigenesis could not be precisely evaluated. To address this issue, further experiments with IL-4R $\alpha^{\Delta\text{IEC}}$ mice were performed.

As observed with IL-4R $\alpha^{\text{del/del}}$ mice, it was shown that deletion of *Il-4r α* specifically in IEC during steady-state conditions did not induce any tumor-promoter phenotype, whereas during colitis-associated tumor model IL-4R α loss modulated tumorigenesis. Intriguingly, IL-4R $\alpha^{\Delta\text{IEC}}$ mice showed significantly reduced tumor growth but no differences in tumor initiation. This interesting finding made us speculate that *Il-4r α* loss in other cell types than enterocytes might also play a role during colorectal tumorigenesis. It is well known that in collaboration to intrinsic cellular mechanisms to counter tumorigenesis (e.g. activation of tumor suppressor genes), the immune system plays a critical role in the identification and elimination of transformed cells. This extraordinary action is executed based on the expression of molecules produced during cellular stress response and by the detection of specific tumor antigens in transformed cells [273-275]. Therefore, it was considered that *Il-4r α* expression in immune cells could affect tumor immune

surveillance. Moreover, it has been already shown that during the early stages of tumorigenesis some signaling pathways activated by transformed cells may disturb innate immune response against the establishment of tumors and consequently even accelerate their development and growth [276, 277]. This issue will be further addressed by future studies, but the preliminary data obtained by using mice with *Il-4r α* -specific deletion in myeloid cells indicate that *Il-4r α* expression in macrophages and neutrophils could influence colorectal tumor immune surveillance (unpublished, data not shown), explaining why IL-4R $\alpha^{\Delta\text{IEC}}$ mice did not present differences in tumor initiation.

Focusing on the direct effects of *Il-4r α* loss in enterocytes it was further demonstrated that tumors from IL-4R $\alpha^{\Delta\text{IEC}}$ mice also exhibited reduced proliferation by a clear reduction in phosphorylated Histone H3, once more denoting cell cycle arrest at the G2-phase. Additionally, although significant differences in apoptosis between IL-4R α -deficient and proficient tumors could not be detected by cleaved-CASPASE 3, at the early stages of tumorigenesis *Il-4r α* -deficient enterocytes were highly susceptible to DSS-induced apoptosis caused by reduced BCL-2 and BCL-XL expression (Figure 28 C and data not shown, respectively). These findings support the idea that one of the reasons for reduced tumorigenesis in *Il-4r α* -deficient mice is the death of the initiated epithelium. This action prevents the accumulation of transformed epithelial cells, which can trigger intestinal tumor development due to a dysregulation in their genetic program controlling proliferation and apoptosis [203, 278]. BCL-2 plays a crucial role in regulating cell survival through protein-protein interactions with other Bcl-2-related family members, including BCL-XL and the death agonists BAD and BAX [279]. The expression of these anti-apoptotic proteins can be a direct consequence of IL-4 and STAT3-mediated transcriptional regulation, therefore explaining their reduced expression [203, 248, 257, 280-282]. Interestingly, it was observed that although IL-4R α -deficient IEC presented enhanced apoptosis, there were no differences in the resolution of inflammation at day 15 of the AOM/DSS regime. This finding could be theoretically caused by the inability of IL-4R $\alpha^{\Delta\text{IEC}}$ mice to recruit inflammatory cells into the *lamina propria* after DSS exposure. Supporting this hypothesis, RT-PCR analysis for chemoattractants and inflammatory

cytokines expression did not reveal any differences between the two genotypes at this time point (d15).

Furthermore, it could be speculated that *Il-4* α loss in IEC may be compensated by other factors involved in mucosal wound healing which were not evaluated in this study and remain to be determined such as, pancreatitis associated protein (PAP), heat shock proteins (HSPs) and Toll-like receptors (TLR) [283-285]. It has been suggested that PAP represents an anti-inflammatory mechanism in colitis due to its ability to inhibit NF- κ B activation, decrease cytokine production and adhesion molecule expression in inflamed tissue [286-288]. Thus, PAP could counteract the inflammatory response by inhibiting leukocyte recruitment into the intestine.

During colitis, intestinal epithelial cells secrete many pro-inflammatory cytokines and chemokines. The regulation of this secretion is necessary to prevent chronic inflammation and extra mucosal damage. HSPs play a major role protecting against inflammation by inhibiting pro-inflammatory cytokine production. Moreover, It has been shown that HSP70 has important anti-apoptotic effects on IEC and can protect them from DSS-induced colitis [289, 290]. Additionally, TLR expression has been already correlated with intestinal epithelial cell protection during bacterial LPS-induced inflammation. Moreover, TLR can mediate IEC responses during the development of colitis [291-293]. Hence, TLR can modulate colonic homeostasis protecting IECs from injury.

Lastly, it has been shown by elegant studies on colitis-associated cancer that aberrant epithelial proliferation during inflammatory insults can predispose to neoplastic transformation [197, 201, 203, 294-296]. Therefore, the finding that IL-4R $\alpha^{\Delta IEC}$ mice presented reduced IEC proliferation at the regenerative phase after acute DSS-induced colitis could represent another mechanism by which these animals exhibited reduced tumorigenesis.

5.3 *Stat6* deletion promotes colorectal tumorigenesis by inducing aberrant overexpression of STAT3 during colitis-associated tumor

In vitro and *in vivo* studies support the concept that STAT6 is crucial to transcriptional activation in response to IL-4 and IL-13 stimulation, highlighting

the importance of STAT6 to IL-4 signaling inducible genes [124, 142, 297, 298]. Therefore, it was hypothesized that *Stat6* ablation during colitis-associated tumor model would generate similar results as the ones obtained with *Il-4Rα* knockout mice. The results obtained demonstrated that *Stat6* loss did not perturb intestinal homeostasis in steady-state conditions; however, it strongly modulated colorectal tumorigenesis. Conversely to what was observed in *IL-4Rα^{del/del}* and *IL-4Rα^{ΔIEC}* mice, *Stat6^{-/-}* mice showed increased tumor formation and enhanced tumor growth when compared to WT mice. Interestingly, although tumors from both genotypes did not show differences regarding tumor cell proliferation or apoptosis, *Stat6*-deficient tumors exhibited significantly enhanced STAT3 activity.

It is well known that many cytokine receptors are phosphorylated on their cytoplasmic tyrosine residues in response to stimuli, and that these phosphorylated residues can function as docking sites for Stats and other signaling molecules [299]. Most important, previous experiments using *Stat*-deficient cells showed that when the dominant STAT does not occupy its cytokine receptor, another STAT member might take over the unoccupied receptor and be activated in response to stimuli signaling through this receptor [300, 301]. This effect can be observed in *Stat1*-deficient mouse embryonic fibroblasts (MEFs). STAT1 is the main transcription factors of IFN γ , and noticeably under normal physiological conditions, STAT3 activation can also be faintly observed upon IFN γ stimulation. However, in *Stat1*-deficient MEFs Src Kinases trigger robust STAT3 tyrosine phosphorylation upon IFN γ stimulation [300]. Furthermore, Costa-Pereira and colleagues demonstrated a similar switch in MEFs lacking STAT3. In this scenario, stimulation with IL-6 mediates an IFN γ -like response, including STAT1 activation and expression of IFN γ related genes [302]. It is relevant to mention that STAT3 and STAT6 have similar structures and are both phosphorylated on tyrosine residues by Janus kinases upon cytokine stimulation. Both Stats form dimers through their reciprocal SH2 domain and translocate to the nucleus to activate the transcription of their target genes [144, 301]. Thereby, the loss of *Stat6* in IEC could induce a STAT3 compensatory activation. In line, the unexpected STAT3 overexpression in *Stat6*-deficient tumors cells could

also be explained by IL-4 signaling being able to activate the downstream signaling pathways JAK, PI3K/AKT and MAPK/ERK, which can further promote STAT3 expression [136, 137, 303]. Therefore, it is theoretically conceivable that in the absence of STAT6, these signaling pathways become sensitized to stimuli transmitted through IL-4R α and IL-13R α 1 due to the unmasking of tyrosine residues on the cytoplasmic domain of those receptors (which were previously blocked by the physical presence of STAT6). Indeed, western blot analysis of tumor lysates shows strong ERK phosphorylation in *Stat6*-deficient tumors. Moreover, it cannot be excluded that STAT6 ablation might affect IL-4R α physical interaction with IL-13R α 1, causing conformational changes in the receptor complex favoring the recruitment and activation of STAT3 [304]. These hypotheses need to be further evaluated in the context of colitis-associated tumorigenesis, but our results support the idea that *Stat6*-deficiency during colitis-associated tumorigenesis leads to STAT3 compensatory activation.

Additionally, it was shown that P53 activity, which is crucial for cell-autonomous mechanisms such as cell cycle regulation, senescence and apoptosis and which tumor-suppressor function is well established in colorectal cancer [205, 305], is highly decreased in *Stat6*^{-/-} tumors. P53 can be regulated by many different factors, and recent reports showed a direct and indirect cross-talk with STAT3 [306-310]. STAT3 activation is able to disrupt P53 function through various mechanisms. First, it is suggested that STAT3 might directly bind and interact with the P53 promoter and exert inhibitory effects on its activity [306, 309]. Second, STAT3 may induce the expression of molecules that can repress the transcriptional activity of P53 such as Fat10 [307]. Last, *Stat3* might transcriptionally induce molecules that increase MDM2 expression and consequently increase P53 protein degradation. Thus, the high STAT3 activity found in *Stat6*-deficient tumors provides a functional explanation for the observations on P53 decreased expression [310].

In addition to the above hypothesis, it is suggested that the total cellular levels of P53 are not strictly regulated by the ratio of its production, but by the ratio of its degradation [311]. Therefore, it could be speculated that

Stat6 deficiency could directly increase P53 degradation, which usually is mediated by ubiquitination and proteasomal degradation [312, 313]. However, the activity of MDM2 – P53 major negative regulator – and other ubiquitin ligases involved in this process were not assessed and remain to be evaluated.

5.4 DSS-induced colitis is exacerbated in *Stat6*^{-/-} mice

The current literature on STAT6 contribution to intestinal inflammation is sparse and notably contradictory depending on the model studied [249, 314, 315]. In the current work, it was demonstrated that loss of *Stat6* in IEC at the early stages of carcinogenesis leads to a strong inflammatory response and to a tumor-promoter phenotype. These findings are in agreement with the previous work of Elrod and colleagues [249], as this study also shows that DSS-induced colitis is exacerbated in *Stat6*^{-/-} mice. Furthermore, adoptive transfer experiments support the idea that the severe colitis phenotype observed in *Stat6*^{-/-} mice is probably due to intrinsic IEC changes caused by *Stat6* loss. DSS-induced colitis does not require T or B cells, as demonstrated by experiments with C.B17 severe immune deficient mice. In fact, the immune response in these mice is largely based on macrophages and myeloid-derived cytokines, such as IL-6 and IL-11 [316]. For this reason BMDM from *Stat6*^{-/-} mice were analyzed, and in contrast to what was proposed in previous studies [249, 315], *Stat6*-deficient macrophages did not present enhanced nitric oxide cytotoxicity (Figure 32 I) or showed reduced expression of canonical Wnt ligands (data not shown), which could regulate colitis severity. Nevertheless, additional experiments are needed to clarify the impact of *Stat6* deficiency in other immune cells than macrophages during AOM/DSS-induced colitis.

Additionally, it was demonstrated that due to the extensive tissue damage during colitis, *Stat6*^{-/-} mice have significantly increased expression of inflammatory cytokines and chemokines. Strong IL-6, IL-10, and IL-11 expression during colitis are known to induce STAT3 activation in IEC, which in *Stat6*-deficient enterocytes could disturb the regeneration phase and induce aberrant hyperproliferation. Moreover, the mutual positive feedback loop between STAT3, IL-6, IL-10 and IL-11 could lead to tumor formation and

tumor maintenance in long-term experiments with AOM/DSS [317]. The higher proliferative rates observed in *Stat6*-deficient IEC on day 15 of the AOM/DSS regime (regenerative phase) support this hypothesis. Lastly, the evaluation of the STAT6 contribution in colitis-independent tumor models remains to be evaluated.

5.5 *Stat6* expression protects IEC from AOM-induced DNA damage and apoptosis

Based on the existing literature, this is the first study to show that *Stat6*-deficient IEC are highly susceptible to DNA damage caused by AOM followed by reduced P53 effector response. It is unknown how STAT6 expression could participate in DNA damage response, but it could be speculated that its loss may disturb the activity of molecules involved in this process, such as ataxia-telangiectasia mutated (ATM), ataxia-telangiectasia mutated and Rad3-related (ATR) and DNA-dependent protein kinase catalytic subunit (DNA-PK), among others. The proper function of these kinases is crucial for detection of DNA breaks, DNA repair and further activation of downstream effectors proteins, in particular, X-ray repair cross-complementary protein 4 (XRCC4), implicated in non-homologous end joining (NHEJ) DNA repair, cell division cycle 25 (CDC25), associated with cell cycle arrest, and P53, which can be involved in the two previous outcomes, plus apoptosis [318-320].

Alkylating agents are considered to induce P53-dependent apoptosis in IEC within the first hours after its administration, generally through the activation of pro-apoptotic proteins such as PUMA, BAX, and NOXA. [321-325]. Therefore, it was reasoned that reduced P53 activation in IEC upon AOM administration would suppress the initial apoptotic response preventing loss of the initiated epithelia that would subsequently increase tumorigenesis in *Stat6*^{-/-} mice. Instead, *Stat6*-deficient enterocytes presented increased apoptotic rates upon the initial AOM challenge.

Whereas P53 reduced activity can be related to increased DNA damage in *Stat6*^{-/-} mice, its reduced activation cannot be linked to the enhanced apoptotic phenotype. These findings are supported by the strong

evidence that IEC-specific deletion of P53 does not cause spontaneous or AOM-induced apoptosis *in vivo* [205], suggesting that the AOM-induced apoptosis detected in *Stat6*-deficient IEC is a P53-independent event. Moreover, the involvement of P63 and P73 in P53-independent apoptosis could probably be neglected in *Stat6*-deficient IEC as these transcription factors ordinarily induce *Puma* and *Bax* expression to trigger mitochondrial membrane permeabilization [326, 327]. Both *Puma* and *Bax* mRNA levels were not found altered between WT and *Stat6*-deficient IEC at this time point. Thus, the underlying mechanisms that led to Caspase 3 cleavage and the possible involvement of other molecules such as Caspase 8 and 9, BID and DIABLO in this process still need to be evaluated.

REFERENCES

1. Standring S, G.H., *Gray's anatomy: the anatomical basis of clinical practice*. 40th ed. 2008, Edinburg: Churchill Livingstone.
2. Weaver, L.T., S. Austin, and T.J. Cole, *Small intestinal length: a factor essential for gut adaptation*. Gut, 1991. **32**(11): p. 1321-3.
3. Aron-Wisnewsky, J., J. Dore, and K. Clement, *The importance of the gut microbiota after bariatric surgery*. Nat Rev Gastroenterol Hepatol, 2012. **9**(10): p. 590-8.
4. Nguyen, T.L.A., et al., *How informative is the mouse for human gut microbiota research?* Disease Models & Mechanisms, 2015. **8**(1): p. 1-16.
5. Droy-Dupre, L., et al., *A multiparametric approach to monitor the effects of gamma-secretase inhibition along the whole intestinal tract*. Dis Model Mech, 2012. **5**(1): p. 107-14.
6. Barker, N., M. van de Wetering, and H. Clevers, *The intestinal stem cell*. Genes Dev, 2008. **22**(14): p. 1856-64.
7. Abdul Khalek, F.J., G.I. Gallicano, and L. Mishra, *Colon cancer stem cells*. Gastrointest Cancer Res, 2010(Suppl 1): p. S16-23.
8. Troughton, W.D. and J.S. Trier, *Paneth and goblet cell renewal in mouse duodenal crypts*. J Cell Biol, 1969. **41**(1): p. 251-68.
9. Crosnier, C., D. Stamataki, and J. Lewis, *Organizing cell renewal in the intestine: stem cells, signals and combinatorial control*. Nat Rev Genet, 2006. **7**(5): p. 349-59.
10. van der Flier, L.G. and H. Clevers, *Stem cells, self-renewal, and differentiation in the intestinal epithelium*. Annu Rev Physiol, 2009. **71**: p. 241-60.
11. Peterson, L.W. and D. Artis, *Intestinal epithelial cells: regulators of barrier function and immune homeostasis*. Nat Rev Immunol, 2014. **14**(3): p. 141-53.
12. Humphries, A. and N.A. Wright, *Colonic crypt organization and tumorigenesis*. Nat Rev Cancer, 2008. **8**(6): p. 415-24.
13. Barker, N., et al., *Identification of stem cells in small intestine and colon by marker gene Lgr5*. Nature, 2007. **449**(7165): p. 1003-7.
14. Sangiorgi, E. and M.R. Capecchi, *Bmi1 is expressed in vivo in intestinal stem cells*. Nat Genet, 2008. **40**(7): p. 915-20.
15. Barker, N., *Adult intestinal stem cells: critical drivers of epithelial homeostasis and regeneration*. Nat Rev Mol Cell Biol, 2014. **15**(1): p. 19-33.
16. Rothenberg, M.E., et al., *Identification of a cKit(+) colonic crypt base secretory cell that supports Lgr5(+) stem cells in mice*. Gastroenterology, 2012. **142**(5): p. 1195-1205 e6.
17. Ross, M.P., W., *Histology: a text and atlas*. 5th ed. 2006, USA: Lippincott Williams & Wilkins. 906.
18. Sandle, G.I., *Salt and water absorption in the human colon: a modern appraisal*. Gut, 1998. **43**(2): p. 294-9.

19. Cardell, R.R., Jr., S. Badenhauen, and K.R. Porter, *Intestinal triglyceride absorption in the rat. An electron microscopical study.* J Cell Biol, 1967. **34**(1): p. 123-55.
20. Kim, Y.S. and S.B. Ho, *Intestinal goblet cells and mucins in health and disease: recent insights and progress.* Curr Gastroenterol Rep, 2010. **12**(5): p. 319-30.
21. William K. Ovalle, P.C.N., *Netter's Essential Histology.* 2008: SAUNDERS-ELSEVIER.
22. Bergstrom, K.S., et al., *Goblet Cell Derived RELM-beta Recruits CD4+ T Cells during Infectious Colitis to Promote Protective Intestinal Epithelial Cell Proliferation.* PLoS Pathog, 2015. **11**(8): p. e1005108.
23. Velich, A., et al., *Colorectal cancer in mice genetically deficient in the mucin Muc2.* Science, 2002. **295**(5560): p. 1726-9.
24. Rudolph, U., et al., *Ulcerative colitis and adenocarcinoma of the colon in G alpha i2-deficient mice.* Nat Genet, 1995. **10**(2): p. 143-50.
25. Hermiston, M.L. and J.I. Gordon, *Inflammatory bowel disease and adenomas in mice expressing a dominant negative N-cadherin.* Science, 1995. **270**(5239): p. 1203-7.
26. Engle, S.J., et al., *Transforming growth factor beta1 suppresses nonmetastatic colon cancer at an early stage of tumorigenesis.* Cancer Res, 1999. **59**(14): p. 3379-86.
27. Gunawardene, A.R., B.M. Corfe, and C.A. Staton, *Classification and functions of enteroendocrine cells of the lower gastrointestinal tract.* Int J Exp Pathol, 2011. **92**(4): p. 219-31.
28. Melmed, P.M.C.S., *Endocrinology: Basic and Clinical Principles.* The Endocrine System of the Gastrointestinal Tract, ed. R.F. Gary A. Wittert, John E. Morley. 1997: Humana Press.
29. Sjolund, K., et al., *Endocrine cells in human intestine: an immunocytochemical study.* Gastroenterology, 1983. **85**(5): p. 1120-30.
30. Schonhoff, S.E., M. Giel-Moloney, and A.B. Leiter, *Minireview: Development and differentiation of gut endocrine cells.* Endocrinology, 2004. **145**(6): p. 2639-44.
31. Bertrand, P.P. and R.L. Bertrand, *Serotonin release and uptake in the gastrointestinal tract.* Auton Neurosci, 2010. **153**(1-2): p. 47-57.
32. Skibicka, K.P., *The central GLP-1: implications for food and drug reward.* Front Neurosci, 2013. **7**: p. 181.
33. Furness, J.B., et al., *The gut as a sensory organ.* Nat Rev Gastroenterol Hepatol, 2013. **10**(12): p. 729-40.
34. Rindi, G., et al., *The "normal" endocrine cell of the gut: changing concepts and new evidences.* Ann N Y Acad Sci, 2004. **1014**: p. 1-12.
35. Rhodin, J. and T. Dalhamn, *Electron microscopy of the tracheal ciliated mucosa in rat.* Z Zellforsch Mikrosk Anat, 1956. **44**(4): p. 345-412.
36. Jarvi, O. and O. Keyrilainen, *On the cellular structures of the epithelial invasions in the glandular stomach of mice caused by intramural application of 20-methylcholantrén.* Acta Pathol Microbiol Scand Suppl, 1956. **39**(Suppl 111): p. 72-3.
37. Jarvi, O., et al., *The cytologic diagnosis of pulmonary carcinoma.* Acta Pathol Microbiol Scand Suppl, 1962. **Suppl 154**: p. 177-8.

38. Luciano, L., E. Reale, and H. Ruska, [*On a "chemoreceptive" sensory cell in the tachea of the rat*]. *Z Zellforsch Mikrosk Anat*, 1968. **85**(3): p. 350-75.
39. Luciano, L., E. Reale, and H. Ruska, [*Brush cells in the alveolar epithelium of the rat lung*]. *Z Zellforsch Mikrosk Anat*, 1969. **95**(2): p. 198-201.
40. Hofer, D. and D. Drenckhahn, *Identification of brush cells in the alimentary and respiratory system by antibodies to villin and fimbrin*. *Histochemistry*, 1992. **98**(4): p. 237-42.
41. Chang, L.Y., R.R. Mercer, and J.D. Crapo, *Differential distribution of brush cells in the rat lung*. *Anat Rec*, 1986. **216**(1): p. 49-54.
42. Hammond, J.B. and L. LaDeur, *Fibrillovesicular cedlls in the fundic glands of the canine stomach: evidence for a new cell type*. *Anat Rec*, 1968. **161**(4): p. 393-411.
43. Luciano, L., E. Reale, and H. Ruska, [*On a glycogen containing brusc cell in the rectum of the rat*]. *Z Zellforsch Mikrosk Anat*, 1968. **91**(1): p. 153-8.
44. Isomaki, A.M., *A new cell type (tuft cell) in the gastrointestinal mucosa of the rat. A transmission and scanning electron microscopic study*. *Acta Pathol Microbiol Scand A*, 1973: p. Suppl 240:1-35.
45. Wattel, W. and J.J. Geuze, *The cells of the rat gastric groove and cardia. An ultrastructural and carbohydrate histochemical study, with special reference to the fibrillovesicular cells*. *Cell Tissue Res*, 1978. **186**(3): p. 375-91.
46. Tsubouchi, S. and C.P. Leblond, *Migration and turnover of entero-endocrine and caveolated cells in the epithelium of the descending colon, as shown by radioautography after continuous infusion of 3H-thymidine into mice*. *Am J Anat*, 1979. **156**(4): p. 431-51.
47. Luciano, L., M. Castellucci, and E. Reale, *The brush cells of the common bile duct of the rat. This section, freeze-fracture and scanning electron microscopy*. *Cell Tissue Res*, 1981. **218**(2): p. 403-20.
48. Luciano, L. and E. Reale, *Brush cells of the mouse gallbladder. A correlative light- and electron-microscopical study*. *Cell Tissue Res*, 1990. **262**(2): p. 339-49.
49. Hofer, D. and D. Drenckhahn, *Identification of the taste cell G-protein, alpha-gustducin, in brush cells of the rat pancreatic duct system*. *Histochem Cell Biol*, 1998. **110**(3): p. 303-9.
50. Reid, L., et al., *The mysterious pulmonary brush cell: a cell in search of a function*. *Am J Respir Crit Care Med*, 2005. **172**(1): p. 136-9.
51. Gerbe, F., et al., *Distinct ATOH1 and Neurog3 requirements define tuft cells as a new secretory cell type in the intestinal epithelium*. *J Cell Biol*, 2011. **192**(5): p. 767-80.
52. Noah, T.K., B. Donahue, and N.F. Shroyer, *Intestinal development and differentiation*. *Exp Cell Res*, 2011. **317**(19): p. 2702-10.
53. von Moltke, J., et al., *Tuft-cell-derived IL-25 regulates an intestinal ILC2-epithelial response circuit*. *Nature*, 2016. **529**(7585): p. 221-5.
54. Howitt, M.R., et al., *Tuft cells, taste-chemosensory cells, orchestrate parasite type 2 immunity in the gut*. *Science*, 2016. **351**(6279): p. 1329-33.
55. van Es, J.H., et al., *Dll1+ secretory progenitor cells revert to stem cells upon crypt damage*. *Nat Cell Biol*, 2012. **14**(10): p. 1099-104.
56. Hofer, D., E. Asan, and D. Drenckhahn, *Chemosensory Perception in the Gut*. *News Physiol Sci*, 1999. **14**: p. 18-23.

57. Gill, S.R., et al., *Metagenomic analysis of the human distal gut microbiome*. Science, 2006. **312**(5778): p. 1355-9.
58. Sartor, R.B., *Microbial influences in inflammatory bowel diseases*. Gastroenterology, 2008. **134**(2): p. 577-94.
59. Eckburg, P.B., et al., *Diversity of the human intestinal microbial flora*. Science, 2005. **308**(5728): p. 1635-8.
60. Palmer, C., et al., *Development of the human infant intestinal microbiota*. PLoS Biol, 2007. **5**(7): p. e177.
61. Johansson, M.E., et al., *The inner of the two Muc2 mucin-dependent mucus layers in colon is devoid of bacteria*. Proc Natl Acad Sci U S A, 2008. **105**(39): p. 15064-9.
62. Gallo, R.L. and L.V. Hooper, *Epithelial antimicrobial defence of the skin and intestine*. Nat Rev Immunol, 2012. **12**(7): p. 503-16.
63. Chassard, C. and C. Lacroix, *Carbohydrates and the human gut microbiota*. Curr Opin Clin Nutr Metab Care, 2013. **16**(4): p. 453-60.
64. Fukuda, S., et al., *Bifidobacteria can protect from enteropathogenic infection through production of acetate*. Nature, 2011. **469**(7331): p. 543-7.
65. Lawley, T.D., et al., *Antibiotic treatment of clostridium difficile carrier mice triggers a supershedder state, spore-mediated transmission, and severe disease in immunocompromised hosts*. Infect Immun, 2009. **77**(9): p. 3661-9.
66. Osawa, N. and S. Mitsuhashi, *Infection of Germfree Mice with Shigella Flexneri 3a*. Jpn J Exp Med, 1964. **34**: p. 77-80.
67. Bohnhoff, M., B.L. Drake, and C.P. Miller, *Effect of streptomycin on susceptibility of intestinal tract to experimental Salmonella infection*. Proc Soc Exp Biol Med, 1954. **86**(1): p. 132-7.
68. Hentges, D.J. and R. Freter, *In vivo and in vitro antagonism of intestinal bacteria against Shigella flexneri. I. Correlation between various tests*. J Infect Dis, 1962. **110**: p. 30-7.
69. Hooper, L.V. and A.J. Macpherson, *Immune adaptations that maintain homeostasis with the intestinal microbiota*. Nat Rev Immunol, 2010. **10**(3): p. 159-69.
70. Stecher, B. and W.D. Hardt, *Mechanisms controlling pathogen colonization of the gut*. Curr Opin Microbiol, 2011. **14**(1): p. 82-91.
71. Tremaroli, V. and F. Backhed, *Functional interactions between the gut microbiota and host metabolism*. Nature, 2012. **489**(7415): p. 242-9.
72. Sjogren, K., et al., *The gut microbiota regulates bone mass in mice*. J Bone Miner Res, 2012. **27**(6): p. 1357-67.
73. Glaister, J.R., *Factors affecting the lymphoid cells in the small intestinal epithelium of the mouse*. Int Arch Allergy Appl Immunol, 1973. **45**(5): p. 719-30.
74. Lee, Y.K. and S.K. Mazmanian, *Has the microbiota played a critical role in the evolution of the adaptive immune system?* Science, 2010. **330**(6012): p. 1768-73.
75. Jostins, L., et al., *Host-microbe interactions have shaped the genetic architecture of inflammatory bowel disease*. Nature, 2012. **491**(7422): p. 119-24.

76. Sun, L., G.M. Nava, and T.S. Stappenbeck, *Host genetic susceptibility, dysbiosis, and viral triggers in inflammatory bowel disease*. Curr Opin Gastroenterol, 2011. **27**(4): p. 321-7.
77. Seksik, P., et al., *Alterations of the dominant faecal bacterial groups in patients with Crohn's disease of the colon*. Gut, 2003. **52**(2): p. 237-42.
78. Rajilic-Stojanovic, M., et al., *Phylogenetic analysis of dysbiosis in ulcerative colitis during remission*. Inflamm Bowel Dis, 2013. **19**(3): p. 481-8.
79. Machiels, K., et al., *A decrease of the butyrate-producing species Roseburia hominis and Faecalibacterium prausnitzii defines dysbiosis in patients with ulcerative colitis*. Gut, 2014. **63**(8): p. 1275-83.
80. He, Q., et al., *Dysbiosis of the fecal microbiota in the TNBS-induced Crohn's disease mouse model*. Appl Microbiol Biotechnol, 2016. **100**(10): p. 4485-94.
81. Kang, S., et al., *Dysbiosis of fecal microbiota in Crohn's disease patients as revealed by a custom phylogenetic microarray*. Inflamm Bowel Dis, 2010. **16**(12): p. 2034-42.
82. Duboc, H., et al., *Connecting dysbiosis, bile-acid dysmetabolism and gut inflammation in inflammatory bowel diseases*. Gut, 2013. **62**(4): p. 531-9.
83. Frank, D.N., et al., *Molecular-phylogenetic characterization of microbial community imbalances in human inflammatory bowel diseases*. Proc Natl Acad Sci U S A, 2007. **104**(34): p. 13780-5.
84. Dalal, S.R. and E.B. Chang, *The microbial basis of inflammatory bowel diseases*. J Clin Invest, 2014. **124**(10): p. 4190-6.
85. Kim, E.R. and D.K. Chang, *Colorectal cancer in inflammatory bowel disease: the risk, pathogenesis, prevention and diagnosis*. World J Gastroenterol, 2014. **20**(29): p. 9872-81.
86. Schwabe, R.F. and C. Jobin, *The microbiome and cancer*. Nat Rev Cancer, 2013. **13**(11): p. 800-12.
87. Biedermann, L. and G. Rogler, *The intestinal microbiota: its role in health and disease*. Eur J Pediatr, 2015. **174**(2): p. 151-67.
88. Arthur, J.C., et al., *Intestinal inflammation targets cancer-inducing activity of the microbiota*. Science, 2012. **338**(6103): p. 120-3.
89. Irrazabal, T., et al., *The multifaceted role of the intestinal microbiota in colon cancer*. Mol Cell, 2014. **54**(2): p. 309-20.
90. Mowat, A.M. and W.W. Agace, *Regional specialization within the intestinal immune system*. Nat Rev Immunol, 2014. **14**(10): p. 667-85.
91. Eberl, G. and M. Lochner, *The development of intestinal lymphoid tissues at the interface of self and microbiota*. Mucosal Immunol, 2009. **2**(6): p. 478-85.
92. Tomasello, E. and S. Bedoui, *Intestinal innate immune cells in gut homeostasis and immunosurveillance*. Immunol Cell Biol, 2013. **91**(3): p. 201-3.
93. Neutra, M.R., N.J. Mantis, and J.P. Kraehenbuhl, *Collaboration of epithelial cells with organized mucosal lymphoid tissues*. Nat Immunol, 2001. **2**(11): p. 1004-9.
94. O'Brien, L.M., et al., *Eosinophil-nerve interactions and neuronal plasticity in rat gut associated lymphoid tissue (GALT) in response to enteric parasitism*. J Neuroimmunol, 2008. **197**(1): p. 1-9.

95. Sipos, F., et al., *The possible role of isolated lymphoid follicles in colonic mucosal repair*. *Pathol Oncol Res*, 2010. **16**(1): p. 11-8.
96. Neutra, M.R., A. Frey, and J.P. Kraehenbuhl, *Epithelial M cells: gateways for mucosal infection and immunization*. *Cell*, 1996. **86**(3): p. 345-8.
97. Siebers, A. and B.B. Finlay, *M cells and the pathogenesis of mucosal and systemic infections*. *Trends Microbiol*, 1996. **4**(1): p. 22-9.
98. Mantis, N.J., et al., *Selective adherence of IgA to murine Peyer's patch M cells: evidence for a novel IgA receptor*. *J Immunol*, 2002. **169**(4): p. 1844-51.
99. Neutra, M.R., et al., *Transport of membrane-bound macromolecules by M cells in follicle-associated epithelium of rabbit Peyer's patch*. *Cell Tissue Res*, 1987. **247**(3): p. 537-46.
100. Jung, C., J.P. Hugot, and F. Barreau, *Peyer's Patches: The Immune Sensors of the Intestine*. *Int J Inflam*, 2010. **2010**: p. 823710.
101. Mitragotri, S., *Immunization without needles*. *Nat Rev Immunol*, 2005. **5**(12): p. 905-16.
102. Coombes, J.L. and F. Powrie, *Dendritic cells in intestinal immune regulation*. *Nat Rev Immunol*, 2008. **8**(6): p. 435-46.
103. Scott, C.L., A.M. Aumeunier, and A.M. Mowat, *Intestinal CD103+ dendritic cells: master regulators of tolerance?* *Trends Immunol*, 2011. **32**(9): p. 412-9.
104. Bogunovic, M., et al., *Origin of the lamina propria dendritic cell network*. *Immunity*, 2009. **31**(3): p. 513-25.
105. Schulz, O., et al., *Intestinal CD103+, but not CX3CR1+, antigen sampling cells migrate in lymph and serve classical dendritic cell functions*. *J Exp Med*, 2009. **206**(13): p. 3101-14.
106. Cerovic, V., et al., *Intestinal CD103(-) dendritic cells migrate in lymph and prime effector T cells*. *Mucosal Immunol*, 2013. **6**(1): p. 104-13.
107. Lee, S.H., P.M. Starkey, and S. Gordon, *Quantitative-Analysis of Total Macrophage Content in Adult-Mouse Tissues - Immunochemical Studies with Monoclonal-Antibody F4/80*. *Journal of Experimental Medicine*, 1985. **161**(3): p. 475-489.
108. Bain, C.C. and A.M. Mowat, *Macrophages in intestinal homeostasis and inflammation*. *Immunol Rev*, 2014. **260**(1): p. 102-17.
109. Farache, J., et al., *Contributions of dendritic cells and macrophages to intestinal homeostasis and immune defense*. *Immunol Cell Biol*, 2013. **91**(3): p. 232-9.
110. Delamarre, L., et al., *Differential lysosomal proteolysis in antigen-presenting cells determines antigen fate*. *Science*, 2005. **307**(5715): p. 1630-4.
111. Charles A Janeway, J., Paul Travers, Mark Walport, and Mark J Shlomchik, *Immunobiology: Principles of innate and adaptive immunity*. 2001, New York: Garland Science.
112. Salmi, M. and S. Jalkanen, *Lymphocyte homing to the gut: attraction, adhesion, and commitment*. *Immunol Rev*, 2005. **206**: p. 100-13.
113. Nutt, S.L., et al., *The generation of antibody-secreting plasma cells*. *Nat Rev Immunol*, 2015. **15**(3): p. 160-71.
114. Andersen, M.H., et al., *Cytotoxic T cells*. *J Invest Dermatol*, 2006. **126**(1): p. 32-41.

115. Hirahara, K. and T. Nakayama, *CD4+ T-cell subsets in inflammatory diseases: beyond the Th1/Th2 paradigm*. Int Immunol, 2016. **28**(4): p. 163-71.
116. Kiraz, Y., Y. Baran, and A. Nalbant, *T cells in tumor microenvironment*. Tumour Biol, 2016. **37**(1): p. 39-45.
117. Barnes, M.J. and F. Powrie, *Regulatory T cells reinforce intestinal homeostasis*. Immunity, 2009. **31**(3): p. 401-11.
118. Rubtsov, Y.P., et al., *Regulatory T cell-derived interleukin-10 limits inflammation at environmental interfaces*. Immunity, 2008. **28**(4): p. 546-58.
119. Howard, M., et al., *Identification of a T cell-derived b cell growth factor distinct from interleukin 2*. J Exp Med, 1982. **155**(3): p. 914-23.
120. Paul, W.E., *History of interleukin-4*. Cytokine, 2015. **75**(1): p. 3-7.
121. Ahdieh, M., T. Vandenbos, and A. Youakim, *Lung epithelial barrier function and wound healing are decreased by IL-4 and IL-13 and enhanced by IFN-gamma*. Am J Physiol Cell Physiol, 2001. **281**(6): p. C2029-38.
122. Yan, D., et al., *STAT3 and STAT6 Signaling Pathways Synergize to Promote Cathepsin Secretion from Macrophages via IRE1alpha Activation*. Cell Rep, 2016. **16**(11): p. 2914-27.
123. Zurawski, G. and J.E. de Vries, *Interleukin 13 elicits a subset of the activities of its close relative interleukin 4*. Stem Cells, 1994. **12**(2): p. 169-74.
124. Shimoda, K., et al., *Lack of IL-4-induced Th2 response and IgE class switching in mice with disrupted Stat6 gene*. Nature, 1996. **380**(6575): p. 630-3.
125. de Waal Malefyt, R., et al., *Differential regulation of IL-13 and IL-4 production by human CD8+ and CD4+ Th0, Th1 and Th2 T cell clones and EBV-transformed B cells*. Int Immunol, 1995. **7**(9): p. 1405-16.
126. Terabe, M., et al., *NKT cell-mediated repression of tumor immunosurveillance by IL-13 and the IL-4R-STAT6 pathway*. Nat Immunol, 2000. **1**(6): p. 515-20.
127. Nelms, K., et al., *The IL-4 receptor: signaling mechanisms and biologic functions*. Annu Rev Immunol, 1999. **17**: p. 701-38.
128. Gallina, G., et al., *Tumors induce a subset of inflammatory monocytes with immunosuppressive activity on CD8+ T cells*. J Clin Invest, 2006. **116**(10): p. 2777-90.
129. Miossec, P., et al., *Inhibition of the production of proinflammatory cytokines and immunoglobulins by interleukin-4 in an ex vivo model of rheumatoid synovitis*. Arthritis Rheum, 1992. **35**(8): p. 874-83.
130. de Waal Malefyt, R., et al., *Effects of IL-13 on phenotype, cytokine production, and cytotoxic function of human monocytes. Comparison with IL-4 and modulation by IFN-gamma or IL-10*. J Immunol, 1993. **151**(11): p. 6370-81.
131. Urban, J.F., Jr., et al., *IL-13, IL-4Ralpha, and Stat6 are required for the expulsion of the gastrointestinal nematode parasite Nippostrongylus brasiliensis*. Immunity, 1998. **8**(2): p. 255-64.
132. Huaux, F., et al., *Dual roles of IL-4 in lung injury and fibrosis*. J Immunol, 2003. **170**(4): p. 2083-92.

133. Leopold Wager, C.M. and F.L. Wormley, Jr., *Classical versus alternative macrophage activation: the Ying and the Yang in host defense against pulmonary fungal infections*. *Mucosal Immunol*, 2014. **7**(5): p. 1023-35.
134. Martinez, F.O. and S. Gordon, *The M1 and M2 paradigm of macrophage activation: time for reassessment*. *F1000Prime Rep*, 2014. **6**: p. 13.
135. Mantovani, A., et al., *The chemokine system in diverse forms of macrophage activation and polarization*. *Trends Immunol*, 2004. **25**(12): p. 677-86.
136. LaPorte, S.L., et al., *Molecular and structural basis of cytokine receptor pleiotropy in the interleukin-4/13 system*. *Cell*, 2008. **132**(2): p. 259-72.
137. Heller, N.M., et al., *Type I IL-4Rs selectively activate IRS-2 to induce target gene expression in macrophages*. *Sci Signal*, 2008. **1**(51): p. ra17.
138. Chiaramonte, M.G., et al., *Regulation and function of the interleukin 13 receptor alpha 2 during a T helper cell type 2-dominant immune response*. *J Exp Med*, 2003. **197**(6): p. 687-701.
139. Fichtner-Feigl, S., et al., *IL-13 signaling through the IL-13alpha2 receptor is involved in induction of TGF-beta1 production and fibrosis*. *Nat Med*, 2006. **12**(1): p. 99-106.
140. Gandhi, N.A., et al., *Targeting key proximal drivers of type 2 inflammation in disease*. *Nat Rev Drug Discov*, 2016. **15**(1): p. 35-50.
141. Luzina, I.G., et al., *Regulation of inflammation by interleukin-4: a review of "alternatives"*. *J Leukoc Biol*, 2012. **92**(4): p. 753-64.
142. Kaplan, M.H., et al., *Stat6 is required for mediating responses to IL-4 and for development of Th2 cells*. *Immunity*, 1996. **4**(3): p. 313-9.
143. Takeda, K., et al., *Essential role of Stat6 in IL-4 signalling*. *Nature*, 1996. **380**(6575): p. 627-30.
144. Wurster, A.L., T. Tanaka, and M.J. Grusby, *The biology of Stat4 and Stat6*. *Oncogene*, 2000. **19**(21): p. 2577-84.
145. Schroder, A.J., et al., *Cutting edge: STAT6 serves as a positive and negative regulator of gene expression in IL-4-stimulated B lymphocytes*. *J Immunol*, 2002. **168**(3): p. 996-1000.
146. Kotanides, H. and N.C. Reich, *Interleukin-4-induced STAT6 recognizes and activates a target site in the promoter of the interleukin-4 receptor gene*. *J Biol Chem*, 1996. **271**(41): p. 25555-61.
147. Schindler, U., et al., *Components of a Stat recognition code: evidence for two layers of molecular selectivity*. *Immunity*, 1995. **2**(6): p. 689-97.
148. Mikita, T., et al., *Requirements for interleukin-4-induced gene expression and functional characterization of Stat6*. *Mol Cell Biol*, 1996. **16**(10): p. 5811-20.
149. Fujisawa, T., B.H. Joshi, and R.K. Puri, *IL-13 regulates cancer invasion and metastasis through IL-13Ralpha2 via ERK/AP-1 pathway in mouse model of human ovarian cancer*. *Int J Cancer*, 2012. **131**(2): p. 344-56.
150. Todaro, M., et al., *Apoptosis resistance in epithelial tumors is mediated by tumor-cell-derived interleukin-4*. *Cell Death Differ*, 2008. **15**(4): p. 762-72.
151. Barderas, R., et al., *High expression of IL-13 receptor alpha2 in colorectal cancer is associated with invasion, liver metastasis, and poor prognosis*. *Cancer Res*, 2012. **72**(11): p. 2780-90.
152. Fujisawa, T., et al., *A novel role of interleukin-13 receptor alpha2 in pancreatic cancer invasion and metastasis*. *Cancer Res*, 2009. **69**(22): p. 8678-85.

153. Nguyen, V., et al., *IL-13Ralpha2-Targeted Therapy Escapees: Biologic and Therapeutic Implications*. Transl Oncol, 2011. **4**(6): p. 390-400.
154. Todaro, M., et al., *Autocrine production of interleukin-4 and interleukin-10 is required for survival and growth of thyroid cancer cells*. Cancer Res, 2006. **66**(3): p. 1491-9.
155. Prokopchuk, O., et al., *Interleukin-4 enhances proliferation of human pancreatic cancer cells: evidence for autocrine and paracrine actions*. Br J Cancer, 2005. **92**(5): p. 921-8.
156. Joshi, B.H., et al., *Interleukin-4 receptor alpha overexpression in human bladder cancer correlates with the pathological grade and stage of the disease*. Cancer Med, 2014. **3**(6): p. 1615-28.
157. Koller, F.L., et al., *Epithelial interleukin-4 receptor expression promotes colon tumor growth*. Carcinogenesis, 2010. **31**(6): p. 1010-7.
158. Joshi, B.H., et al., *In situ expression of interleukin-4 (IL-4) receptors in human brain tumors and cytotoxicity of a recombinant IL-4 cytotoxin in primary glioblastoma cell cultures*. Cancer Res, 2001. **61**(22): p. 8058-61.
159. Wang, H.W. and J.A. Joyce, *Alternative activation of tumor-associated macrophages by IL-4: priming for protumoral functions*. Cell Cycle, 2010. **9**(24): p. 4824-35.
160. Ostrand-Rosenberg, S., *Immune surveillance: a balance between protumor and antitumor immunity*. Curr Opin Genet Dev, 2008. **18**(1): p. 11-8.
161. Li, B.H., et al., *Stat6 activity-related Th2 cytokine profile and tumor growth advantage of human colorectal cancer cells in vitro and in vivo*. Cell Signal, 2012. **24**(3): p. 718-25.
162. Bankaitis, K.V. and B. Fingleton, *Targeting IL4/IL4R for the treatment of epithelial cancer metastasis*. Clin Exp Metastasis, 2015. **32**(8): p. 847-56.
163. Todaro, M., et al., *Colon cancer stem cells dictate tumor growth and resist cell death by production of interleukin-4*. Cell Stem Cell, 2007. **1**(4): p. 389-402.
164. Ferlay, J., et al., *Cancer incidence and mortality worldwide: sources, methods and major patterns in GLOBOCAN 2012*. Int J Cancer, 2015. **136**(5): p. E359-86.
165. Filho, G.B., *Bogliolo*. 8th ed. 2011: Guanabara Koogan. 1524.
166. Hannan, L.M., E.J. Jacobs, and M.J. Thun, *The association between cigarette smoking and risk of colorectal cancer in a large prospective cohort from the United States*. Cancer Epidemiol Biomarkers Prev, 2009. **18**(12): p. 3362-7.
167. Beyaz, S., et al., *High-fat diet enhances stemness and tumorigenicity of intestinal progenitors*. Nature, 2016. **531**(7592): p. 53-8.
168. Schmid, D. and M.F. Leitzmann, *Television viewing and time spent sedentary in relation to cancer risk: a meta-analysis*. J Natl Cancer Inst, 2014. **106**(7).
169. Jaspersion, K.W., et al., *Hereditary and familial colon cancer*. Gastroenterology, 2010. **138**(6): p. 2044-58.
170. Lasry, A., A. Zinger, and Y. Ben-Neriah, *Inflammatory networks underlying colorectal cancer*. Nat Immunol, 2016. **17**(3): p. 230-40.
171. Eaden, J.A., K.R. Abrams, and J.F. Mayberry, *The risk of colorectal cancer in ulcerative colitis: a meta-analysis*. Gut, 2001. **48**(4): p. 526-35.
172. Abraham, C. and J.H. Cho, *Inflammatory bowel disease*. N Engl J Med, 2009. **361**(21): p. 2066-78.

173. Melton, G.B., et al., *Do preoperative factors predict subsequent diagnosis of Crohn's disease after ileal pouch-anal anastomosis for ulcerative or indeterminate colitis?* Colorectal Dis, 2010. **12**(10): p. 1026-32.
174. Baumgart, D.C. and S.R. Carding, *Inflammatory bowel disease: cause and immunobiology*. Lancet, 2007. **369**(9573): p. 1627-40.
175. Bollrath, J., *Diverse functions of Stat3 in intestinal epithelial cells during inflammation-associated and sporadic carcinogenesis*, in *Biology*. 2010, Technischen Universität München: Munich, Germany.
176. Fearon, E.R., *Molecular genetics of colorectal cancer*. Annu Rev Pathol, 2011. **6**: p. 479-507.
177. Aoki, K. and M.M. Taketo, *Adenomatous polyposis coli (APC): a multi-functional tumor suppressor gene*. J Cell Sci, 2007. **120**(Pt 19): p. 3327-35.
178. Sansom, O.J., et al., *Loss of Apc in vivo immediately perturbs Wnt signaling, differentiation, and migration*. Genes Dev, 2004. **18**(12): p. 1385-90.
179. Zumbunn, J., et al., *Binding of the adenomatous polyposis coli protein to microtubules increases microtubule stability and is regulated by GSK3 beta phosphorylation*. Curr Biol, 2001. **11**(1): p. 44-9.
180. Kobayashi, M., et al., *Nuclear translocation of beta-catenin in colorectal cancer*. Br J Cancer, 2000. **82**(10): p. 1689-93.
181. Vogelstein, B., et al., *Genetic alterations during colorectal-tumor development*. N Engl J Med, 1988. **319**(9): p. 525-32.
182. Fujii, S., T. Fujimori, and H. Kashida, *Ulcerative colitis-associated neoplasia*. Pathol Int, 2002. **52**(3): p. 195-203.
183. Kheirleiseid, E.A., et al., *Mismatch repair protein expression in colorectal cancer*. J Gastrointest Oncol, 2013. **4**(4): p. 397-408.
184. Fishel, R., *Mismatch repair, molecular switches, and signal transduction*. Genes Dev, 1998. **12**(14): p. 2096-101.
185. Boland, C.R. and A. Goel, *Microsatellite instability in colorectal cancer*. Gastroenterology, 2010. **138**(6): p. 2073-2087 e3.
186. Wheeler, J.M., W.F. Bodmer, and N.J. Mortensen, *DNA mismatch repair genes and colorectal cancer*. Gut, 2000. **47**(1): p. 148-53.
187. Duval, A. and R. Hamelin, *Mutations at coding repeat sequences in mismatch repair-deficient human cancers: Toward a new concept of target genes for instability*. Cancer Research, 2002. **62**(9): p. 2447-2454.
188. Jabbari, K. and G. Bernardi, *Cytosine methylation and CpG, TpG (CpA) and TpA frequencies*. Gene, 2004. **333**: p. 143-9.
189. Lao, V.V. and W.M. Grady, *Epigenetics and colorectal cancer*. Nat Rev Gastroenterol Hepatol, 2011. **8**(12): p. 686-700.
190. Samowitz, W.S., et al., *Evaluation of a large, population-based sample supports a CpG island methylator phenotype in colon cancer*. Gastroenterology, 2005. **129**(3): p. 837-45.
191. Toyota, M., et al., *CpG island methylator phenotype in colorectal cancer*. Proc Natl Acad Sci U S A, 1999. **96**(15): p. 8681-6.
192. Jones, P.A., *Functions of DNA methylation: islands, start sites, gene bodies and beyond*. Nat Rev Genet, 2012. **13**(7): p. 484-92.
193. Jjingo, D., et al., *On the presence and role of human gene-body DNA methylation*. Oncotarget, 2012. **3**(4): p. 462-74.

194. Nazemalhosseini Mojarad, E., et al., *The CpG island methylator phenotype (CIMP) in colorectal cancer*. Gastroenterol Hepatol Bed Bench, 2013. **6**(3): p. 120-8.
195. Sturlan, S., et al., *Interleukin-10-deficient mice and inflammatory bowel disease associated cancer development*. Carcinogenesis, 2001. **22**(4): p. 665-71.
196. Lee, G., et al., *Phosphoinositide 3-kinase signaling mediates beta-catenin activation in intestinal epithelial stem and progenitor cells in colitis*. Gastroenterology, 2010. **139**(3): p. 869-81, 881 e1-9.
197. Grivennikov, S.I., *Inflammation and colorectal cancer: colitis-associated neoplasia*. Semin Immunopathol, 2013. **35**(2): p. 229-44.
198. Kaler, P., et al., *The NF-kappaB/AKT-dependent Induction of Wnt Signaling in Colon Cancer Cells by Macrophages and IL-1beta*. Cancer Microenviron, 2009. **2**(1): p. 69-80.
199. Brown, J.B., et al., *Mesalamine inhibits epithelial beta-catenin activation in chronic ulcerative colitis*. Gastroenterology, 2010. **138**(2): p. 595-605, 605 e1-3.
200. Oguma, K., et al., *Activated macrophages promote Wnt signalling through tumour necrosis factor-alpha in gastric tumour cells*. EMBO J, 2008. **27**(12): p. 1671-81.
201. Greten, F.R., et al., *IKKbeta links inflammation and tumorigenesis in a mouse model of colitis-associated cancer*. Cell, 2004. **118**(3): p. 285-96.
202. Bollrath, J. and F.R. Greten, *IKK/NF-kappaB and STAT3 pathways: central signalling hubs in inflammation-mediated tumour promotion and metastasis*. EMBO Rep, 2009. **10**(12): p. 1314-9.
203. Bollrath, J., et al., *gp130-mediated Stat3 activation in enterocytes regulates cell survival and cell-cycle progression during colitis-associated tumorigenesis*. Cancer Cell, 2009. **15**(2): p. 91-102.
204. Fang, H.Y. and F.R. Greten, *Cell Autonomous and Non-Autonomous Functions of IKKbeta and NF-kappaB during the Pathogenesis of Gastrointestinal Tumors*. Cancers (Basel), 2011. **3**(2): p. 2214-22.
205. Schwitalla, S., et al., *Loss of p53 in Enterocytes Generates an Inflammatory Microenvironment Enabling Invasion and Lymph Node Metastasis of Carcinogen-Induced Colorectal Tumors*. Cancer Cell, 2013. **23**(1): p. 93-106.
206. Park, J., et al., *MLLT11/AF1q boosts oncogenic STAT3 activity through Src-PDGFR tyrosine kinase signaling*. Oncotarget, 2016.
207. Song, L., et al., *Activation of Stat3 by receptor tyrosine kinases and cytokines regulates survival in human non-small cell carcinoma cells*. Oncogene, 2003. **22**(27): p. 4150-65.
208. Yu, H., M. Kortylewski, and D. Pardoll, *Crosstalk between cancer and immune cells: role of STAT3 in the tumour microenvironment*. Nat Rev Immunol, 2007. **7**(1): p. 41-51.
209. Hirano, T., K. Ishihara, and M. Hibi, *Roles of STAT3 in mediating the cell growth, differentiation and survival signals relayed through the IL-6 family of cytokine receptors*. Oncogene, 2000. **19**(21): p. 2548-56.
210. Grivennikov, S.I. and M. Karin, *Dangerous liaisons: STAT3 and NF-kappaB collaboration and crosstalk in cancer*. Cytokine Growth Factor Rev, 2010. **21**(1): p. 11-9.

211. Siveen, K.S., et al., *Targeting the STAT3 signaling pathway in cancer: role of synthetic and natural inhibitors*. Biochim Biophys Acta, 2014. **1845**(2): p. 136-54.
212. Schwitalla, S., *The role of IKK β --dependent NF - κ B signaling on different stages of intestinal carcinogenesis*, in *Lehrstuhl für Biotechnologie der Nutztiere*. 2012, TECHNISCHE UNIVERSITÄT MÜNCHEN: Munich. p. 147.
213. Karin, M., et al., *NF-kappaB in cancer: from innocent bystander to major culprit*. Nat Rev Cancer, 2002. **2**(4): p. 301-10.
214. Haura, E.B., J. Turkson, and R. Jove, *Mechanisms of disease: Insights into the emerging role of signal transducers and activators of transcription in cancer*. Nat Clin Pract Oncol, 2005. **2**(6): p. 315-24.
215. Schwitalla, S., et al., *Intestinal tumorigenesis initiated by dedifferentiation and acquisition of stem-cell-like properties*. Cell, 2013. **152**(1-2): p. 25-38.
216. Hayden, M.S. and S. Ghosh, *Shared principles in NF-kappaB signaling*. Cell, 2008. **132**(3): p. 344-62.
217. Hayden, M.S. and S. Ghosh, *NF-kappaB, the first quarter-century: remarkable progress and outstanding questions*. Genes Dev, 2012. **26**(3): p. 203-34.
218. Karin, M., *Nuclear factor-kappaB in cancer development and progression*. Nature, 2006. **441**(7092): p. 431-6.
219. Rezapour, S., et al., *STC1 and NF-kappaB p65 (Rel A) is Constitutively Activated in Colorectal Cancer*. Clin Lab, 2016. **62**(3): p. 463-9.
220. Giri, D.K. and B.B. Aggarwal, *Constitutive activation of NF-kappaB causes resistance to apoptosis in human cutaneous T cell lymphoma HuT-78 cells. Autocrine role of tumor necrosis factor and reactive oxygen intermediates*. J Biol Chem, 1998. **273**(22): p. 14008-14.
221. Braunstein, S., S.C. Formenti, and R.J. Schneider, *Acquisition of stable inducible up-regulation of nuclear factor-kappaB by tumor necrosis factor exposure confers increased radiation resistance without increased transformation in breast cancer cells*. Mol Cancer Res, 2008. **6**(1): p. 78-88.
222. Jackson-Bernitsas, D.G., et al., *Evidence that TNF-TNFR1-TRADD-TRAF2-RIP-TAK1-IKK pathway mediates constitutive NF-kappaB activation and proliferation in human head and neck squamous cell carcinoma*. Oncogene, 2007. **26**(10): p. 1385-97.
223. De, S., J.K. Dermawan, and G.R. Stark, *EGF receptor uses SOS1 to drive constitutive activation of NFkappaB in cancer cells*. Proc Natl Acad Sci U S A, 2014. **111**(32): p. 11721-6.
224. Fearon, E.R. and B. Vogelstein, *A genetic model for colorectal tumorigenesis*. Cell, 1990. **61**(5): p. 759-67.
225. Tong, Y., W. Yang, and H.P. Koeffler, *Mouse models of colorectal cancer*. Chin J Cancer, 2011. **30**(7): p. 450-62.
226. De Robertis, M., et al., *The AOM/DSS murine model for the study of colon carcinogenesis: From pathways to diagnosis and therapy studies*. J Carcinog, 2011. **10**: p. 9.
227. Karim, B.O. and D.L. Huso, *Mouse models for colorectal cancer*. Am J Cancer Res, 2013. **3**(3): p. 240-50.
228. Wali, R.K., et al., *Inhibition of O(6)-methylguanine-DNA methyltransferase increases azoxymethane-induced colonic tumors in rats*. Carcinogenesis, 1999. **20**(12): p. 2355-60.

229. Pegg, A.E., *Methylation of the O6 position of guanine in DNA is the most likely initiating event in carcinogenesis by methylating agents*. Cancer Invest, 1984. **2**(3): p. 223-31.
230. Clapper, M.L., H.S. Cooper, and W.C. Chang, *Dextran sulfate sodium-induced colitis-associated neoplasia: a promising model for the development of chemopreventive interventions*. Acta Pharmacol Sin, 2007. **28**(9): p. 1450-9.
231. Egger, B., et al., *Characterisation of acute murine dextran sodium sulphate colitis: cytokine profile and dose dependency*. Digestion, 2000. **62**(4): p. 240-8.
232. Aust, D.E., et al., *Altered distribution of beta-catenin, and its binding proteins E-cadherin and APC, in ulcerative colitis-related colorectal cancers*. Mod Pathol, 2001. **14**(1): p. 29-39.
233. Bolt, A.B., et al., *Azoxymethane induces K1-ras activation in the tumor resistant AKR/J mouse colon*. Mol Carcinog, 2000. **27**(3): p. 210-8.
234. De Filippo, C., et al., *Mutations of the Apc gene in experimental colorectal carcinogenesis induced by azoxymethane in F344 rats*. Br J Cancer, 1998. **77**(12): p. 2148-51.
235. Kobaek-Larsen, M., et al., *Review of colorectal cancer and its metastases in rodent models: comparative aspects with those in humans*. Comp Med, 2000. **50**(1): p. 16-26.
236. Erdman, S.H., et al., *Assessment of mutations in Ki-ras and p53 in colon cancers from azoxymethane- and dimethylhydrazine-treated rats*. Mol Carcinog, 1997. **19**(2): p. 137-44.
237. Pallangyo, C.K., P.K. Ziegler, and F.R. Greten, *IKKbeta acts as a tumor suppressor in cancer-associated fibroblasts during intestinal tumorigenesis*. J Exp Med, 2015. **212**(13): p. 2253-66.
238. Noben-Trauth, N., et al., *An interleukin 4 (IL-4)-independent pathway for CD4+ T cell IL-4 production is revealed in IL-4 receptor-deficient mice*. Proc Natl Acad Sci U S A, 1997. **94**(20): p. 10838-43.
239. Herbert, D.R., et al., *Alternative macrophage activation is essential for survival during schistosomiasis and downmodulates T helper 1 responses and immunopathology*. Immunity, 2004. **20**(5): p. 623-35.
240. Madison, B.B., et al., *Cis elements of the villin gene control expression in restricted domains of the vertical (crypt) and horizontal (duodenum, cecum) axes of the intestine*. J Biol Chem, 2002. **277**(36): p. 33275-83.
241. West, G.A., et al., *Interleukin 4 in inflammatory bowel disease and mucosal immune reactivity*. Gastroenterology, 1996. **110**(6): p. 1683-95.
242. Nielsen, O.H., et al., *Involvement of interleukin-4 and -10 in inflammatory bowel disease*. Dig Dis Sci, 1996. **41**(9): p. 1786-93.
243. Marchenko, N.D., et al., *Stress-mediated nuclear stabilization of p53 is regulated by ubiquitination and importin-alpha3 binding*. Cell Death Differ, 2010. **17**(2): p. 255-67.
244. Marine, J.C., *p53 stabilization: the importance of nuclear import*. Cell Death Differ, 2010. **17**(2): p. 191-2.
245. Calon, A., et al., *Dependency of colorectal cancer on a TGF-beta-driven program in stromal cells for metastasis initiation*. Cancer Cell, 2012. **22**(5): p. 571-84.

246. Calon, A., et al., *Stromal gene expression defines poor-prognosis subtypes in colorectal cancer*. Nat Genet, 2015. **47**(4): p. 320-9.
247. Isella, C., et al., *Stromal contribution to the colorectal cancer transcriptome*. Nat Genet, 2015. **47**(4): p. 312-9.
248. Aronica, M.A., S. Goenka, and M. Boothby, *IL-4-dependent induction of BCL-2 and BCL-X(L)IN activated T lymphocytes through a STAT6- and pi 3-kinase-independent pathway*. Cytokine, 2000. **12**(6): p. 578-87.
249. Elrod, J.W., et al., *DSS-induced colitis is exacerbated in STAT-6 knockout mice*. Inflamm Bowel Dis, 2005. **11**(10): p. 883-9.
250. Rutschman, R., et al., *Cutting edge: Stat6-dependent substrate depletion regulates nitric oxide production*. J Immunol, 2001. **166**(4): p. 2173-7.
251. Chen, J. and X.F. Huang, *The signal pathways in azoxymethane-induced colon cancer and preventive implications*. Cancer Biol Ther, 2009. **8**(14): p. 1313-7.
252. Ward, J.M., R.S. Yamamoto, and C.A. Brown, *Pathology of intestinal neoplasms and other lesions in rats exposed to azoxymethane*. J Natl Cancer Inst, 1973. **51**(3): p. 1029-39.
253. Raju, J., *Azoxymethane-induced rat aberrant crypt foci: relevance in studying chemoprevention of colon cancer*. World J Gastroenterol, 2008. **14**(43): p. 6632-5.
254. Loughery, J., et al., *Critical role for p53-serine 15 phosphorylation in stimulating transactivation at p53-responsive promoters*. Nucleic Acids Res, 2014. **42**(12): p. 7666-80.
255. Chao, C., et al., *Phosphorylation of murine p53 at ser-18 regulates the p53 responses to DNA damage*. Proc Natl Acad Sci U S A, 2000. **97**(22): p. 11936-41.
256. Furtek, S.L., et al., *Strategies and Approaches of Targeting STAT3 for Cancer Treatment*. ACS Chem Biol, 2016. **11**(2): p. 308-18.
257. Bromberg, J.F., et al., *Stat3 as an oncogene*. Cell, 1999. **98**(3): p. 295-303.
258. Epling-Burnette, P.K., et al., *Inhibition of STAT3 signaling leads to apoptosis of leukemic large granular lymphocytes and decreased Mcl-1 expression*. J Clin Invest, 2001. **107**(3): p. 351-62.
259. Catlett-Falcone, R., et al., *Constitutive activation of Stat3 signaling confers resistance to apoptosis in human U266 myeloma cells*. Immunity, 1999. **10**(1): p. 105-15.
260. Kanda, N., et al., *STAT3 is constitutively activated and supports cell survival in association with survivin expression in gastric cancer cells*. Oncogene, 2004. **23**(28): p. 4921-9.
261. Iwamaru, A., et al., *A novel inhibitor of the STAT3 pathway induces apoptosis in malignant glioma cells both in vitro and in vivo*. Oncogene, 2007. **26**(17): p. 2435-44.
262. Zhang, J., et al., *The cell death regulator GRIM-19 is an inhibitor of signal transducer and activator of transcription 3*. Proc Natl Acad Sci U S A, 2003. **100**(16): p. 9342-7.
263. Blaskovich, M.A., et al., *Discovery of JSI-124 (cucurbitacin I), a selective Janus kinase/signal transducer and activator of transcription 3 signaling pathway inhibitor with potent antitumor activity against human and murine cancer cells in mice*. Cancer Res, 2003. **63**(6): p. 1270-9.

264. Grivennikov, S., et al., *IL-6 and Stat3 are required for survival of intestinal epithelial cells and development of colitis-associated cancer*. *Cancer Cell*, 2009. **15**(2): p. 103-13.
265. Putoczki, T.L., et al., *Interleukin-11 is the dominant IL-6 family cytokine during gastrointestinal tumorigenesis and can be targeted therapeutically*. *Cancer Cell*, 2013. **24**(2): p. 257-71.
266. Liu, T., et al., *Inhibitory effects of cucurbitacin B on laryngeal squamous cell carcinoma*. *Eur Arch Otorhinolaryngol*, 2008. **265**(10): p. 1225-32.
267. Su, Y., et al., *JSI-124 inhibits glioblastoma multiforme cell proliferation through G(2)/M cell cycle arrest and apoptosis augment*. *Cancer Biol Ther*, 2008. **7**(8): p. 1243-9.
268. Dong, Y., et al., *Clinical relevance of cyclin B1 overexpression in laryngeal squamous cell carcinoma*. *Cancer Lett*, 2002. **177**(1): p. 13-9.
269. Hassan, K.A., et al., *Cyclin B1 overexpression and resistance to radiotherapy in head and neck squamous cell carcinoma*. *Cancer Res*, 2002. **62**(22): p. 6414-7.
270. Li, J.Q., et al., *Cyclin B1, unlike cyclin G1, increases significantly during colorectal carcinogenesis and during later metastasis to lymph nodes*. *Int J Oncol*, 2003. **22**(5): p. 1101-10.
271. Fang, Y., et al., *Chk1-induced CCNB1 overexpression promotes cell proliferation and tumor growth in human colorectal cancer*. *Cancer Biol Ther*, 2014. **15**(9): p. 1268-79.
272. Carey, G.B., et al., *IL-4 protects the B-cell lymphoma cell line CH31 from anti-IgM-induced growth arrest and apoptosis: contribution of the PI-3 kinase/AKT pathway*. *Cell Res*, 2007. **17**(11): p. 942-55.
273. Swann, J.B. and M.J. Smyth, *Immune surveillance of tumors*. *J Clin Invest*, 2007. **117**(5): p. 1137-46.
274. Burnet, F.M., *The concept of immunological surveillance*. *Prog Exp Tumor Res*, 1970. **13**: p. 1-27.
275. Ehrlich, P., *Über den jetzigen Stand der Karzinomforschung*. *Ned. Tijdschr. Genees.*, 1909. **5**: p. 273-290.
276. Raulet, D.H. and N. Guerra, *Oncogenic stress sensed by the immune system: role of natural killer cell receptors*. *Nat Rev Immunol*, 2009. **9**(8): p. 568-80.
277. Zanoni, I. and F. Granucci, *Regulation and dysregulation of innate immunity by NFAT signaling downstream of pattern recognition receptors (PRRs)*. *Eur J Immunol*, 2012. **42**(8): p. 1924-31.
278. Gunther, C., et al., *Regulation and pathophysiological role of epithelial turnover in the gut*. *Semin Cell Dev Biol*, 2014. **35**: p. 40-50.
279. Huang, Z., *The chemical biology of apoptosis. Exploring protein-protein interactions and the life and death of cells with small molecules*. *Chem Biol*, 2002. **9**(10): p. 1059-72.
280. Bhattacharya, S., R.M. Ray, and L.R. Johnson, *STAT3-mediated transcription of Bcl-2, Mcl-1 and c-IAP2 prevents apoptosis in polyamine-depleted cells*. *Biochem J*, 2005. **392**(Pt 2): p. 335-44.
281. Rahaman, S.O., et al., *Inhibition of constitutively active Stat3 suppresses proliferation and induces apoptosis in glioblastoma multiforme cells*. *Oncogene*, 2002. **21**(55): p. 8404-13.

282. Stephanou, A., et al., *Opposing actions of STAT-1 and STAT-3 on the Bcl-2 and Bcl-x promoters*. Cell Death Differ, 2000. **7**(3): p. 329-30.
283. Greten, F.R. and M. Karin, *The IKK/NF-kappaB activation pathway-a target for prevention and treatment of cancer*. Cancer Lett, 2004. **206**(2): p. 193-9.
284. Iizuka, M. and S. Konno, *Wound healing of intestinal epithelial cells*. World J Gastroenterol, 2011. **17**(17): p. 2161-71.
285. Cario, E., *Toll-like receptors in inflammatory bowel diseases: a decade later*. Inflamm Bowel Dis, 2010. **16**(9): p. 1583-97.
286. Ogawa, H., et al., *Increased expression of HIP/PAP and regenerating gene III in human inflammatory bowel disease and a murine bacterial reconstitution model*. Inflamm Bowel Dis, 2003. **9**(3): p. 162-70.
287. A. Shytenberg, E.K., Y. Lin, A. Schwartzman, H. Zhang, M.E. Zenilman, *Up-regulation of pancreatitis-associated protein in a rat model of inflammatory bowel disease*. J Surg Res, 2003. **114**(2): p. 292-293.
288. Gironella, M., et al., *Anti-inflammatory effects of pancreatitis associated protein in inflammatory bowel disease*. Gut, 2005. **54**(9): p. 1244-53.
289. Sikora, A. and E. Grzesiuk, *Heat shock response in gastrointestinal tract*. J Physiol Pharmacol, 2007. **58 Suppl 3**: p. 43-62.
290. Tanaka, K., et al., *Genetic evidence for a protective role for heat shock factor 1 and heat shock protein 70 against colitis*. J Biol Chem, 2007. **282**(32): p. 23240-52.
291. Abreu, M.T., et al., *Decreased expression of Toll-like receptor-4 and MD-2 correlates with intestinal epithelial cell protection against dysregulated proinflammatory gene expression in response to bacterial lipopolysaccharide*. J Immunol, 2001. **167**(3): p. 1609-16.
292. Hausmann, M., et al., *Toll-like receptors 2 and 4 are up-regulated during intestinal inflammation*. Gastroenterology, 2002. **122**(7): p. 1987-2000.
293. Singh, J.C., et al., *Toll-like receptor-mediated responses of primary intestinal epithelial cells during the development of colitis*. Am J Physiol Gastrointest Liver Physiol, 2005. **288**(3): p. G514-24.
294. Rigby, R.J., et al., *Suppressor of cytokine signaling 3 (SOCS3) limits damage-induced crypt hyper-proliferation and inflammation-associated tumorigenesis in the colon*. Oncogene, 2007. **26**(33): p. 4833-41.
295. Terzic, J., et al., *Inflammation and colon cancer*. Gastroenterology, 2010. **138**(6): p. 2101-2114 e5.
296. Jess, T., C. Rungoe, and L. Peyrin-Biroulet, *Risk of colorectal cancer in patients with ulcerative colitis: a meta-analysis of population-based cohort studies*. Clin Gastroenterol Hepatol, 2012. **10**(6): p. 639-45.
297. Linehan, L.A., et al., *STAT6 is required for IL-4-induced germline Ig gene transcription and switch recombination*. J Immunol, 1998. **161**(1): p. 302-10.
298. O'Reilly, S., et al., *IL-13 mediates collagen deposition via STAT6 and microRNA-135b: a role for epigenetics*. Sci Rep, 2016. **6**: p. 25066.
299. Stahl, N., et al., *Choice of STATs and other substrates specified by modular tyrosine-based motifs in cytokine receptors*. Science, 1995. **267**(5202): p. 1349-53.
300. Qing, Y. and G.R. Stark, *Alternative activation of STAT1 and STAT3 in response to interferon-gamma*. J Biol Chem, 2004. **279**(40): p. 41679-85.

301. Murray, P.J., *The JAK-STAT signaling pathway: input and output integration*. J Immunol, 2007. **178**(5): p. 2623-9.
302. Costa-Pereira, A.P., et al., *Mutational switch of an IL-6 response to an interferon-gamma-like response*. Proc Natl Acad Sci U S A, 2002. **99**(12): p. 8043-7.
303. Lee, P.J., et al., *ERK1/2 mitogen-activated protein kinase selectively mediates IL-13-induced lung inflammation and remodeling in vivo*. J Clin Invest, 2006. **116**(1): p. 163-73.
304. Constantinescu, S.N., *Gathering support for critical mass: interleukin 4 receptor signaling requires clustering in endosomes*. Biophys J, 2014. **107**(11): p. 2479-80.
305. Iacopetta, B., *TP53 mutation in colorectal cancer*. Hum Mutat, 2003. **21**(3): p. 271-6.
306. Niu, G., et al., *Role of Stat3 in regulating p53 expression and function*. Mol Cell Biol, 2005. **25**(17): p. 7432-40.
307. Choi, Y., J.K. Kim, and J.Y. Yoo, *NFkappaB and STAT3 synergistically activate the expression of FAT10, a gene counteracting the tumor suppressor p53*. Mol Oncol, 2014. **8**(3): p. 642-55.
308. Hallenborg, P., et al., *MDM2 facilitates adipocyte differentiation through CRTC-mediated activation of STAT3*. Cell Death Dis, 2016. **7**(6): p. e2289.
309. Wormann, S.M., et al., *Loss of P53 Function Activates JAK2-STAT3 Signaling to Promote Pancreatic Tumor Growth, Stroma Modification, and Gemcitabine Resistance in Mice and Is Associated With Patient Survival*. Gastroenterology, 2016. **151**(1): p. 180-193 e12.
310. Yu, H., et al., *LIF negatively regulates tumour-suppressor p53 through Stat3/ID1/MDM2 in colorectal cancers*. Nat Commun, 2014. **5**: p. 5218.
311. Vogelstein, B., D. Lane, and A.J. Levine, *Surfing the p53 network*. Nature, 2000. **408**(6810): p. 307-10.
312. Scheffner, M., et al., *The HPV-16 E6 and E6-AP complex functions as a ubiquitin-protein ligase in the ubiquitination of p53*. Cell, 1993. **75**(3): p. 495-505.
313. Yang, Y., C.C. Li, and A.M. Weissman, *Regulating the p53 system through ubiquitination*. Oncogene, 2004. **23**(11): p. 2096-106.
314. Rosen, M.J., et al., *STAT6 deficiency ameliorates severity of oxazolone colitis by decreasing expression of claudin-2 and Th2-inducing cytokines*. J Immunol, 2013. **190**(4): p. 1849-58.
315. Cosin-Roger, J., et al., *The activation of Wnt signaling by a STAT6-dependent macrophage phenotype promotes mucosal repair in murine IBD*. Mucosal Immunol, 2016. **9**(4): p. 986-98.
316. Dieleman, L.A., et al., *Dextran sulfate sodium-induced colitis occurs in severe combined immunodeficient mice*. Gastroenterology, 1994. **107**(6): p. 1643-52.
317. Rokavec, M., et al., *IL-6R/STAT3/miR-34a feedback loop promotes EMT-mediated colorectal cancer invasion and metastasis*. The Journal of Clinical Investigation, 2014. **124**(4): p. 1853-67.
318. Sulli, G., R. Di Micco, and F. d'Adda di Fagagna, *Crosstalk between chromatin state and DNA damage response in cellular senescence and cancer*. Nat Rev Cancer, 2012. **12**(10): p. 709-20.

-
319. Menon, V. and L. Povirk, *Involvement of p53 in the repair of DNA double strand breaks: multifaceted Roles of p53 in homologous recombination repair (HRR) and non-homologous end joining (NHEJ)*. Subcell Biochem, 2014. **85**: p. 321-36.
 320. Jackson, S.P., *Sensing and repairing DNA double-strand breaks*. Carcinogenesis, 2002. **23**(5): p. 687-96.
 321. Toft, N.J., et al., *Msh2 status modulates both apoptosis and mutation frequency in the murine small intestine*. Proc Natl Acad Sci U S A, 1999. **96**(7): p. 3911-5.
 322. Oda, E., et al., *Noxa, a BH3-only member of the Bcl-2 family and candidate mediator of p53-induced apoptosis*. Science, 2000. **288**(5468): p. 1053-8.
 323. Qiu, W., et al., *PUMA suppresses intestinal tumorigenesis in mice*. Cancer Res, 2009. **69**(12): p. 4999-5006.
 324. Hu, Y., R.K. Le Leu, and G.P. Young, *Absence of acute apoptotic response to genotoxic carcinogens in p53-deficient mice is associated with increased susceptibility to azoxymethane-induced colon tumours*. Int J Cancer, 2005. **115**(4): p. 561-7.
 325. Pietsch, E.C., et al., *The p53 family and programmed cell death*. Oncogene, 2008. **27**(50): p. 6507-21.
 326. Bender, T. and J.C. Martinou, *Where killers meet--permeabilization of the outer mitochondrial membrane during apoptosis*. Cold Spring Harb Perspect Biol, 2013. **5**(1): p. a011106.
 327. Flores, E.R., et al., *p63 and p73 are required for p53-dependent apoptosis in response to DNA damage*. Nature, 2002. **416**(6880): p. 560-4.

ABBREVIATIONS

| | |
|-------------------------------|---|
| AOM | Azoxymethane |
| APC | Adenomatous polyposis coli |
| BCL2 | Pro apoptotic B cell lymphoma 2 |
| Bcl-xl | B-cell lymphoma-extra large |
| Bmi1 | Bmi1 polycombo ring finger |
| BrdU | Bromodesoxyuridine |
| CAC | Colitis-associated colon cancer |
| CCL | Chemokine C-C motif ligand |
| CD | Cluster of differentiation |
| CD | Crohn's disease |
| CKIT | Mas cell growth factor receptor |
| COX2 | Cyclooxygenase 2 |
| CRC | Colorectal cancer |
| CXCL | Chemokine ligand C-X-C motif |
| DC | Dendritic cell |
| DEPC | Diethylpyrocarbonate |
| DMEM | Dulbecco's modified eagle medium |
| DNA | Deoxyribonucleic acid |
| DNMT | DNA methyltransferase |
| dNTP | Deoxynucleotide triphosphate |
| DSS | Dextran sodium sulphate |
| DTT | Dithiothreitol |
| ECM1 | Extracellular matrix protein 1 |
| EEC | Enteroendocrine cell |
| EDTA | Ethylenediaminetetraacetic acid |
| ELISA | Enzyme-linked immunosorbent assay |
| FAE | Follicle associated epithelium |
| FAP | Familial adenomatous polyposis |
| Fcgbp | Fc gamma binding protein |
| FCS | Fetal calf serum |
| H&E | Hamatoxylin and eosin |
| HRP | Horseradish peroxidase |
| IBD | Inflammatory bowel disease |
| IEC | Intestinal epithelial cells |
| IEL | Intraepithelial lymphocyte |
| IFNγ | Interferon γ |
| IHC | Immunohistochemistry |
| IL | Interleukin |
| iNOS | Inducible nitric oxide |
| IP | Intraperitoneal |
| IV | Intravenous |
| JNK | C-Jun-N-terminal kinase |
| Lgr5 | Leucine-rich repeat-containing G-protein coupled receptor 5 |
| LIF | Leukemia inhibitor factor |
| LOH | Loss of heterozygosity |
| LP | <i>Lamina propria</i> |

| | |
|--------------------------------|--|
| MAPK | Mitogen-activated protein kinase |
| MHC | Major histocompatibility complex |
| MIP | Macrophage inflammatory protein |
| MMP | Matrix metalloproteinase |
| mRNA | Messenger RNA |
| MUC2 | Mucin 2 |
| NaCl | Sodium chloride |
| NF-κB | Nuclear factor kappa-light-chain-enhancer of activated B cells |
| NHEJ | Non-homologous end joining |
| NK | Natural killer |
| NLRs | NOD-like receptors |
| PAMPS | Pathogen-associated molecular patterns |
| PBS | Phosphate buffered saline |
| FFPE | Paraformaldehyde fixed paraffin embedded |
| PFA | Paraformaldehyde |
| PMSF | Phenylmethylsulfonyl fluoride |
| Poly I:C | Polyinosinic : polycytidylic acid |
| PP | Peyer's Patch |
| PRRs | Pattern recognition receptors |
| RNA | Ribonucleic acid |
| RELMβ | Resistin-like molecule beta |
| ROS | Reactive oxygen species |
| RT-PCR | Real time-polymerase chain reaction |
| SEM | Standard error of the mean |
| SNPs | Single nucleotide polymorphisms |
| STAT | Signal transducer and activator of transcription |
| TA | Transitory amplifying |
| TEMED | Tetramethylethylenediamine |
| TFF3 | Intestinal trefoil factor 3 |
| Th | T helper |
| TLR | Toll-like receptor |
| TNFα | Tumor necrosis factor α |
| TRPM5 | Transient receptor potential cation channel subfamily M member 5 |
| TUNEL | TdT-mediated dUTP-biotin nick end labeling |
| VEGF | Vascular endothelial growth factor |
| WNT | Mouse homolog of wingless |

Other common abbreviations may not be listed here

ACKNOWLEDGEMENTS

I would like to thank all people involved in this work. Especially my husband Roberto, my dear colleagues from AG Greten (Öz, Michaela, Mallika, Varga, Paul, Little Boll, Tobias, Facial, Jalaj, Little, Gölfem, Kerstin, Saskia, Christin D, Kathleen, Hanna, Eva, Charles, Marina, Delis and Pumpkin) and my supervisor Prof. Florian Richard Greten, who invested in my career as no one else ever did. Also, I thank Birgitta Michels for introducing me to the amazing world of text formatting and Sebastian Ebert from his help with bioinformatics.

I would like to thank the support from IMPRS-LS coordinator office during this period. Thanks Hans-Jörg, Ingrid and Maxi.

Last, but not least I would like to thank my grandmother for dedicating to me her last years of sanity, and teaching me that even when we do not have anything valuable to share, we still can share love.

Eidesstattliche Erklärung

Ich versichere hiermit an Eides statt, dass die vorgelegte Dissertation von mir selbständig und ohne unerlaubte Hilfe angefertigt ist.

München, den 27.10.2016

Tiago De Oliveira

(Unterschrift)

Erklärung

Hiermit erkläre ich, *

- ☒ dass die Dissertation nicht ganz oder in wesentlichen Teilen einer anderen Prüfungskommission vorgelegt worden ist.
- ☒ dass ich mich anderweitig einer Doktorprüfung ohne Erfolg **nicht** unterzogen habe.
- ☐ dass ich mich mit Erfolg der Doktorprüfung im Hauptfach
und in den Nebenfächern
bei der Fakultät für der
(Hochschule/Universität)
unterzogen habe.
- ☐ dass ich ohne Erfolg versucht habe, eine Dissertation einzureichen oder mich der Doktorprüfung zu unterziehen.

München, den 27.10.2016

Tiago De Oliveira

(Unterschrift)

*) Nichtzutreffendes streichen

CURRICULUM VITAE

Tiago Azambuja De Oliveira

LANGUAGES: Portuguese (mother language); English (Proficient); German (beginner); Spanish (beginner)

EDUCATION

| | | |
|--------------------------|---|----------------------------|
| 10/2010 – actual | Doctorate Candidate International Max Planck Research School (IMPRS-LS) PhD Program “Life Sciences” Faculty of Biology, Ludwig Maximilian Universität, Munich (LMU), Research on colorectal tumorigenesis and tumor microenvironment performed at the Department of Immunology, of Technische Universität München, Munich (TUM) and Department of Tumor Cell-Stroma Interaction and Tumor Microenvironment at Georg-Speyer-Haus Institute, Frankfurt am Main. Thesis topic ‘Divergent Functions of IL-4R α and STAT6 in a Model of Colitis- Associated Carcinogenesis. Supervision by Univ.-Prof. Dr. Florian R. Greten (Georg-Speyer-Haus) and Prof. Dr. Heinrich Leonhardt (Faculty of Biology, Ludwig Maximilian Universität, Munich) | Munich/ Frankfurt, Germany |
| 08/2004 – 04/2006 | Specialization in Oncology Medical Nursing Specialization in Oncology at the Institute of Education and Research (IEP Moinhos de Vento, in Portuguese), of the Moinhos de Vento Hospital Thesis on ‘Medical nurse attendance and breast cancer’. (Achieved 9,5 GPA on a scale of 10,0) Supervision by Dr. Maira Caleffi, MD, PhD and Dr. Paula Raffin Pohlmann, MD, PhD | Porto Alegre, Brazil |
| 1/2000 – 11/2004 | Bachelor and State Examination (Licentiate) on Medical Nurse Medical Nurse Faculty of the Pelotas Federal University (FE-UFPEL) Diploma Thesis on ‘Medical Nurse Cognizance in the Chemotherapy Unit’ (Achieved 8,7 GPA on a scale of 10,0) | Pelotas, Brazil |

PUBLICATIONS

1. Diamanti MA, Gupta J, Bennecke M, De Oliveira T, Ramakrishnan M, Braczynski AK, Richter B, Beli P, Hu Y, Saleh M, Mittelbronn M, Dikic I, Greten FR. IKK α controls ATG16L1 degradation to prevent ER stress during inflammation. J Exp Med. 2017 Feb;214(2):423-437.
2. Varga J, De Oliveira T, Greten FR. The architect that never sleeps: Tumor induced plasticity. FEBS Lett. 2014 Aug 1;588(15):2422-7.
3. De Oliveira T, Abiatari I, Raulefs S, Sauliunaite D, Erkan M, Kong B, Friess H, Michalski CW, Kleeff J. Syndecan-2 promotes perineural invasion and cooperates with K-ras to induce an invasive pancreatic cancer cell phenotype. Mol Cancer. 2012 Apr 3;11:19.
4. Hong X, Michalski CW, Kong B, Zhang W, Raggi MC, Sauliunaite D, De Oliveira T, Friess H, Kleeff J. ALCAM is associated with chemoresistance and tumor cell adhesion in pancreatic cancer. J Surg Oncol. 2010 Jun 1;101(7):564-9.
5. Abiatari I & DeOliveira T*, Kerkadze V, Schwager C, Esposito I, Giese NA, Huber P, Bergman F, Abdollahi A, Friess H, Kleeff J. Consensus transcriptome signature of perineural invasion in pancreatic carcinoma. Mol Cancer Ther. 2009 Jun;8(6):1494-504. (*shared first authorship)
6. Ivane Abiatari, Sonja Gillen, Tiago De Oliveira, Theresa Klose, Kong Bo, Nathalia A. Giese, Helmut Friess and Jörg Kleeff. The microtubule-associated protein MAPRE2 is involved in perineural invasion of pancreatic cancer cells. Int J Oncol 2009;35(5):1111-6.
7. Abiatari I, Esposito I, De Oliveira T, Felix K, Xin H, Penzel R, Giese T, Friess H, Kleeff J. Moesin-dependent cytoskeleton remodeling is associated with an anaplastic phenotype of pancreatic cancer. J Cell Mol Med. 2009.

APPENDIX

Figure copyrights

Figure 1: License Number 3913561058828

License date: Jul 21, 2016

Licensed Content Publisher: Nature Publishing Group

Figure 2: © 2015. Published by The Company of Biologists Ltd

This is an Open Access article distributed under the terms of the Creative Commons Attribution License (<http://creativecommons.org/licenses/by/3.0>), which permits unrestricted use, distribution and reproduction in any medium provided that the original work is properly attributed.

Figure 3: © 2012. Published by The Company of Biologists Ltd

This is an Open Access article distributed under the terms of the Creative Commons Attribution Non-Commercial Share Alike License (<http://creativecommons.org/licenses/by-nc-sa/3.0>), which permits unrestricted non-commercial use, distribution and reproduction in any medium provided that the original work is properly cited and all further distributions of the work or adaptation are subject to the same Creative Commons License terms.

Figure 4: License Number 3913061411638

License date: Jul 20, 2016

Licensed Content Publisher: Nature Publishing Group

Figure 5: License Number 3913070214380

License date: Jul 20, 2016

Licensed Content Publisher: Nature Publishing Group

Figure 6 Micrography: Order License ID 4038741461633

Confirmation Number: 11622063

Licensed Content Publisher: Rockefeller University Press

Figure 7-8 Micrography: Electron Microscopy Research Laboratory

<http://www.kumc.edu/emrl.html>

"The Electron Microscope Research Laboratory is supported, in part, by NIH/NIGMS COBRE grant P20GM104936. The JEOL JEM-1400 transmission electron microscope was purchased with funds from NIH grant 1S10RR027564."

Figure 7-8 Diagrams: License Number 3913661319912

License date: Jul 21, 2016

Licensed Content Publisher: Nature Publishing Group

Figure 9 Diagram: Copyright © 1999, © 1999 Int. Physiol. Sci/Am.Physiol.Soc.

Permission for use in Thesis/Dissertation is not required

Figure 9 Histology: License Number 3913070420203

License date: Jul 20, 2016

Licensed Content Publisher: Nature Publishing Group

Figure 10: License Number 4038751360312

License date: Jan 30, 2017

Licensed Content Publisher: Elsevier

Figure 11: Order License ID 3913080663272
Confirmation Number: 11578043
Licensed Content Publisher: American Society for Clinical Investigation

Figure 12: License Number 3913081076846
License date: Jul 20, 2016
Licensed Content Publisher: Elsevier

Figure 13: License Number 3913081211303
License date: Jul 20, 2016
Licensed Content Publisher: Nature Publishing Group

Figure 14: License Number 3913081415668
License date: Jul 20, 2016
Licensed Content Publisher: Nature Publishing Group

Figure 16: Copyright © 2014 Faculty of 1000 Ltd
All F1000Prime Reports articles are distributed under the terms of the Creative Commons Attribution-Non Commercial License, which permits non-commercial use, distribution, and reproduction in any medium, provided the original work is properly cited.

Figure 17: License Number 3913100029317
License date: Jul 20, 2016
Licensed Content Publisher: Nature Publishing Group

Figure 18: License Number 3913100359622
License date: Jul 20, 2016
Licensed Content Publisher: Springer

Figure 19: License Number 3913100517416
License date: Jul 20, 2016
Licensed Content Publisher: Nature Publishing Group

Figure 20: Copyright © 2011, Annual Reviews
Material may be republished in Thesis/Dissertation without obtaining additional permission from Annual Reviews, providing that the author and the original source of publication are fully acknowledged.

Table 1: Copyright © 2011 Robertis
This is an open-access article distributed under the terms of the Creative Commons Attribution-Noncommercial-Share Alike 3.0 Unported, which permits unrestricted use, distribution, and reproduction in any medium, provided the original work is properly cited.

Figure 21: Anyone may, without requesting permission, use original figures or tables published in PNAS for noncommercial and educational use (i.e., in review article, in a book that is not for sale), provided that the full journal reference is cited and, for articles published in volumes 90-105 (1993-2008), “copyright (copyright year) National Academy of Sciences”.

Figure 22: License Number 3914120055642
License date: Jul 22, 2016
Licensed Content Publisher: Elsevier

Figure 23: Copyright © 2002, by the American Society for Biochemistry and Molecular Biology. The publisher allows article reuse in thesis or dissertations at no charge (additional letter of permission under request).

Figure 24: License Number 3914120730615
License date: Jul 22, 2016
Licensed Content Publisher: Elsevier